Proceedings of the 8th Working Meeting on European VLBI for Geodesy and Astrometry

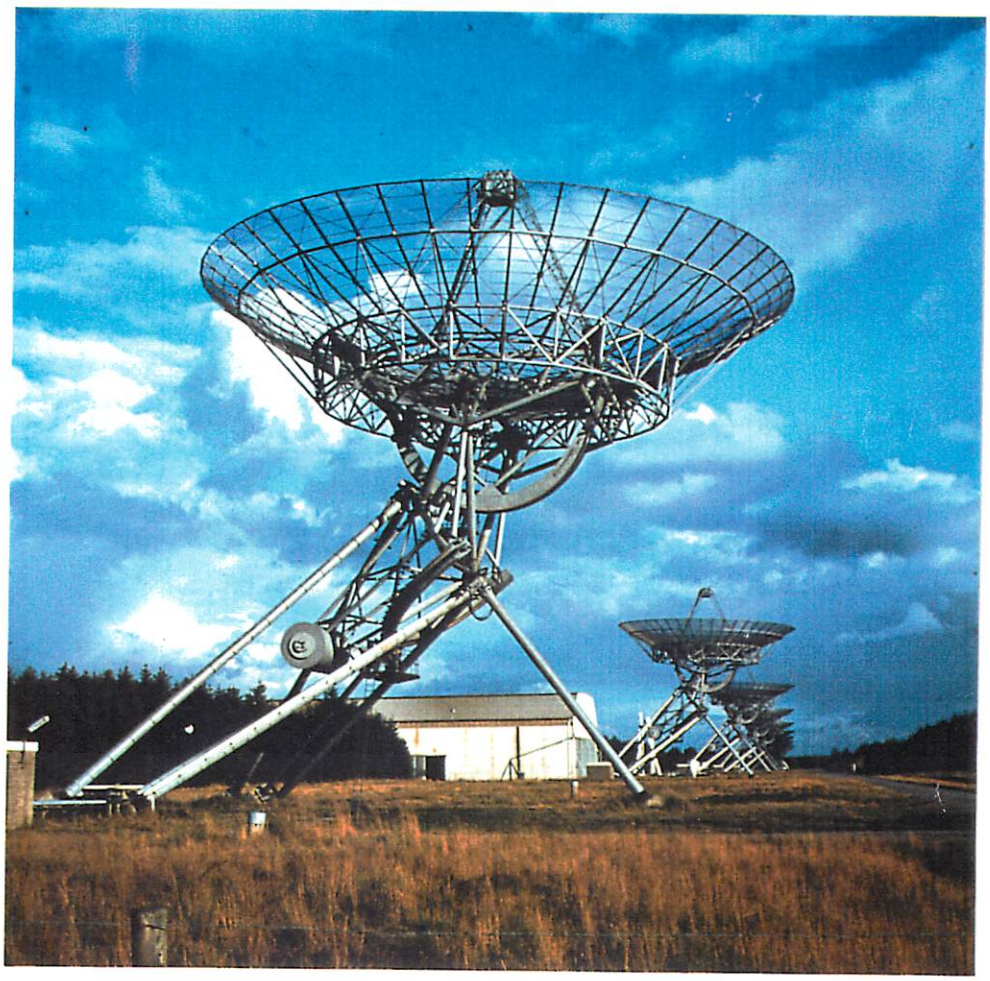

June 13th-14th 1991
Dwingeloo, The Netherlands

Proceedings of the 8th Working Meeting on European VLBI for Geodesy and Astrometry

Report MDTNO-R-9243
Survey Department of Rijkswaterstaat
Delft, The Netherlands

TABLE OF CONTENTS

Table of contents		i
Preface		iii
The 8th Working Meeting on European VLBI for Geodesy and Astrometry		v
List of participants		ix
Station reports		
J. Campbell	The European Geodetic VLBI Network - Status Report	I-1
R. Kilger	Status Report of RT-Wettzell	I-5
B. Pernice, L. Garramone V. Luceri	Matera VLBI status report	I-9
P. Tomasi	Medicina and Noto stations: status report	I-17
A. Rius	Madrid status report	I-20
F.J.J. Brouwer, R.E. Molendijk, R.T. Schilizzi	Status report NL-VLBI	I-22
A. Nothnagel	Status Report Hartebeesthoek Radio Astronomy Observatory	I-24
G. Elgered, R.T.K. Jaldehag, J.M. Johansson, B.I. Nilsson, B.I. Rönnäng	Geodesy VLBI Activities at the Onsala Space Observatory Status Report for 1990-1991	I-25
Status reports on systems and campaigns		
A. Müskens	Report about the Geodetic Use of the MarkIIIA Correlator in Bonn	II-1
K. Jaldehag	New S/X Feed Systems for the SEST and the Onsala Radio Telescopes	II-5
A. Nothnagel	IRIS-S Data Analysis at the Bonn Geodetic Institute	II-12
N. Rebai, G. Petit	Preliminary Results of the 1989 Mobile VLBI European Campaign	II-18
H. Hase, V. Tornatore	Analysis of Recent European VLBI Experiments	II-23

H. Seeger	not published here, see Proceedings of the AGU Chapman Conference on Geodetic VLBI, April 22-26, 1991, page 411-418	

Astrometry

G. Petit, J-F. Lestrade, T. Fayard, A. Rius	VLBI Observations of Millisecond Pulsars	III-1
J.M. Parades, M. Massi, R. Estalella, M. Felli	VLBI Observations of the HIPPARCOS Radiostar LSI+61°303	III-7
M.J. Rioja P. Elósegui J.M. Marcaide	Third epoch of Pair of Quasars 1038+528 A,B: Preliminary results	III-10

Computing methods in Geodetic VLBI

E. Sardón, A. Rius, N. Zarraoa	Kalman analysis of Geodetic VLBI Observables	IV-1
G. Elgered, J.M. Johansson, B.O. Rönnäng	Variations in the Wet Path Delay	IV-7
G. Zeppenfeld	Source structure enhanced MKIII Data Analysis Software	IV-16
H. Steufmehl	AUTOSKED - Automatic Creation of Optimised VLBI Observing Schedules	IV-22
H.-G. Scherneck	A Parameterized Solid Earth Tide Model for VLBI: Quality Assessment	IV-30
B. Plietker, H. Schuh	Free Network Adjustment in VLBI Data Analysis	IV-39
B. Plietker, H. Schuh	Definition of DOP factors for VLBI-solutions	IV-47
H. Schuh	Design of an Expert System for VLBI Data Analysis	IV-53
N. Zarraoa, A. Rius, E. Sardón	Introduction to the OCCAM V2.0 Models	IV-59

Preface

This report collects all contributions to the 8th Working Meeting on European VLBI for Geodesy and Astrometry.

In the first part of these proceedings a short overview of the meeting has been given, followed by a list of participants.

The second part contains all written (scientific) contributions sent to us by the participants. The total list of papers has been divided into four categories, according to the set-up of the programme of the Working Meeting: first the station reports from the different countries, secondly the status reports on campaigns and system related matters, followed by the papers concerning the astrometric applications of VLBI and finally all papers referring to computational methods in Geodetic VLBI.

The meeting has been supported by:

- The Netherlands Geodetic Commission.
- Leids Kerkhoven Bosscha Fund.
- The Survey Department of Rijkswaterstaat.
- The Netherlands Foundation for Research in Astronomy.

This support is gratefully acknowledged.

I also want to thank my co-convenor Ger de Bruyn and especially Ronald Molendijk and Anton Jongeneelen who served as the local organizing committee, whereas Ronald also served as editor of these proceedings.

I hope - and trust - that all participants can look back on a both fruitful - in the scientific sense - and pleasant Working Meeting, and look forward to the next one.

Frits J.J. Brouwer,
convenor

The 8th Working Meeting on European VLBI for Geodesy and Astrometry

The 8th Working Meeting on European VLBI for Geodesy and Astrometry has been held on 13th and 14th June 1991 at the Netherlands Foundation for Research in Astronomy facilities in Dwingeloo, The Netherlands.

The official part of the meeting started with a lunch on Thursday. Participants who had arrived the day before visited the Westerbork Synthesis Radio Telescope in the morning.

The scientific programme had been divided into four parts, containing respectively status reports from the different countries, reports on systems and campaigns, activities in the field of astrometry and finally recent developments in computing methods in geodetic VLBI.

After lunch time Frits Brouwer (convenor) followed by Wim Brouw (NFRA institute) gave a short introduction mentioning some statistics and historical facts about the preceding meetings.
The meeting itself started with James Campbell (page I-1) sketching the history and present status of European VLBI and summarising the contents and goals of this meeting. He paid special attention to some vital subjects like the funding (NASA-DOSE project, EC proposal SCIENCE plan) and the correlation situation. He concluded by emphasising the importance of this kind of meetings for inter-European scientific and technical cooperation.

Session I: Station reports

Till coffee break status reports from the groups in the different countries were presented containing information on organisation, participation in campaigns, (proposed) developments in instrumentation and research. The reports presented were successively the status report of RT Wettzell (D) by Richard Kilger (page I-5), the Matera (I) VLBI status report by Bartolomeo Pernice (page I-9), the Medicina and Noto (I) status report by Paolo Tomasi (page I-17), the Madrid DSN (ESP) status report by Antonio Rius (page I-20), the Dutch status report by Richard Schilizzi (page I-22), the status of the Hartebeesthoek Radio Astronomy Observatory (RSA) by Axel Nothnagel (page I-24), the Onsala (S) Status Report by Gunnar Elgered (page I-25) and finally Stan Gorgolewski with a status report of the Torun Radio Astronomy Observatory (PL), where a new (renovated) telescope is planned to be operational by spring 1993 after which further extension of geodetic VLBI to the east will be possible.

Session II: Status reports on systems and campaigns

After the break the meeting was continued with a session containing reports on systems and campaigns.
Arno Müskens (page II-1) started with a report on the present status of the MKIIIA Correlator in Bonn. He emphasised the limited capacity as the most

important bottleneck at the moment.
An overview of progress and future plans at the ERS/VLBI station O'Higgins in Antarctica was given by Hayo Hase, followed by Kenneth Jaldehag (page II-5) with some interesting features about the new S/X feed systems for the SEST and Onsala Radio Telescopes. Axel Nothnagel (page II-12) continued with an overview of the IRIS-S activities at the Bonn Geodetic Institute. The last two presentations on Thursday contained both results of computations on observed VLBI campaigns. Gérard Petit (page II-18) informed the participants about the results of the 1989 Mobile VLBI European campaign, analysed with the MODEST software, the successor of the MASTERFIT software from JPL.
Hayo Hase and Vincenza Tornatore (page II-23) presented a recent analysis of European VLBI experiments situated in the tectonically interesting Mediterranean with a comparison of VLBI results and geophysical models.

The rest of the first day was spent in one of the conference hotels in Hoogeveen with an informal dinner offered by the Dutch sponsors of the meeting.

Session III: Astrometry

In the first session on Friday attention was paid to astrometry.
Gérard Petit (page III-1) reported about the results and the progress of research on observations of millisecond pulsars. Josep Parades (page III-7) followed with some results observing the radiostar LSI+61303 to link the Hipparcos reference frame and the extra-galactic one through VLBI observations.
Anton Jongeneelen continued with an overview of phase referencing using the Dutch DEGRIAS software on a project dealing with the detection of proper motion of M81 using two reference sources. Finally Maria Rioja (page III-10) presented some results of differential astrometry on the pair of quasars 1038+52 A&B.

Session IV: Computing methods in Geodetic VLBI

The fourth session contained all topics related to computing methods in Geodetic VLBI. Esther Sardon (page IV-1) started with some results on the utilisation of Kalman analysis to Geodetic VLBI observables. Following the good results (less memory, stochastic modelling atmosphere) there are plans to implement this approach in the next version of the OCCAM software.
Gunnar Elgered (page IV-7) dealt in his talk with results of handling the variations in the wet path delay; Günter Zeppenfeld (page IV-16) told about his results on applying source structure corrections in the data analysis software and Axel Nothnagel (page IV-22) presented the status of the automatic creation of optimised VLBI observing schedules.
Hans-Georg Scherneck (page IV-30) followed with the presentation of a new parameterised earth tide model for VLBI, especially meaningful as a new model for computation of the station displacement due to earth tides.
Berthold Plietker and Harald Schuh (page IV-39) presented some results on

research on free network adjustment in VLBI data analysis and the applicability of DOP-factors for VLBI-solutions (page IV-47).
The morning session was concluded by Nestor Zarraoa (page IV-59) providing all participants some background information about the new OCCAM software

After a short walk to the radiotelescope for the common group photo, everybody met in the restaurant for lunch.
During lunch the Madrid group gave, in continuation of the introduction earlier, a short instruction and demonstration of the OCCAM software.

After lunch Hermann Seeger gave an introduction to the TIGO concept (Transportable Integrated Geodynamical Observations) and the corresponding IfAG-plans to support VLBI in the southern Hemisphere. With this in mind he also emphasised that additional correlator capacity would be necessary.
Harald Schuh (page IV-53) introduced his idea about the design of an expert system for VLBI data analysis because of the complexity of the data-editing and decision process on model parameters in view of the large amount of data.
Stan Gorgolewski examined the possibilities and the application of Space VLBI station coordinates. Finally Bartolomeo Pernice presented some results on recent data analysis from Matera.

General discussion

The meeting ended with a general discussion on present day topics. The main items discussed were the developments on the correlator situation like the necessity of new centres, an proposed upgrade of the existing instrumentation (MARK-IIIA/MARK-IV developments) and related problems like the extension of the EVN network.
The meeting was then adjourned with the agreement to have the next meeting in Matera (Italy). As stated during the presentation of the Torun status report by Stan Gorgolewski, for the meeting after the next one the geodetic and astrometric VLBI community would be welcome in Poland.

List of participants

name	institute	country
Gérard Petit	B.I.P.M.	FRANCE
Patrick Charlot	Observatoire de Paris / IERS	FRANCE
Harald Schuh	DLR, MD-TK/E	GERMANY
James Campbell	Geodetic Institute, Univ. of Bonn	GERMANY
Hayo Hase	Geodetic Institute, Univ. of Bonn	GERMANY
Axel Nothnagel	Geodetic Institute, Univ. of Bonn	GERMANY
Arno Müskens	Geodetic Institute, Univ. of Bonn	GERMANY
Günter Zeppenfeld	Geodetic Institute, Univ. of Bonn	GERMANY
Berthold Plietker	Inst. für Photogr., Univ. Stuttgart	GERMANY
Gerhard Schindler	Institut für Angewandte Geodäsie	GERMANY
Hermann Seeger	Institut für Angewandte Geodäsie	GERMANY
Richard Kilger	Satellitenbeobachtungsstation Wettzell	GERMANY
Luciano Garramone	Centro di Geodesia Spaziale	ITALY
Vincenza Luceri	Centro di Geodesia Spaziale	ITALY
Bartolomeo Pernice	Centro di Geodesia Spaziale	ITALY
Paolo Tomasi	Instituto di Radioastronomia CNR	ITALY
Vincenza Tornatore	Instituto di Radioastronomia CNR	ITALY
Stan Gorgolewski	TRAO, Nic. Copernicus Univ.	POLAND
Antonio Rius	Instituto de Astronomia y Geodesia	SPAIN
Esther Sardon	Instituto de Astronomia y Geodesia	SPAIN
Nestor Zarraoa	Instituto de Astronomia y Geodesia	SPAIN
Maria-José Rioja	Instituto de Astrofysica de Andalucia	SPAIN
Josep Parades	Univ. de Barcelona	SPAIN
Gunnar Elgered	Onsala Space Observatory	SWEDEN
Kenneth Jaldehag	Onsala Space Observatory	SWEDEN
Hans-Georg Scherneck	Uppsala University	SWEDEN
Thomas Schildknecht	Astronomical Inst., University of Bern	SWITZERLAND
Wim Brouw	NFRA	THE NETHERLANDS
Ger de Bruyn	NFRA	THE NETHERLANDS
Richard Schilizzi	NFRA	THE NETHERLANDS
Frits Brouwer	RWS/Survey Department	THE NETHERLANDS
Ronald Molendijk	RWS/Survey Department	THE NETHERLANDS
Anton Jongeneelen	Sterrewacht Leiden	THE NETHERLANDS
Rudolf le Poole	Sterrewacht Leiden	THE NETHERLANDS

SESSION 1

status reports

The European Geodetic VLBI-Network - Status Report

J. Campbell

Geodetic Institute, University of Bonn
Bonn, Fed. Rep. of Germany

ABSTRACT: In 1990 Europe has seen a rapid expansion of its geodetic VLBI-net with the establishment of several new stations with full geodetic capability, especially in the Mediterranean. Thus one of the world's most densely spaced VLBI-networks of fixed stations for regional crustal motion research has been created. In order to provide a sound basis for regular observations in this network, proposals have been presented to NASA and to the European Community. EC-funding is expected for the support of network operations, whereas correlator expansion at the MPIfR in Bonn will be subjet to an inter-agency agreement between radioastronomers and geodesists in Germany.

1. THE EUROPEAN GEODETIC VLBI NETWORK

The successful start of multistation-observations among geodetically equipped radio telescopes in western Europe in 1989 marks the beginning of a truly European crustal dynamics program (Campbell 1989). The establishment in the Mediterranean of three new stations fully capable of operating in the geodetic mode has been a major breakthrough, which would not have occurred without the strong commitment of Italian scientific community in favour of VLBI. Now the network comprises six stations, the two base stations in the central and northern part of Europe (Wettzell in eastern Bavaria and Onsala in southern Sweden), the NASA/DSN-Station of Robledo west of Madrid in central Spain and three stations in Italy, i.e. Medicina near Bologna in northern Italy, Matera west of Bari in southern Italy and Noto at the south-eastern tip of Sicily. The coverage of this network represents an excellent geometric configuration, because it allows the determination of relative motions between some of the most important crustal blocks in the European plate puzzle (Campbell, 1987).

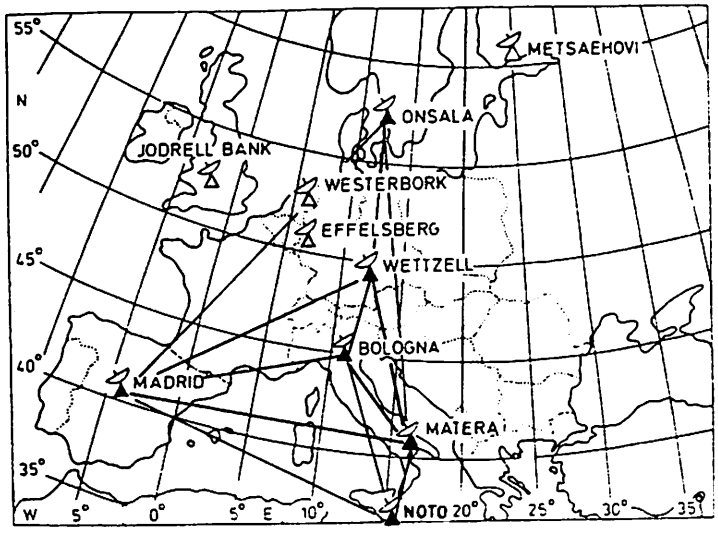

The European VLBI network in 1990

In these proceedings, reports about the status of the new stations and of the results of the first campaigns with more than two active stations in Europe are presented by the various groups involved.

2. DATA PROCESSING AND ANALYSIS CAPABILITIES

2.1 Correlator Situation

In Europe, at present there is just one MkIII correlation facility, operated by the Max-Planck-Institute for Radio Astronomy in Bonn, FRG. With the introduction of the high density head system and a new design of correlator modules, this correlator has been gradually transformed into the MkIIIA version. At present five tape units are available, two of which offer also normal density playback. In combination with ten correlator modules (plus one spare) this allows the correlation of a five station mode C experiment in one pass. Problems with the reliability of playback quality and with the limited coputation speed of the HP 1000F machine still persist and this is why normally only 4 stations can be made to run satisfactorily. Further improvements in the playback elctronics are being implemented and two new tape units (one VLBA and one Penny&Giles machine) will be available as spares during this year (1991) (see also A. Müskens in these proceedings).

2.2 Correlator Plans at MPIfR

The development of the next generation MkIV system, which includes such features as a fourfold data rate for higher delay resolution and greater sensitivity, improved fied systems for easier observing and an upgraded correlator with new design for faster and more efficient processing, requires a timely discussion on the Europeans side on how to keep systems updated and operational.

Negociations have begun between the Max-Planck-Institute in Bonn and the Institute for Applied Geodesy in Frankfurt to embark on a joint project to build at the MPIfR in Bonn a copy of the new MkIV-correlator with the support of the Haystack group. Progress in this work will of course entirely depend on the time scale envisaged for the development of the MkIV correlator at Haystack. The present estimate for this development is two years, if the funding level is not less the $500k per year. If the work can start in 1992 the earliest start in Bonn would be in 1993. With appropriate funding the new Bonn correlator could then be available from 1995, but 1996 seems more realistic. In the meantime an interim solution has to be found in order to increase the correlator power in relation to increasing demand. At present one solution appears to be the reactivation of the old MkIII correlator modules and to add the necessary tape drives, which could later be upgraded to suit the MkIV norm. This would mean that a 5-station MkIIIA and a 4-station MkIII correlator would be available for simultaneous use in the years 1992-1996.

2.3 Geodetic Processing

The geodetic VLBI group includes one geodetic correlation supervisor and a contingent of student labor to carry out the correlation of geodetic experiments within the time allocated by the MPIfR to geodesy (25% of the total time). The CALC/SOLVE package to produce geodetic results is available both at the MPIfR and at the Geodetic Institute of the University of Bonn. The VLBI-Group at the Geodetic Institute is using this software for several ongoing projects, such as the analysis of IRIS-S (South) and some of the CDP-campaigns, Intensive UT1- and Polar Motion observations, special experiments for relativity and tests on schedule optimization and source structure effects. In parallel, the Bonn VLBI software system (BVSS) has been developed into a full-grown multi-station analysis system with special features by the Spanish VLBI group in Madrid (Zarraoa et al. in these proceedings). More VLBI-analysis software is available also in the other European countries such as in Italy, France, the Netherlands and in Sweden.

3. NASA RESEARCH ANNOUNCEMENT DYNAMICS OF THE SOLID EARTH (DOSE)

The NASA Research Announcement 'Dynamics of the Solid Earth' (DOSE) of December 28, 1990 introduces a program which is essentially a continuation of the CDP, albeit with a much larger scope adapted to the themes of the U.S. Global Change Research Program. In order to avoid a fragmentation of the European efforts in this field, the WEGENER-group took the initiative to collect and coordinate the European proposals relevant to the NASA announcement.

The WEGENER group (Working-group of European Geo-scientists for the Establishment of Networks for Earth-science Research), which up to now has mainly taken care of the SLR work, has been re-organised to include also the other geodynamical observing techniques. At special meetings in Frankfurt and Kootwijk the European geoscientists interested in this program met and dicussed the primary goals under which the individual proposals in response to the NASA announcement should be sent in. These goals are the investigation of the kinematics and dynamics of the south-western boundary of the Eurasian plate, the study of post-glacial uplift in Fennoscandia and the study of the relationships between changes of height, changes of sea level and global warming. In addition a commitment is made to continue the support of global programs. A total of 28 individual proposals from institutions in 24 different countries have been submitted jointly to NASA under an agreed upon management structure.

The proposal for European geodetic VLBI has been included in the WEGENER joint proposal for two obvious reasons:

- For the European geodetic VLBI community it will be essential that the planned activities become part of the follow-up NASA program in the same way as has been the case with the CDP, to ensure that the necessary hard- and software support as well as the ability to use US telescopes and the CDP databases will continue to be available.

- The aims of the VLBI basline measurements largely coincide with the goals of WEGENER and will benefit from close cooperation and coordination of efforts.

It should be noted that the participation in the NASA program does not include any form of financial support. This is why in a separate move an application for financial support has been submitted to the EC.

4. EC - PROPOSAL FOR EUROPEAN GEODETIC VLBI

An application for financial support of the planned regular VLBI campaigns for crustal motion in Europe has been presented to the European Commission under the so-called Science Plan for the years 1988-1992. This funding concept aims at 'improving the quality and efficacy of scientific and technical research in all member states' and tries to 'overcome the traditional European weakness of isolation and fragmentation'. The specific objects of the plan include the promotion of training and improvement of mobility of European researchers, the further development of cooperation and the setting up of 'intra-European cooperation- and interchange networks'.

The support method consists of either twinning or operations contracts and provides funds to cover costs for travel, extra staff and extra equipment needed for the proposed project. The total funding available for any one project of three years duration is relatively small (500 kECU, = 700k$), but seems just about adequate to cover the extra costs arising from the carrying out of the proposed VLBI-campaigns.

The idea of this proposal is to mobilise the inherent potential of the European VLBI-network to determine crustal motions in the active zones between the African and Eurasian plates. Up

to now this potential has been largely used by the U.S.A. through the channels of the NASA Crustal Dynamics Project. This project will come to an end of 1991, and discussions with NASA officials showed that they would welcome the shifting of the initiative to the European side. This of course means that the Europeans have to provide all the services in organisation and data processing which have been mainly in the hands of the NASA-Goddard Space Flight Center VLBI Group.

The operations contract of the EC Science Plan binds together six participants, which are represented by the five institutions supporting the geodetic VLBI activities at the observatories, and a coordinating centre, which is identical with the scheduling and processing center for geodetic VLBI in Bonn. The contract members are: Geodetic Institute, University of Bonn (coordinator); Istituto di Radioastronomia Bologna (CNR), Centro di Geodesia Spaziale Matera (ASI); Instituto de Astronomia y Geodesia, University of Madrid (CSIC); Rijkswaterstaat, Meetkundige dienst, Delft; Onsala Space Observatory, Technical University of Göteborg; Satellitenbeobachtungsstation Wettzell (IfAG, Frankfurt).

The proposed funding scheme is largely made up of manpower costs, which are seen as a vital stimulus for the proliferation of the application of the VLBI technology in Europe. There is a great need of young experts to be trained when they graduate or are leaving the universities. Due to the lack of appropriate temporary positions, it has been exceedingly difficult to find experienced staff in this new field. There is only one full position of a scientist, who is designed to act as the prime coordinator and investigator. For the other positions graduate or post graduate students will be employed in accordance with the available conditions in each country.

The running costs such as travel, tape shipments and consumables are required on the marginal level and are very small compared to the total cost of operating and maintaining the observatories. The total EC-contribution of about 800 kECU for this project, which combines 6 different groups from 5 different countries has been based on the average funding level of about 400 kECU for 3 countries with 4 organisations.

The proposal of a European VLBI network should be optimally suited for the Science funding scheme and it is hoped that it will make its way successfully throug the different stages of evaluation and selection at the EC in Brussels.

5. REFERENCES

Campbell, J.: European VLBI for Geodynamics. Proc 3rd Int. Conf. on the WEGENER/MEDLAS Project, Bologna, May 1987, Ed. by P. Baldi and S. Zerbini, Publication of the University of Bologna, p. 361-374, 1988

Campbell, J.: Status report on global and European VLBI. Proc 7th Working Meeting on European VLBI for Geodesy and Astrometry, Ed. by A. Rius, Consejo Superior de Investigaciones Cientificas, Madrid, October 1989

Wettzell, MAY 29TH, 1991

STATUS REPORT OF RT-WETTZELL

This report presents an overview of the activities at radiotelescope Wettzell regarding observing and upgrading the hardware of our VLBI-system since our last meeting in Madrid.
Since Wettzell is a station, dedicated 100% to geodesy, our observing activities do not change much through the years. A board, whose members are
- Prof. Dr. H. Seeger, President of IfAG, Frankfurt,
- Prof. Dr. M. Schneider, Technical University of Munich,
- Prof. Dr. J. Campbell, Geodetic Institute of University of Bonn,
- Dr. W. Schlueter, Satellitenbeobachtungsstation Wettzell,

decide over additional observations of our radiotelescope.

- IRIS-A : The continuous participation in IRIS-A is still our major effort in geodetic observing campaigns. The net normally consists of the radiotelescopes:
  - Westford, Massachusetts,
  - Richmond, Florida,
  - Mojave, California,
  - Wettzell, FRG and
  - Onsala, Sweden, (about once per month).

  The IRIS-A session is an old observing session, its history reaches back to the year 1980. There have been some changes through the years to improve
  - the geometry of the network,
    (From May 29th to August 7th RT Algonquin will join IRIS-A; this measure will not really improve the geometry of the network, since Algonquin is too close to Westford.
    Plans of NGS to add a telescope in Brazil near Recife to IRIS-A will significantly improve the North-South extension of the network.)
  - the selection of the observed sources,
  - the strategy of the observing schedule,
  - the hardware of the observatories.

  All these measures help to make IRIS-A to one of the most accurate and valuable geodetic measurements.
  One of the last major changes happened at April 22, 1991. The network IRIS-A, now called also network NEOS-B observes weekly:
  - starting at Monday, 8:00 UT and
  - finishing at Tuesday, 8:00 UT.

  An additional network NAVNET, with the additional synonym NEOS-A, consisting of the radiotelescopes
  - Greenbank, West Virginia,
  - Richmond, Florida,
  - Fairbanks, Alasca, and
  - Kokee Park, Hawai,

  observes also weekly, but 3.5 days later,
  - starting at Thursday, 20:00 UT
  - finishing at Friday, 20:00 UT.

  Both nets are expected to measure with highest possible precision:

- the coordinates X+Y of the rotational pole of the earth,
- UT1-UTC, or changes of the length of a day,
- horizontal and vertical components of the baselines between participating observatories, as well as their changes with time,
- the position of the radiotelescopes, thus forming a terrestrial reference frame, serving for instance GPS networks as fiducial reference frame,
- the coefficients of nutation and precession,
- the coordinates of the observed radio sources, thus forming a celestial reference frame,
- the performance of the hydrogen masers at the stations, etc.

The tapes of both networks are correlated at the correlator of the US Naval Observatory in Washington.
The results are published in the monthly issued IRIS, Earth Orientation Bulletin, A+B by NGS [1] and contribute to the earth orientation parameters, published by the BIH.

- IRIS-S : There have been changes in IRIS-S as well. While previously the network operated once per year, performing about six 24h-sessions within one month, it now operates on a regular basis with about twelve 24h-sessions per year. The network normally consists now of following radiotelescopes:
  - Hartebeesthook, Suedafrika,
  - Westford, Massachusetts,
  - Richmond, Florida,
  - Mojave, California, and
  - Wettzell, FRG.

  This session is correlated by the Geodetic Institute of the university in Bonn at the correlator of the Max Planck Institute of Radioastronomy.

- INTENSIVE : Based on the values of X + Y of the rotational pole of the earth and the coordinates of the radio sources it is possible to determine with a single (East West) baseline interferometer:
  - UT1-UTC and the length of day,
  - performance of the hydrogen masers at the observatories and
  - the atmospheric zenith path delay.

  The net consists of the radiotelescopes at Westford and Wettzell, forming an East-West-interferometer with a 6000 km-baseline. 4 radio source are recorded twice in sequence. The measurement is performed once daily at the same siderial time between IRIS-A-sessions. The session runs since April 1984 continuously.
  Correlation is done at WaCo, USNO, within 5 days after recording.
  The results are published in IRIS, Earth Orientation Bulletin, A+B. [1]

- CDP : The radiotelescope Wettzell is integrated in the CDP-program of NASA since 1984.

  Europe : The network consists of the European telescopes:
  - Onsala, Sweden,

- Madrid, Spain,
- Medicina, Noto and Matera, Italy, and
- Wettzell.

Correlation is done by Geodetic Institute in Bonn at the correlator of Max Planck Institute for Radioastronomy.

X-Asia : The network consists of the radiotelescopes
- Hartebeesthook, South Africa,
- DSS 45, Australia, at Tidbinbilla, 34m-RT,
- Hobart, Australia,
- Shanghai, China,
- Kashima, Japan,
- Wettzell, FRG.

The session connects 2 telescopes in Australia (South Pacific) to the telescopes in Asia, Africa and Europe.

R&D-program: NASA (Goddard Space Flight Center) and Haystack Observatory are in the process of improving the hardware of VLBI measuring technique. Main steps towards this goal are:
- doubling of the band width of the upper side bands of the video frequencies from 2 to 4 MHz. The recording speed of the tape unit increases from 120 to 240 ips;
- doubling of the spanned IF-bandwidth
  : in X-Band from 360 to 720 MHz
  : in S-Band from 85 to 125 MHz.

The video frequencies in a R&D sessions are:

X-Band [MHz]	S-Band [MHz]
132.99	200.99
172.99	210.99
272.99	230.99
432.99	285.99
652.99 *	320.99
772.99 *	325.99
832.99 *	
852.99 *	

In order to enable the participation of our radiotelescope in R&D sessions we had to perform following major modifications in our system:

x receiver:
X-Band: replacement of filters and amplifiers
S-Band: replacement of filters
The preamplifiers in the dewar remained unchanged. But it is highly desirable to change these preamplifiers in the dewar against units being tuned to the higher band width.

x MIII-DAT:
Video Converters: Addition of 14 4 MHz-filters
IF-Distributor : Addition of a modul IF3,
reducing the 4 higher IF-Bands (*) with a LO frequency of 500.1 MHz to lower levels, which the video converters are able to process.

R&D-experiments started in Mar 27th, 1989 at the radio telescopes in Westford, Mojave, Fairbanks and Pie Town. Our radiotelescope joined the R&D network since beginning of 1991 and the present network consists of:
- Westford, Mojave, Fairbanks, Los Alamos (VLBA-site)

Kokee Park and Wettzell.
Together with additional measures, as
- better modelling of refraction (wet and dry component) by improved software (Kalman filter) and low elevation observations (El = 2 degree)
- avoiding sources with strucure,
- shorter scans (due to receivers with less noise) and
- more sophisticated strategies regarding sky coverage

the accuracy of R&D measurements has improved by a factor of about 3.

[1] SUBCOMMISSION INTERNATIONAL RADIO INTERFEROMETRIC SURVEYING (IRIS)

IRIS-EARTH ORIENTATION BULLETIN, BULLETIN A
and
IRIS-OBSERVATORIES PERFORMANCE REPORT, BULLETIN B

MATERA VLBI STATUS REPORT

B.Pernice ASI-CGS Matera

L.Garramone
V.Luceri TELESPAZIO-CGS Matera

1. Introduction

This report summarizes the present status (to June 1991) of the VLBI activities at the Matera Center for Space Geodesy (CGS).
In the first part of this report the main characteristics of the VLBI system are described with operating and technical remarks.
In the second part, the VLBI data analysis activities at Matera CGS are described.

2. VLBI system characteristics

In fig.1 there is the block diagram of the Matera VLBI system and TAB.1 describes its main characteristics.

2.1 Operating remarks

Since May 1990, when the VLBI system became operating, Matera partecipated to 3 CDP european experiments (EUROPE....) and to 9 USNO experiments (NAVEX....).
Moreover Matera has plan to partecipate to the USNO NAVNET campaign (weekly) and to the NGS IRIS-A experiments (monthly).
Other dedicated experiments are also planned for S/X band Radio Astronomy and Geodesy.

2.2 Technical remarks

- The first experiment revealed a significant phase drift ($\triangle f/f \approx 5 \times 10^{-14}$) of the Local Oscillator of the Down Converter.
  On February 1991, the origianl L.O. was replaced with the one provided by NASA ($\triangle f/f \leq 1 \times 10^{-14}$).
- Experiments between October 1990 and February 1991 showed low sensitivity in the S-band.

This problem was solved after accurate check and calibration of the S-band.

- RF interferencies in the S-band are present at Matera due to TV relays.
  The effect is significant on two S-band VLBI channels.

2.3 Operating team

The Matera VLBI system is operated by Telespazio under the Italian Space Agency management (Project Manager: B.Pernice).
The operating team is composed by 1 operation manager (shared), 2 system engineer (shared) and 4 technicians (full-time).

3. Data analysis

The data analysis activity at the Matera Space Geodesy Center began with the installation of the Solve program on the HP 9000/835 computer of the Center in May 1990.
In the same period (precisely on the 24th of May) the first 6-hours experiment involving Matera took place.
The obtained data were analyzed with the above-mentioned program and the estimate of the Matera-Wettzell baseline was compared with the same baseline calculated from the laser coordinates of the two sites (TPZ90.1 solution) and the laser-vlbi eccentricity vectors.
A difference of cm. 5 between these two measurements came out (fig. 2).
Later, as a training activity, the data of the IRIS campaign from 1984 to 1988, already processed at GSFC, were analyzed in order to obtain: time serie of baselines and station coordinates, site velocities, earth rotation parameters.
The same parameterization was used for the whole set of data, except few experiments (batch mode with 1 hour for clock and atmosphere, Lanyi model for the calibration of atmosphere, reweighting of the baselines, Westford as master station moved according to the Minster-Jordan model).
From the obtained estimates of the station coordinates and with the determination of the regression lines (fig. 3), the site velocities calculated with three different techniques, that is VLBI, SLR and Minster-Jordan model, were compared (figures 4 and 5).

4. Future plans

4.1 Operation

- The Matera VLBI station is expected to guarantee up to 140 operational days per year.
- An additional High Density VLBI Tape recorder will be procured in the near future.

- Upgrading of the VLBI acquisition system is planned according to the new standard.

4.2 Data analysis

- Data analysis activities will continue in the future, based on the use of CALC-SOLVE software.

  Main goals will include:

  · extension of time series of geodetic parameters (station coordinates, ERP);
  · comparison of Terrestrial Reference System;
  · VLBI versus SLR and GPS;
  · short periodic Polar Motion (provided VLBI data coverage sufficiently long).

TAB. 1

· **ANTENNA RECEIVING SYSTEM**

- 20 m Cassegrain radiotelescope
- 2 m actively controlled subreflector (5 degrees of freedom)
- 0.4 mm overall accuracy of the main reflector surface
- Altazimuth mount with crossing axes
- 2 deg/s max angular velocity (both axes)
- Dual band, S/X conical horn feed
- Two stages, helium cooled fet low-noise RF receiver
- Wide band down-converter

· **DATA ACQUISITION AND TIMING SYSTEM**

- MARK III-A Data Acquisition Terminal with upgrated tape recorder (Signatron Inc. USA)
- HP 1000/A400 field computer
- H-MASER frequency standard EFOS-8 by Oscilloquartz SA-CH host in a dedicated underground room

FIG.1

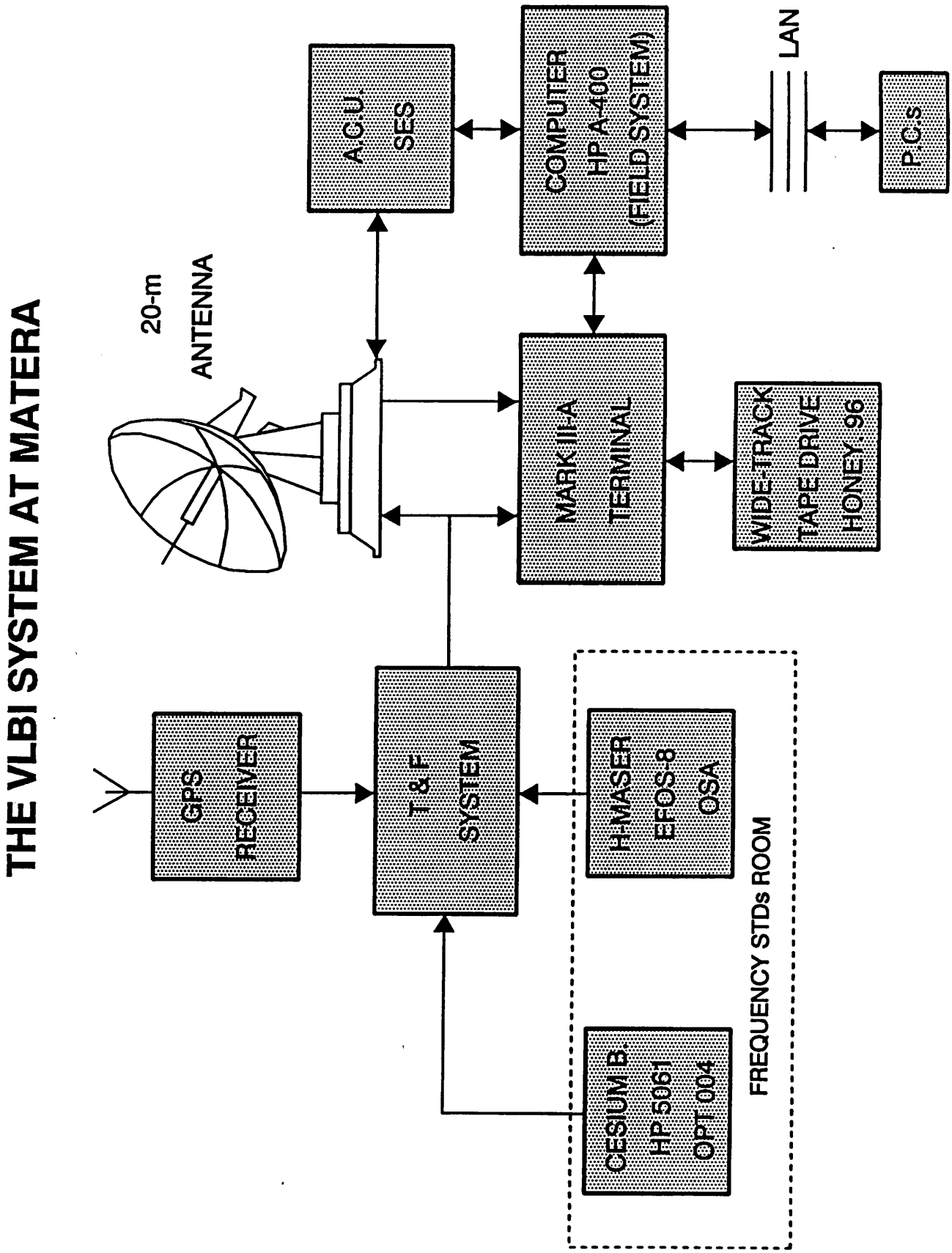
THE VLBI SYSTEM AT MATERA
20-m
ANTENNA
A.C.U
SES
COMPUTER
HP A-400
(FIELD SYSTEM)
LAN
P.C.s
MARK IIIA
TERMINAL
WIDE-TRACK
TAPE DRIVE
HONEY 96
GPS
RECEIVER
T & F
SYSTEM
H-MASER
EFOS-8
OSA
CESIUM B.
HP 5061
OPT 004
FREQUENCY STDs ROOM

VLBI VERSUS SLR INTERCOMPARISON
FOR MATERA-WETTZELL BASELINE

VLBI COORDINATES(1)

	X (mm)	Y (mm)	Z (mm)
MATERA	4641940531 ± 9	1393002006 ± 10	4133325805 ± 10
WETTZELL (Fixed)	4075541655	931734258	4801629697

MAT-WET BASELINE = 990053389 ± 4 mm (VLBI)

SLR COORDINATES (2)

	X (mm)	Y (mm)	Z (mm)
MATERA	4641965215 ± 4	1393069878 ± 7	41332620S5 ± 7
WETTZELL	4075530189 ± 8	931781239 ± 8	4801617 ± 7

SLR → VLBI ECCENTRICITY

	δX (mm)	δY (mm)	δZ (mm)
MATERA(3)	-26118 ± 4	-67073 ± 6	63166 ± 9
WETTZELL(4)	10003 ± 5	-46149 ± 5	11072 ± 5

MAT-WET BASELINE = 990053336 ± 12 mm (SLR-pred.VLBI)

MISCLOSURE
5 cm

NOTES

(1) Telespazio solution from the 6-hour experiment on May 1990.

(2) From the TPZ90 solution extrapolated at epoch of May 1990.

(3) G. Bianco, A. Cenci, A. Caporali: "Geodetic connection of a VLBI radiotelescope to an existing ground reference frame: an application to Matera and Medicina sites" - Presented at the 19th CDP meeting, October 1990.

(4) W. Schluter et al.: "Local Surveys of the Fundamental Station at Wettzell" - October 1990

FIG; 2

FIG.3

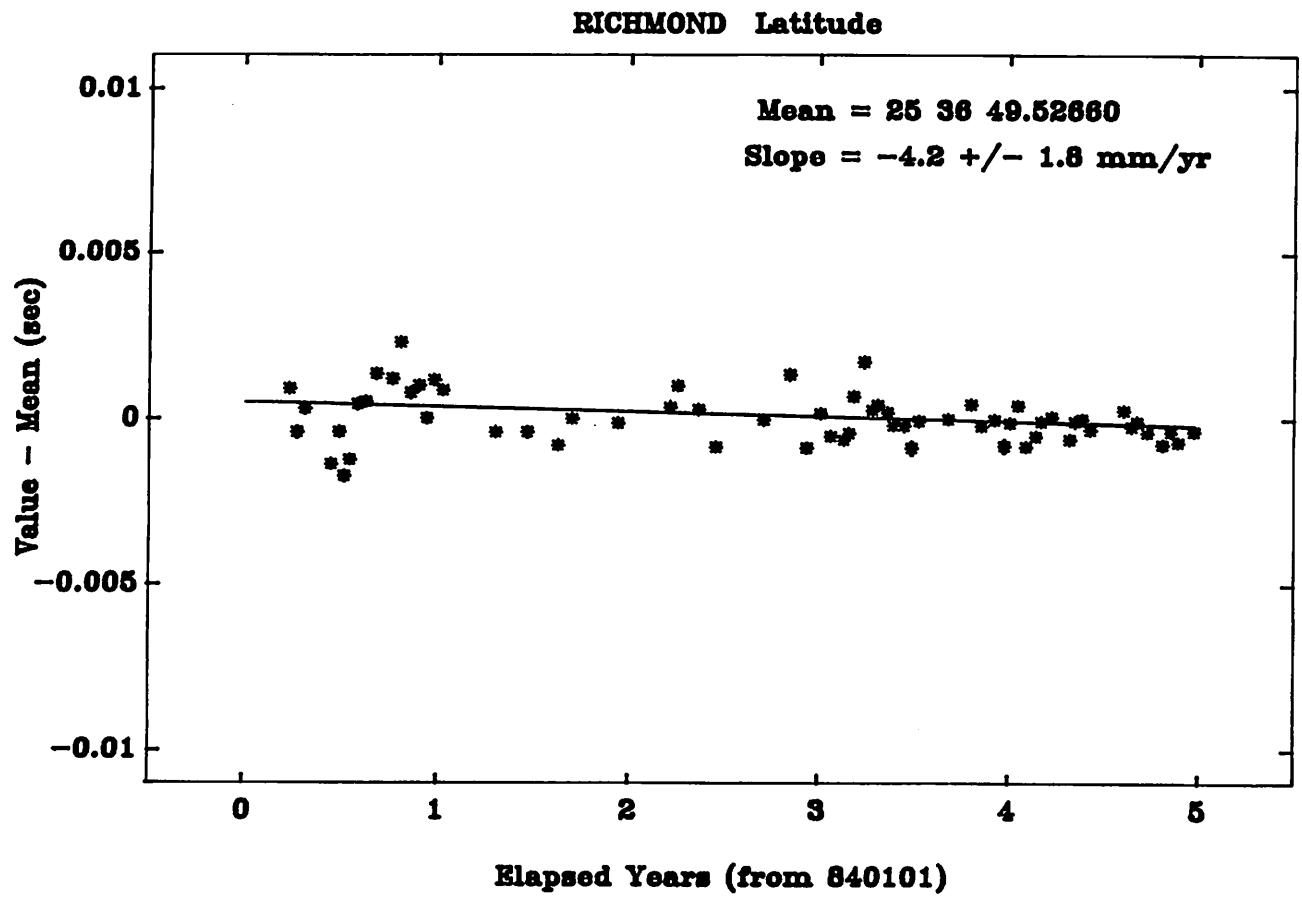
RICHMOND Latitude
Mean = 25 36 49.52660
Slope = −4.2 +/− 1.8 mm/yr
0.01
0.005
0
−0.005
−0.01
Value − Mean (sec)
0
1
2
3
4
5
Elapsed Years (from 840101)

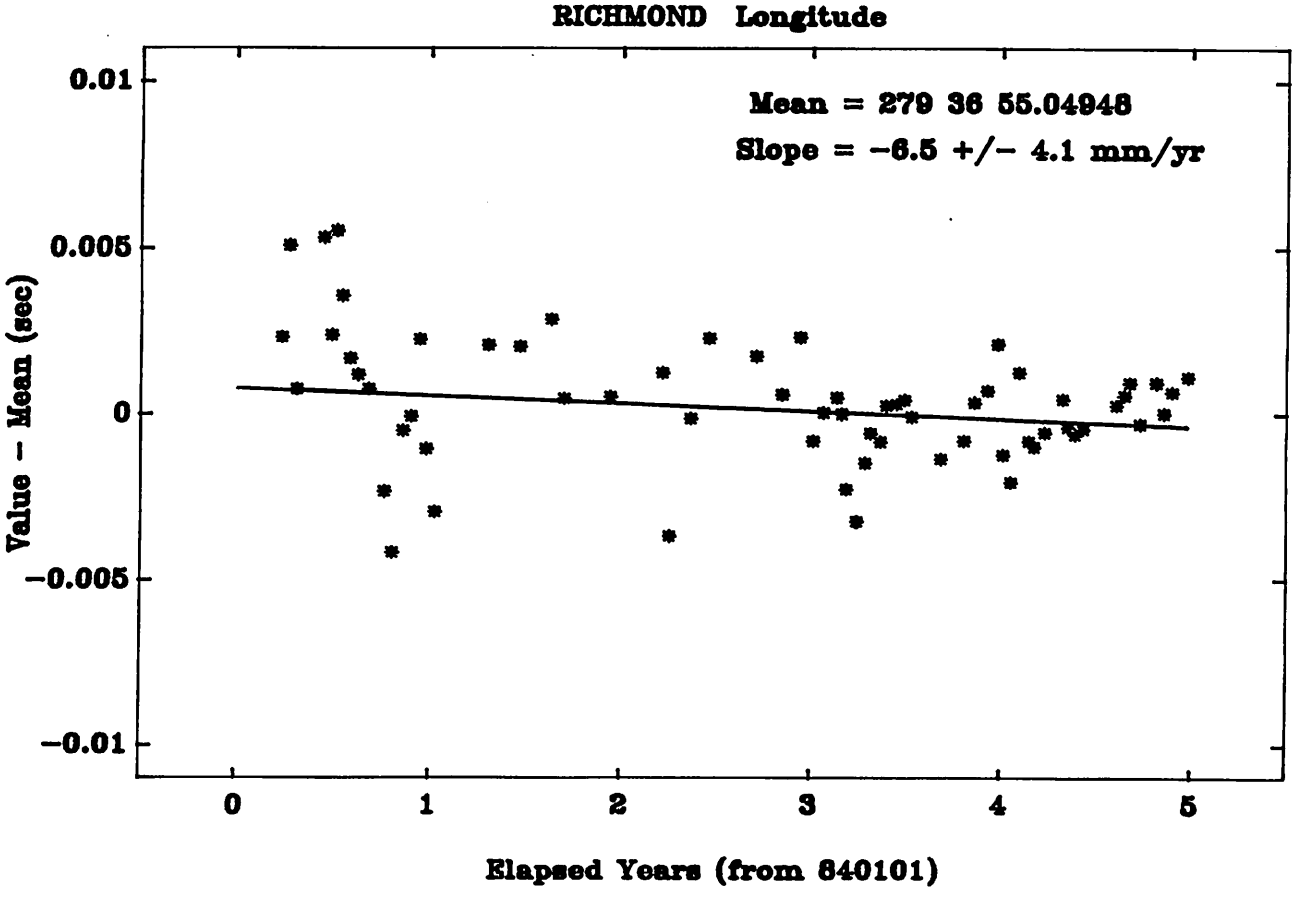
RICHMOND Longitude
Mean = 279 36 55.04948
Slope = −6.5 +/− 4.1 mm/yr
0.01
0.005
0
−0.005
−0.01
Value − Mean (sec)
0
1
2
3
4
5
Elapsed Years (from 840101)

FIG.4

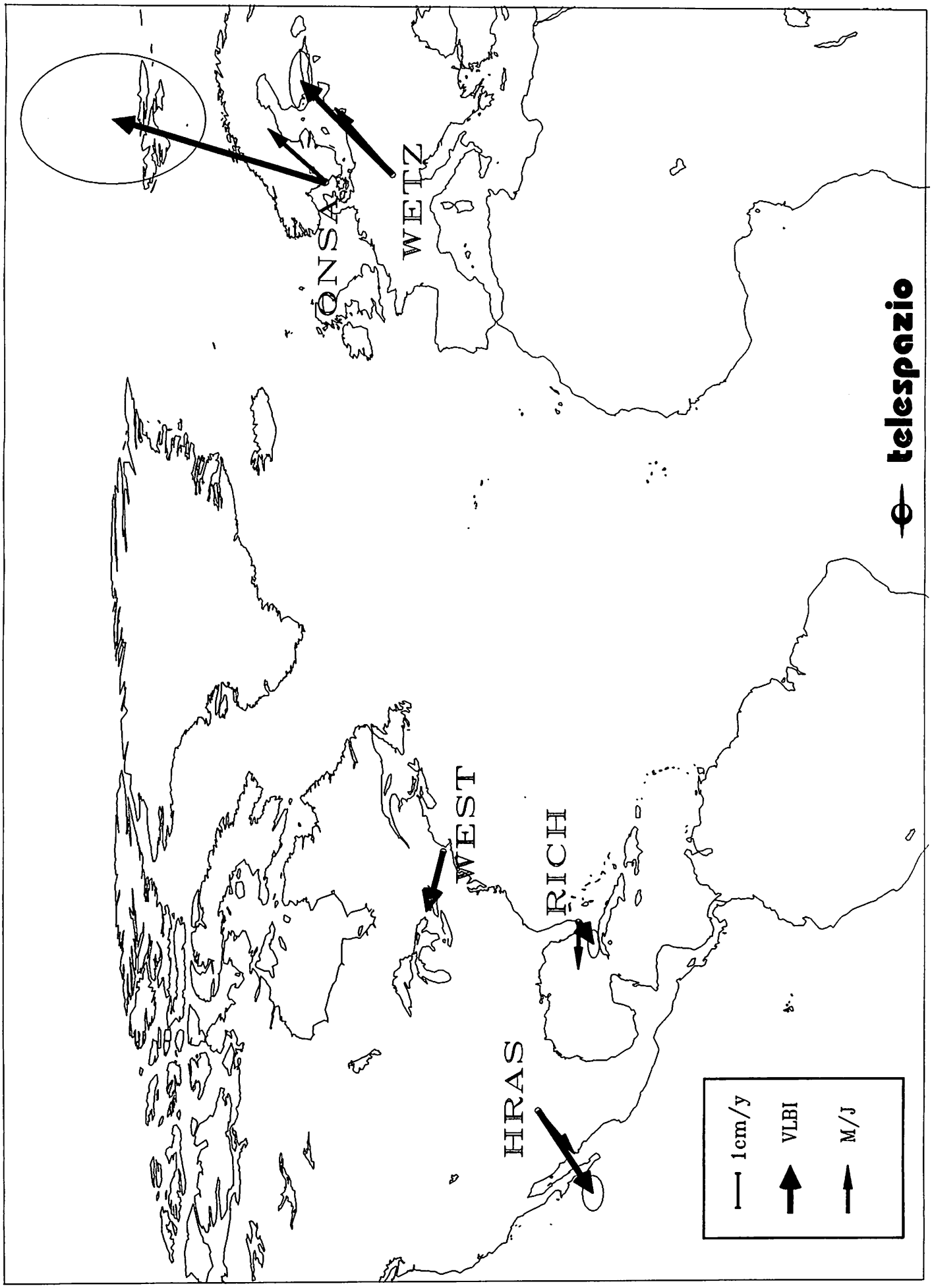

FIG.5

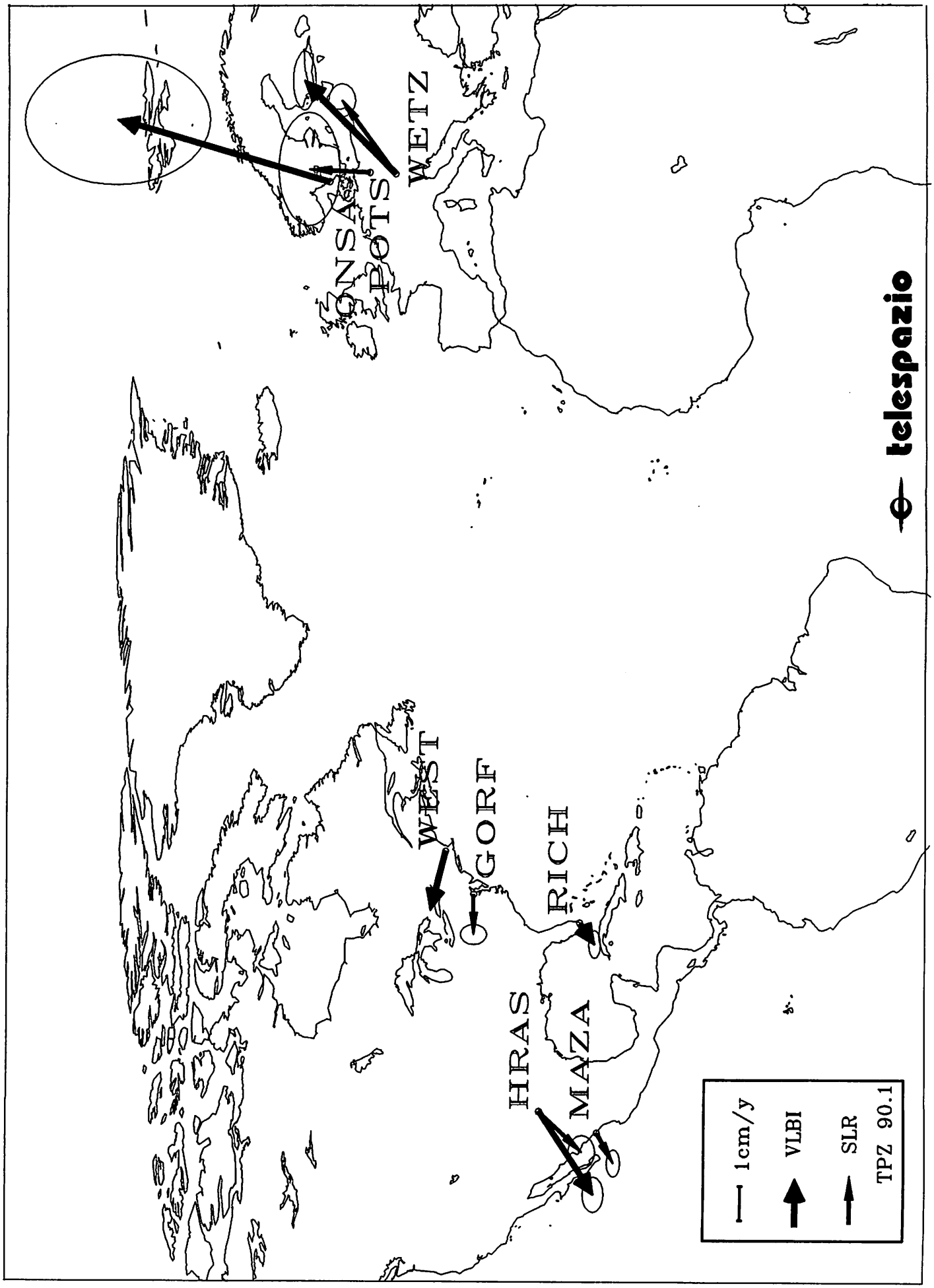
telespazio
WETZ
GONSAVES
POTSD
WEST
GORF
RICH
HRAS
MAZA
1cm/y
VLBI
SLR
TPZ 90.1

Medicina and Noto stations: status report

P. Tomasi

Istituto di Radioastronomia; CNR
Bologna - Italy

1. Introduction

Since 1989 the Istituto di Radioastronomia (I.R.A.) of C.N.R. took part regularly in geodetic V.L.B.I. experiments with the two 32 meters dish antennas: the oldest one near Bologna (the Medicina antenna) and the new one not far from Siracusa (Sicily), (the Noto antenna).

Both these antennas are used mainly for astronomical observations, but a reasonable fraction of their working time is devoted to geodetic V.L.B.I. experiments. In the past the Medicina antenna was involved in IRIS observations, to measure Polar motion and UT1, in EATL experiments, to measure the enlargement of the distance between North-American plate and Eurasian plate, and in a number of ad hoc experiments, with South Africa, Japan and China, together with Wettzell antenna.

May be of interest to remember that the Medicina antenna is fully equipped for V.L.B.I. geodetic observation: S/X cooled receiver with a band of about 500 MHz, MarkIII terminal with high density head recorder and the HP1000 computer, with field system installed, to drive the antenna and the schedule.

The Noto antenna come into operation in March 1989 and its first geodetic V.L.B.I. observation was in June 1989, with an IRIS experiment. During that summer the Noto antenna was heavily involved in EUREF experiment for establishing precise reference points along Europe, with mobile V.L.B.I. antenna.

Differently from the Medicina antenna, the one in Sicily is not fully equipped for geodetic VLBI observations. The S/X receiver is on long term loan from N.A.S.A. and it is uncooled, the antenna site have no MARKIII receiver, and we operate, in this field, only when N.A.S.A (or other agency or Institute) send a terminal to Noto.

2. Recent activity

The main observing program for both antennas, during the last two years, was EUROPE, in order to measure the Eurasian plate deformations, in the south-western Mediterranean, and the horizontal and vertical movements in particular in the colliding zone between Eurasian and African plates.

For these goals the European V.L.B.I. network is really well tailored: a western antenna in Spain near Madrid, three antennas along Italy, from North to South: Medicina, Matera and Noto; and two antennas, Onsala and Wettzell, on stable Eurasian plate, for reference. Preliminary results from observations, have been presented in this meeting by Hase and Tornatore (1991), showing a 1 cm./year velocity at Noto, more or less in the North direction.

Medicina antenna was also involved in the POLAR experiment, for measuring, with large accuracy, the Polar motion.

The Noto antenna took part to an IRIS experiment, immediately after the Sicilian earthquake (12 October 1990). The experiment was made on October 18, and, as expected from the magnitude of the earthquake, no motion was measured within the errors.

From March 1992 the Noto antenna was equipped with a VLBA terminal, assembled with parts from IFAG (Germany) and some others from my institute. In fact IFAG, in order to test the modules and the software, before sending them the new station in Antarctica, agree with IRA to left the modules behind, to be assemble at the Noto station, with the VLBA recorder and within the rack property of Istituto di Radioastronomia. In this way, for about 8 months the Noto station had a full VLBA terminal, and the modules were tested together with the software.

The first test was a full comparison, on the same experiment, between a MARKIII DAT and a VLBA terminal. 12 hours experiment, with both terminals driven manually (the HP1000 refused to start few hours before the experiment), show no different results between data collected by MARKIII and by VLBA terminal. The differences at the correlator (quality factor slightly worst for VLBA) may be due to formatter faults, found and fixed at later experiment. The software for driving the VLBA terminal, provided by Interferometric, was tested in its evolution, and at the end (September 1991) it seems working in every parts.

The Noto site was equipped with Satellite Laser Ranging pad, and that pad was occupied during September 1990 with a SLR successful campaign.

Also GPS campaigns were performed at Noto site by different groups.

More over the monumentation around the antenna was made, and the Italian Space Agency and Telespazio linked the local network. The antenna invariant point will be measured and linked to the local network next year.

From the data analysis point of view, at Bologna we have now an HP9000/360 workstation, with Unix CALC/SOLVE running, and CNPLT, the graphics part of SOLVE, working on the large screen without window (the used graphics library is STARBASE). CATLG is now working and can import database via electronic ftp. The archive facility is still not developed.

3. Future plans

In the next future we will expand our activity within the European network, ready for making much regular European observations along the years.

We are trying to enlarge the capability of the stations with GPS experiment, using V.L.B.I. positions as reference points. We are planning to have a permanent GPS receiver at the stations (probably Rogue), and we are involved directly in two experiments for measuring the absolute sea level rising, using V.L.B.I. and GPS. One is for the "Laguna veneta" near Venice, the other in the southern Mediterranean, near Noto.

At the station workshop, we are making a new S/X receiver with lower temperature and larger band, ready early 1992,

probably for the Noto antenna. In the same time we have already ordered a 4 basebands VLBA terminal. This terminal is not able to make MARKIII compatible geodetic observations, but we are confident to be ready to order the 10 more, along the next year (it will depend on budget). In any case we will have a N.A.S.A MARKIII terminal from January to April 1991, and probably more in autumn if a fully compatible VLBA will not be ready.

Also the data reduction will be keep update: the HP work-station will be moved to 380 for higher speed and a new disk will be added for allowing more room for database. Also the HP700 option will be considered.

In the meantime the software will be updated with the new SOLVE version now working at Goddard Space Flight Centre.

4. References

H. Hase and V. Tornatore: Analysis of recent European VLBI Experiments, Proceedings of the 8th Working Meeting on European VLBI for Geodesy and Astrometry, Dwingeloo, June 1991, in press.

MADRID STATUS REPORT

A. Rius
Instituto de Astronomía y Geodesia, C.S.I.C.-U.C.M.
Madrid, Spain

1. Radioastronomy resources at the Madrid Deep Space Communications Complex

Front ends

DSS63 (70 meter antenna)

Receivers

L Band 1 Cooled FET circular polarization
S Band 2 TWM dual polarization
X Band 2 TWM dual polarization
22GHz 1 TWM LCP polarization

Calibration devices

Noise Diodes in all the receivers
Beam waveguide switching in the 22 GHz receiver
Phase calibration units at the L, S, X receivers
IF Phase calibration system for the 22 GHz receiver

DSS 65 (34 meter antenna)

Receivers
S Band Cooled FET
X Band HEMT and TWM

Calibration devices
Noise Diodes in all the receivers
Phase calibration units in all the receivers

Signal recording and processing

1 VLBI MkIII DAT (2 recorders)
2 VLBI Mk II JPL BWS
1 dedicated microcomputer with A/D and D/A interfaces

Time and frequency

2 Hydrogen MASERS

Water Vapor Radiometer

JPL D1 unit

GPS receiver

SNR-8 ROGUE GPS receiver

Meteorological equipment

Pressure, humidity and temperature sensors.

2. Local Geodetic Ties

Conventional geodetic measurements between the different the VLBI points of DSS63, DSS65, the ROGUE antenna and several geodetic marks have been performed.

3. VLBI experiments

DSS 65 has participated in all the geodetic VLBI experiments in the EUROPE series organized by the NASA Crustal Dynamics Project. Results of these experiments could be found in several papers published in these proceedings.

Detailed information on other experiments performed by the different users of the DSN R/A resources could be found in the document "Radio Astronomy And the Deep Space Network. A report for 1990 JPL 1750-1990" compiled by the Jet Propulsion Laboratory,Telecommunications and Data Acquisition Science Office.

4. OCCAM

The software OCCAM announced during the Madrid meeting and developed in cooperation with the Bonn University group has been released to different interested parties. Details about its availability could be found in these proceedings.

STATUS REPORT NL-VLBI

Frits J.J. Brouwer, Ronald E. Molendijk
(Survey Department RWS, Delft)

Richard T. Schilizzi
(Netherlands Foundation for Research in Astronomy, Dwingeloo)

At the moment, research on Geodetic and Astrometric VLBI in the Netherlands is concentrated at the Netherlands Foundation for Astronomy (NFRA) in Dwingeloo, the University of Leiden and the Survey Department of Rijkswaterstaat in Delft (RWS/MD).

Instrumentation at the WSRT.

Geodetic VLBI equipment:

- one Mk3 terminal with narrow track heads
- one hydrogen maser frequency standard
- S/X receivers being constructed as part of the Multi-Frequency-Frontend project for the WSRT. A prototype frontend is expected to be tested on one of the WSRT telescopes in 1993, and all elements will be outfitted by 1995.

Correlator facilities.

As part of the plan to upgrade EVN facilities, a 20-station correlator has been proposed for joint multi-national/EC funding. It is to be located in Dwingeloo. At the time of the meeting (June 1991), the Netherlands government had committed approximately 20% of the required funding contingent on the remaining funds becoming available. Discussions with other possible partners are on-going. The correlator design will take account of geodetic VLBI requirements

Scientific research on Geodetic and Astrometric VLBI.

The Survey Department of Rijkswaterstaat is responsible for all aspects related to height information in the Netherlands. For detailed studies on sea level changes it is necessary to detect land subsidence at tide gauges.
Geodetic VLBI, in combination with e.g. GPS, can be used for monitoring land subsidence. This is one of the reasons for the Survey Department to continue the work done at the Delft University of Technology in the past years.

During the last one and a half years, most of the time spent on VLBI has been used for the upgrading of the DEGRIAS software, developed at the Delft University of Technology. The difference in the basic geometry between BVSS and DEGRIAS is less than a hundredth of a nanosecond.

Worth mentioning is also that DEGRIAS has been used for phase referenced VLBI in astrometry at the University of Leiden.

After further comparison with BVSS and other software packages DEGRIAS will be used to analyze European VLBI campaigns.
A second goal with respect to the interest of the Survey Department is schedule optimisation for special (European) VLBI height campaigns. First computations have been carried out and in the near future the results will be compared with other work in this field.
In addition to participation in the EC-SCIENCE project with other members of the EVN, the Survey Department is a participant in an EC-EPOCH project (climate change, sea level rise and its impact in Europe). Both projects support the work mentioned above.

Station Report

Hartebeesthoek Radio Astronomy Observatory

Axel Nothnagel
Geodetic Institute of the University of Bonn
Nussallee 17
D-5300 Bonn 1
Federal Republic of Germany

Equipment

Mark III Terminal, regular density (on loan from NGS)

Dicroic S/X feed system, EFOS H-Maser

Future modifications to meet VEGA specifications (VLBI Enhanced Geodetic Accuracy)

System Equivalent Flux Densities (SEFD)

	with Dicroic	without Dicroic	
S-Band	1320 (65 K)	450	
X-Band	5190 (300 K)	5000	
	2100 (120 K)		(GaAsFET on loan)
	1000 (50 K)		(HEMT to be purchased)

Participation in Experiments

12 IRIS-S, 1/month with Wettzell, Westford, Richmond, Mojave (NGS)
12 Southern Hemisphere Survey (SHS), 1/month with Hobart (NGS)
2 SURVEY-S with Hobart (NASA)
2 POLAR-S with Santiago, Hobart, DSS45, [Antarctica] (NASA)
2 X-ASIA with Wettzell, Seshan, Kashima, Hobart, DSS45 (NASA)
1 GLOBAL (48 hours) with Onsala, Santiago, Fairbanks, Westford, Kauai, Hobart (NASA)
28 IRIS-IP4 with Wettzell, Kashima, Hobart (2 hours each) (GIUB)
1 SESH91 with Wettzell, Kashima, Seshan (GIUB)

(All sessions of 24 hour duration, exceptions are marked;
Organising institution in paranthesis)

Geodesy VLBI Activities at the Onsala Space Observatory: Status Report for 1990–1991

G. Elgered, R.T.K. Jaldehag, J.M. Johansson, B.I. Nilsson, B.O. Rönnäng
Onsala Space Observatory
Chalmers University of Technology
S–43900 Onsala, Sweden
phone +46 300 60650, fax +46 300 62621, e-mail geo@oden.oso.chalmers.se

Abstract. This report describes the geodesy VLBI and related activities at the Onsala Space Observatory—including the SEST antenna on La Silla, Chile—during 1990–1991. The performed and planned VLBI observations are summarized; the local footprints mainly maintained using the GPS technique are described; and ongoing technical developments for an improved quality of future geodesy VLBI data are presented.

1. VLBI Observations

IRIS-A

The IRIS-A experiments coordinated by the GRDL at NOAA in the US have had Onsala participation approximately once per month. (A list of abbreviations are found at the end of the paper.) Twelve experiments were performed during 1990 and eleven experiments are planned for 1991. The stations included in these experiments are Westford, MA, Richmond, FL, and Mojave, CA, in the US and Wettzell in Germany. Up to April 1991 these experiments were ran every 5 days. Thereafter, there is one IRIS experiment every 7 days (start Monday morning at 8 UT with a duration of 24 hours). The reason is that another campaign (NAVNET) coordinated by the USNO has one experiment scheduled every Thursday evening resulting in estimated Earth rotation parameters every 3.5 days starting in April 1991.

The European network

The European network—now consisting of three Italian sites (Noto, Matera, and Medicina), Madrid in Spain, Wettzell in Germany and Onsala in Sweden—has proven to be a sensitive network with formal errors of estimated baseline lengths at the few millimeter level (see *e.g.* other contributions in these proceedings and e-mail communication from B. Potash, Interferometrics Inc./NASA/GSFC). Onsala participated in three experiments during 1990 and another three are planned for 1991.

The Global and Polar networks

A 48 hour long Global experiment (suggested by the Onsala staff and coordinated by NASA) was performed in May 1990. The reason was the possibility to include a telescope on the South American plate for the first time, namely the SEST antenna at the ESO site on La Silla, Chile. This telescope—with a diameter of 15 meters—is primarily intended for millimeter and sub-millimeter radio astronomy research. The over all surface accuracy is approximately 70 microns. A photo is shown in Figure 1. In spite of a limited sky coverage due to a safety limit of 50° around the sun and limited time on the telescope to optimize the prototype feed system the formal uncertainty of the estimated baselines to the SEST site was a few centimeters (*Jaldehag*, 1991, these proceedings). The new dedicated geodesy VLBI antenna in Santiago de Chile is planned to replace the SEST antenna in the Global experiment planned for 1991. The use of the SEST telescope in less regular geodesy VLBI experiments may still prove useful in a geophysically interesting area.

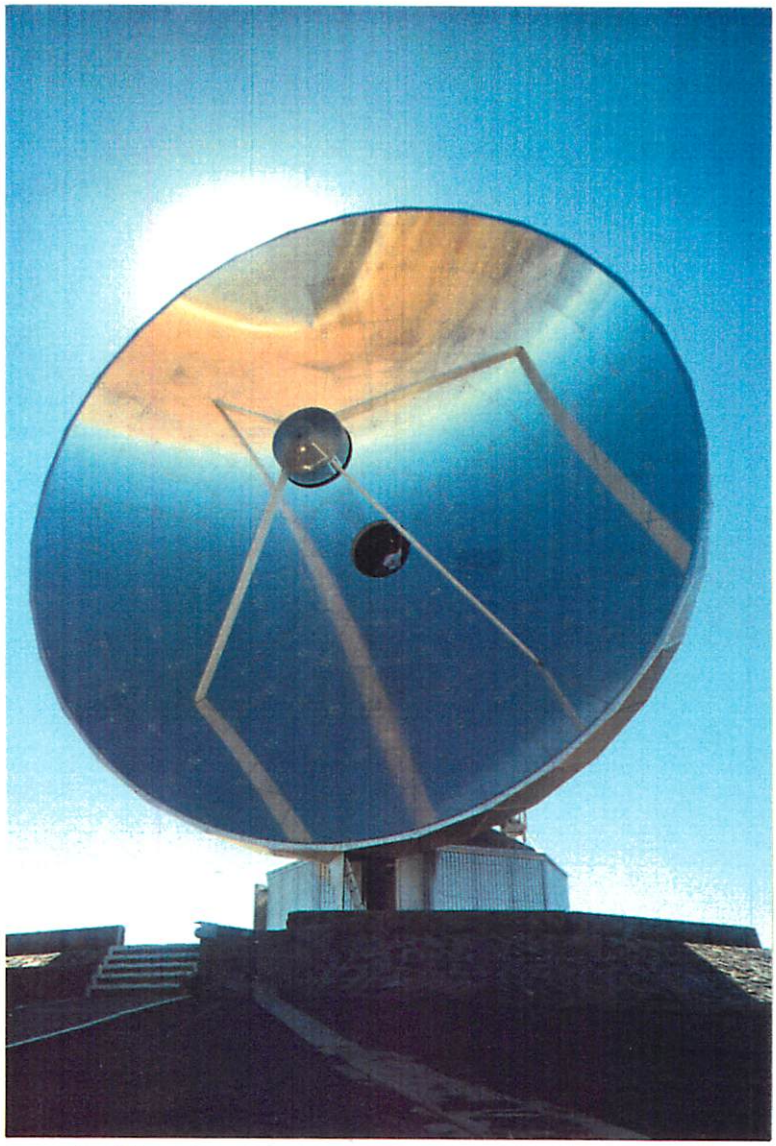

Figure 1. The 15 m telescope for sub-millimeter radio astronomy on La Silla, Chile.

The Polar experiments during 1990 and 1991 have been scheduled simultaneously with IRIS-A experiments. This offers the possibility to study any systematic dependence caused by different networks on the estimated Earth rotation parameters. The used sites are Kashima (Japan), Fairbanks (AL), Haystack (MA), Madrid, Medicina, and Onsala.

2. GPS activities

The increased interest in space geodetic measurements using GPS has first of all resulted in a continuously operating tracking station (in the CIGNET network) at the Onsala site. Furthermore, national interests have been coordinated to make available several GPS receivers for measurement in local networks. It is obvious that it is important to establish and maintain high precision local networks around the VLBI sites. Previously, such a network with baselines of some hundred meters existed at the Onsala site established with "conventional" geodesy. Here we present a summary of the GPS measurements around the Onsala and SEST VLBI sites.

Continuous Operation of the GPS Tracking Station at Onsala

The Onsala site has been a part of CIGNET since December 1987. Excluding shorter time periods of equipment failures data from at least one receiver have been available from this time. Table 1 gives the equipment status over the last years and Figure 2 shows the present configuration.

Table 1. GPS receiver occupation at the Onsala CIGNET site.

Time Period	Receiver	Remark
Dec87–May91	TI-4100	Loan from Statens Kartverk, Norway
Oct90–May91	Ashtech L-XII	Loan from the National Land Survey, Sweden
Jun91–present	Rogue SNR 800	Grant from the Wallenberg Foundation

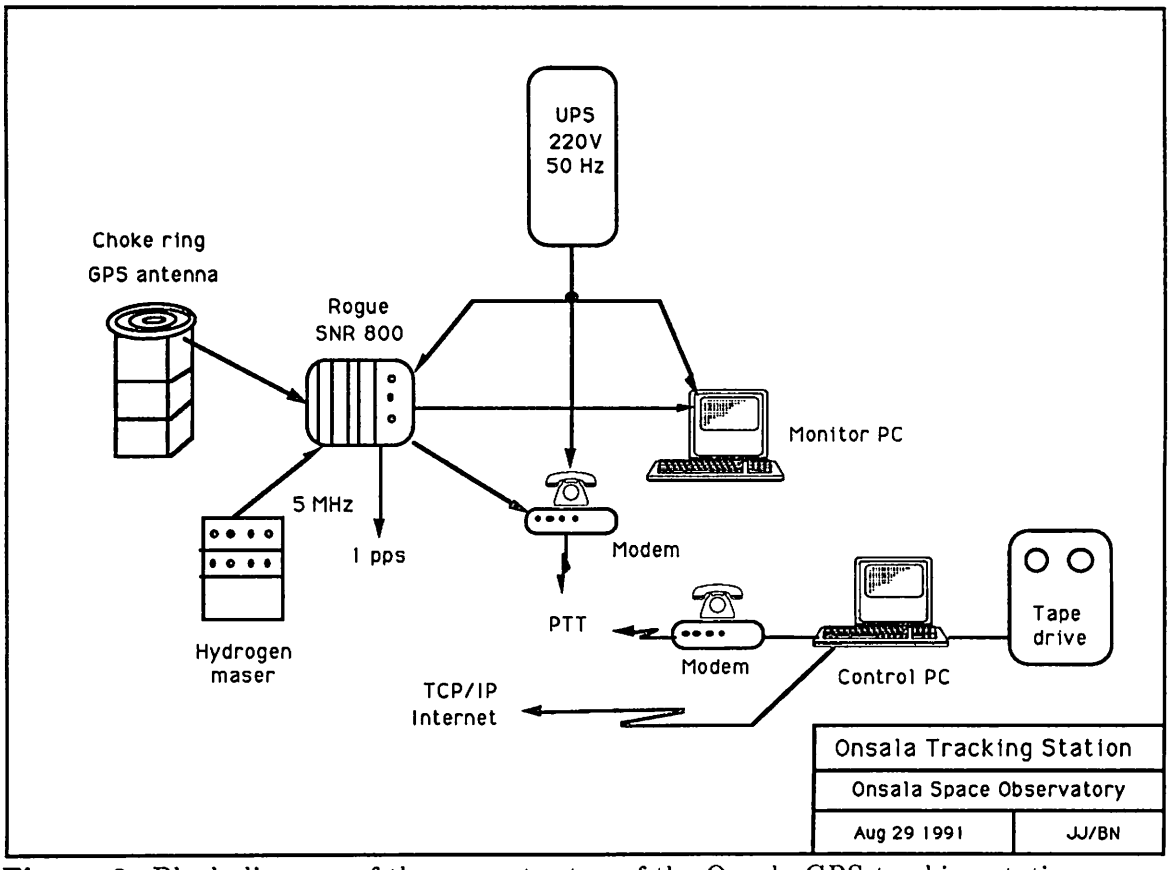

Figure 2. Block diagram of the present setup of the Onsala GPS tracking station.

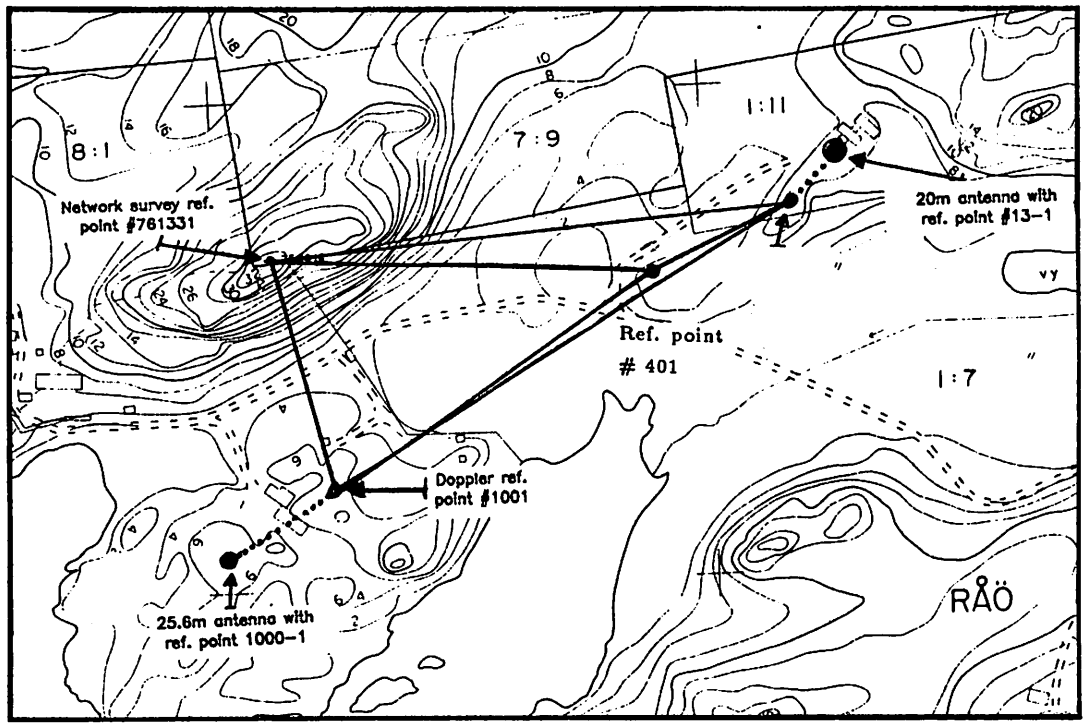

Figure 3. The small footprint at the Onsala VLBI site. The solid lines have been measured using both conventional geodesy and GPS. The VLBI tie (dotted lines) to this network has been obtained using conventional geodesy only. Finally, the baseline between the two telescopes has been estimated from VLBI data (*Lundqvist*, 1984).

Maintenance of the Onsala Local Footprint

A small footprint with the size of a few hundred meters is shown in Figure 3. GPS measurements have verified the consistency with conventional geodesy at the 1–2 millimeter level in all coordinates. A larger footprint, shown in Figure 4, has been measured using dual-frequency GPS receivers in June 1989 and February 1990. A couple of Danish sites have been added to the network and another Swedish site approximately 100 kilometers east of Onsala is planned to be included in early 1992.

Establishment of the SEST Local Footprint

GPS measurements were carried out simultaneously with the GLOBAL VLBI experiment mentioned above. A WM–102 receiver (loan from the National Land Survey, Sweden) was shipped to Chile for several months. In addition to the importance of the footprint itself this work was also called for in order to obtain a South American tie between the VLBI reference network (via the SEST site) and the SLR reference network (via the SLR station on Cerro Tololo). The SEST site was used as a reference site in a larger GPS experiment coordinated by the TUB. In addition to the WM–102 used at SEST, receivers were borrowed from TUB in order to establish the footprint shown in Figure 5.

3. Technical Developments and Plans for the Future

Upgrade of the 20 m telescope

Grants have recently been allocated to upgrade the surface and to install a new steering system on the 20 m telescope. The surface improvement has little impact on the S/X band aperture efficiency (< 1%) since the surface has already an RMS accuracy of approximately 0.25 mm. The new steering system, including numerically controlled motors, are planned to allow for slewing speeds of about 3 °/s.

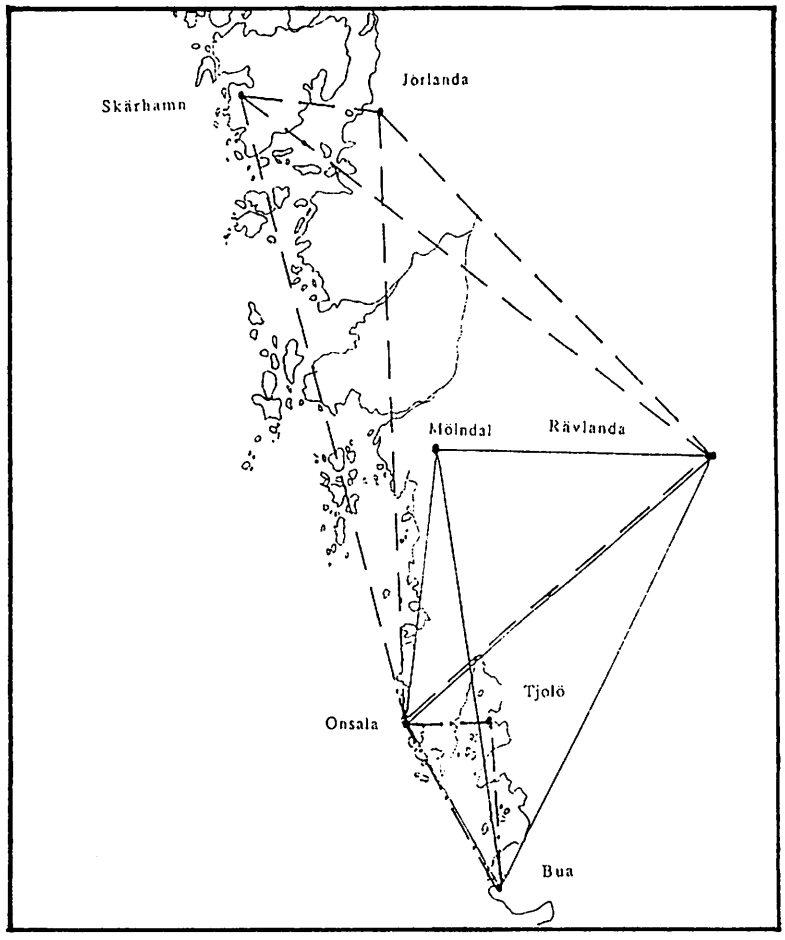

Figure 4. The GPS footprint on the Swedish west coast. The baseline Onsala – Rävlanda is 45 km.

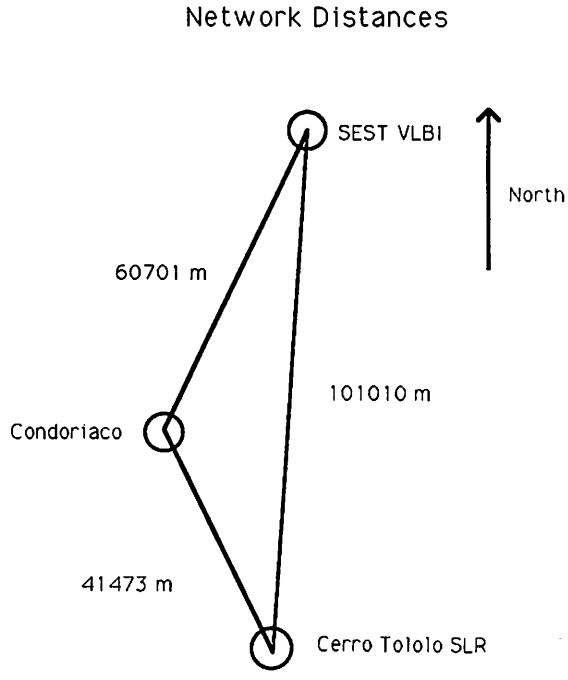

Figure 5. The GPS network used to tie the SLR and VLBI reference frames together in South America.

New S/X band feed systems for Onsala and SEST

The Onsala feed system has been improved using a new design of the dichroic surface and a prototype feed system for SEST has been developed. Further details can be found in *Jaldehag* [1991] (these proceedings).

Improvement of the Onsala Water-Vapor Radiometer (WVR)

A few modifications have been implemented in the WVR. The last VLBI experiment with the old WVR design was carried out in October 1990. The reference loads which were cooled using liquid nitrogen have been removed. Instead, new, more accurate hot reference loads have been installed. Preliminary tests indicate that these will imply an improved accuracy of the inferred atmospheric emission.

New software running on an IBM PC-AT clone will allow more flexible data acquisition and faster slewing rates in azimuth and elevation. Furthermore, it will be possible to slew from horizon to horizon via the zenith direction. This is an important feature which implies that a faster (and therefore more accurate) tip-curve calibration can be performed.

Finally, the WVR will be mounted on a new foundation near the reference marker "Ref. point # 301" shown in Figure 3. The radome of the 20 m telescope gives here a much smaller sky blockage compared to the present location which is approximately half the distance from the 20 m telescope.

List of Abbreviations

CIGNET	Cooperative International GPS Network
ESO	European Southern Observatory
GPS	Global Positioning System
GRDL	Geodetic Research and Development Laboratories
GSFC	Goddard Space Flight Center
IRIS	International Radio Interferometric Surveying
IRIS-A	IRIS Atlantic
NASA	National Aeronautics and Space Administration
NOAA	National Oceanic and Atmospheric Administration
SEST	Swedish–ESO Submillimetre Telescope
SLR	Satellite Laser Ranging
TUB	Technical University, Berlin
USNO	United States Naval Observatory
VLBI	Very-Long-Baseline Interferometry
WVR	Water-Vapor Radiometer

References

Caprette, D.S., Ma, C., & Ryan, J.W., Crustal Dynamics Project Data Analysis–1990, *NASA Technical Memorandum 100765*, 1990.

Jaldehag, R.T.K., New S/X-Band Feed Systems for the SEST and the Onsala Radio Telescopes, *Proc. of the 8th Working Meeting on European VLBI for Geodesy and Astrometry*, this volume, 1991.

Lundqvist, G., Radio Interferometry as a Probe of Tectonic Plate Motion, Doctoral Thesis, Tech. Rept. No. 150, School of Electrical and Computer Engineering, Chalmers Univ. of Tech. Göteborg, Sweden, 1984.

SESSION 2

status reports on systems and campaigns

Report About the Geodetic Use of The MarkIIIA Correlator in Bonn

A. Müskens
Geodätisches Institut der Universität Bonn
Federal Republic of Germany

ABSTRACT: *The present correlator configuration at the MPIfR in Bonn is described. The short and long term planning are discussed as well as the present geodetic policy. A short summary of the global statistics on the correlator time usage for Geodesy and Astronomy of the last few years are given.*

1. Introduction

The MarkIIIA VLBI correlator has set the standard in VLBI instrumentation since the mid of the 1980's. In Europe in Bonn the 'Max-Planck-Institut für Radioastronomie' (MPIfR) has operated a MarkIII correlator of Haystack design since 1982. Developed as an outgrowth of the original MarkIII VLBI system, now the MarkIIIA correlator at Bonn was funded by MPIfR. The Bonn University Geodetic VLBI group has helped to finance an extension of the correlator and has provided operations support by trained students. Therefore the MPIfR commits around 25% of the correlator time to the Geodetic VLBI Group.

The correlation of the IRIS-S experiments (12 times per year / 5 station [Mode B/C]) forms the main part of the geodetic correlation. Additionally extra correlations are done, such as some of the East-Atlantic-Experiments (EATL-n), the EUROPE experiment with the participation of 6 stations (Madrid [Spain] , Matera [Italy], Medicina [Italy], Noto [Italy], Onsala [Sweden], Wettzell [Germany]) and other special experiments which are scheduled by the Geodetic VLBI group (SHAWE,IPM,EOP e.t.c) for measurements of the earth rotation rate and the spin-axis orientation.

2. General aspects of MKIIIA correlator operations

USA (Haystack and USNO correlator)

Both correlators in the USA are configured for split mode operation. Eight drives at Haystack and seven at Washington are equipped with an additional control computer, interface, disks and extra drives. Thus simultaneous correlation of two experiments is possible - for example a three- station (3 baselines) and a four-station (6 baselines) experiment can be done with seven drives total. Moreover, the split correlator operation permits some routine functions, such as fringe search, tape test and recorder maintenance to be done without interrupting the correlation process. In this way the throughput in Washington is sometimes even greater than 100% relative to a single five station correlator operating full time.

Germany (Bonn correlator at MPIfR)

In the beginning the MPIfR acquired a three station MarkIII correlator , designed by Haystack. Expanded with two more playback drives , high density playback heads and new correlator modules, at present we have a five station MarkIIIA processor running. Four of these recorders still have the old wide track heads in addition to narrow track MarkIIIA heads which are on all playback units. The correlator expansion to 12 crates with MarkIIIA modules was completed in December 1990. This gives us now a correlator capacity of max. 10 baselines in mode B/C and 5 baselines in mode A with two spare crates, which are useful for optimal operational processing.

Limited future expansion of the MarkIIIA correlator is planned. Two more tape drives will be installed at the correlator. A 6th playback drive, designed by Penny & Giles who recently started to produce instrumentation recorders, is being installed at the correlator since May this year. This playback drive has been purchased with EEC money and provides a test of playback compatibility with Honeywell based recording systems.
A 7th playback drive has been purchased primarily to develop VLBA-style playback recorder electronics. We hope that one of these recorders will eventually provide a useful 6th station input and will provide more flexible playback at the end of 1991 (2 passes, 6 station Mode B/C).

3. Present situation for geodetic correlation

The fundamental limitation at the MPIfR/Bonn correlator is the present HP1000F correlator control computer power. Operating the five-station correlator, 10 baselines at a time in mode B/C, forces a rather large pre-averageing time of the data (ca. 7 sec), and this effectively prohibits further expansion of the correlator without replacing the computer with a more powerful one. However, plans to replace the old correlator control computer HP1000F by a new model like the HP1000-A990 series have been abandoned.

3.1 Software and periphery

The standard software for schedule preparation (SKED/DRUDG) has been installed on the HP1000-A900 at MPIfR/Bonn, as well as on the HP9000 series330 under HP-UX at the Geodetic Institute at the University of Bonn. In addition the wellknown PC-SCHED program written by Alan Rogers (Haystack) is available on a '386' personal computer at both institutes. The last version of the correlator software from Haystack is installed on the HP1000F correlator control computer. New modified upated software for fringe-fitting, refringing and archiving is running on the A900 as well as the geodetic CALC/SOLVE analysis software (Clark et al, 1988). At the Geodetic Institute the CALC/SOLV software is running on an HP1000F and in the near future also on an HP9000 workstation.

Since May this year a new DAT (Digital Audio Tape) unit has been installed on the A900 for the archiving of correlator and fringe-fitting output. It has replaced the A- and B-tapes archiving (1600bpi, traditional 9-track tapes). With the DAT cassette system a whole correlated experiment can archived in the old A-tape format (file types 50,51,52) on a single cassette which can hold a total of 1.2Gbytes. In the furture a different format may be chosen for archiving. At present the standard SAVEM format insures that the data is readable by the DBFT program for further CALC/SOLV analysis and by MK3IN for fring-fitting in AIPS. In addition we have the possibility to archive the same data in

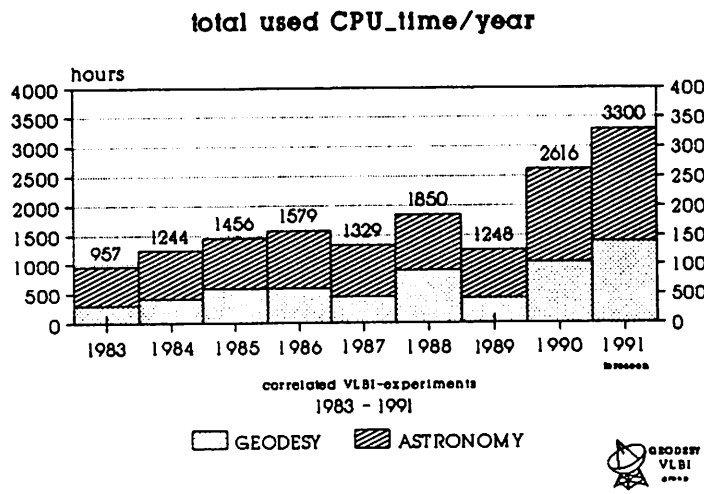

Figure 1: *MarkIIIA Correlator Usage at Bonn/MPIfR* from 1983 to 1991

UNIX readable TAR format which will be used for archiving at some point in the future. This TAR format could be read easily by all foreign users and principal investigators, who could then do the fringe-fitting and further mapping at their own computer systems.

3.2 Geodetic Correlator Usage

The load on the correlator shows us a steady increase from 1986 to 1991 (*see Figure 1*). Due to the initial installation of narrow track heads the correlator was much less used in 1989. A lot of time has been spent on reducing the problems of high error rates of the MKIIIA recordings and into doing other problems of the tape drives - mostly connected with the read interface. In general we could see an increase to more than 3000 hours of real correlator CPU-time per year up to the end of 1991 for both user groups (Astronomy and Geodesy).

4. Outlook

At present the different possibilities of increasing the efficiency of the existing correlator at Bonn are being investigated. The split correlator concept may not really increase the actual productivity of the Bonn correlator as much as it has at both American correlators. The reasons are that geodesists and astronomers (actual 1/3 partition) at MPIfR/Bonn correlator do not simplify simultaneous correlation. Mainly geodesists use the standard recording Mode C and the astronomers Mode A. Besides both users have mostly five participating stations or more. Therefore all available crates are fully loaded. Only during the recorrelation of occasionally less than five stations, fringe-tests and fringe-searching could make a split correlator useful. Additional modification as well as one more drive, additional CPU and hardware for split mode operations and live support could not be realized without extra funding.

It is obvious that the present MPIfR processor centre will be pushed to it limits to handle the needs of future VLBI/VLBA projects for the German Geodetic Community (GGC) and the European Astronomy Community (EAC). For both sides we need greater VLBI sensitivity. Likewise the world wide VLBI activities forced the geodesists to think about a new type of correlator. The actual development of a MarkIV system is an expansion of the MarkIIIA system to cater for operating with wider bandwidth, providing the greater sensitivity to be used in the future. This MarkIV system for example has 14 video converters

each with a maximum bandwidth of 8MHz/sideband and supports 1 or 2bits/sample data replacement format only, support several modes of multiplexing, with a maximum data rate of 1024Mbits/sec on 64 tracks.
For geodesists it is essential that we use the widest available bandwidth (8MHz/sideband) for recording and that in near future we need a correlator capable of wideband processing of a maximum of 7/8 stations to use.

On the correlation side the development of the new MarkIV-system requires of course the construction of a new MarkIV correlator, a project which is being started this year by the Haystack Group. For the geodetic data processing in Europe this means that in some way or another this new development has to be followed on our side. The issue is now being discussed at all levels and before the end of this year a viable option has to be decided upon.

In order to arrive at a financially sound solution, the German geodetic community is seeking to intensify and expand the history partnership with the Max-Planck-Institut for Radio Astronomy at Bonn (MPIfR) to build or contract out a copy of the new MarkIV correlator. The minimum timescale for such an undertaking will be four years. In the meantime, however, the present correlator will have to be improved to be able to handle to increasing demands by both astronomers and geodesists in the coming years.

References

1. Clark,T.A., Corey,B.E., Davis, J.L., Elgered, G., Herring, T.A., Hinteregger, H.F., Knight, C.A., Levine, J.I., Lundqvist, G., Ma, C., Nesman, E.F., Phillips, R.B., Rogers, A.E.E., Ronnäng, B.O., Ryan, J.W., Shupler, B.R., Shaffer, D.B., Shapiro, I.I., Vandenberg, N.R., Webber, J.C., Whitney, A.R., 1985: IEEE Transactions of Geoscience and Remote Sensing, **GE-23**, No. 4, 438

2. The MarkIV VLBI System - next step ; East Coast VLBI group ; October 23.1990

NEW S/X BAND FEED SYSTEMS FOR THE SEST AND THE ONSALA RADIO TELESCOPES

by

Kenneth Jaldehag
Onsala Space Observatory
Chalmers University of Technology
S-439 00 Onsala, Sweden

ABSTRACT. Both the SEST (Swedish-ESO Sub-millimeter Telescope) antenna and the Onsala 20-m antenna are primarily built for radio astronomical research and therefore not directly suited for geo-VLBI. New feed systems are therefore needed to handle simultaneous dual frequency observations and the large bandwidth. This paper will give a few examples of existing feeds for geo-VLBI and describe a new system, with two offset parabolic reflectors fed by horn antennas. The central part of one of the reflectors has been replaced by a plane dichroic surface. This design has the advantage of not interfering with the existing radio astronomical receivers of traditional Cassegrain antennas. The feed system has been tested and used at the SEST antenna, located in the Andes in Chile, during two geo-VLBI experiments in 1990. Theoretical efficiencies are presented and compared with measured values.

1. INTRODUCTION

It is possible to divide the antennas used for geo-VLBI into two categories. The first one is antennas dedicated for geo-VLBI. Dual frequency feed systems for such antennas can be constructed without any concern for receiver and feed systems at other frequencies. Dedicated antennas exist in the US, Germany and Italy. The Cassegrain antenna in Wettzell, Germany, uses a large dual frequency corrugated horn (*Whitington et al.* 1981). Front-fed antennas, such as the VLBI antenna in Westford, MA, USA, use a concentric dual frequency scalar horn design with choke rings.

The second category is antennas primarily built for radio astronomical research, temporarily reconfigured for geo-VLBI. Three examples are the 32-m antenna at the Medicina station, Italy, the Onsala 20-m antenna and the 26-m antenna at Hartebeesthoek, South Africa. Although Medicina is a Cassegrain antenna it uses the same sort of primary feed horn as Westford. By simply removing the subreflector, during geo-VLBI observations, the primary focus becomes available. The Onsala 20-m antenna and the 26-m Hartebeesthoek antenna is supplied with two different kind of feed systems. The present feed system at Onsala uses a large dual mode horn for X-band, located behind an offset parabolic reflector, used for S-band. The central part of the offset reflector is replaced by a dichroic surface, described later in this paper. Hartebeesthoek is supplied with a similar feed system.

Table 1 shows a few parameters, as of August 1991, for the above mentioned antennas.

TABLE 1. PERFORMANCE OF DIFFERENT GEO-VLBI ANTENNAS

Antenna	Diameter D [m]	Aperture Efficiency η_a[%]	System Temperature T_{sys} [K]	Effective Area A_{eff} [m^2]	Sensitivity SEFD [Jy]
		X-band			
Wettzell	20	55	45	173	718
Westford	18	50	55	127	1200
Medicina	32	45	110	362	846
Onsala	20	45	80	141	1562
Hartebeesthoek	26	22	220	117	5190
		S-band			
Wettzell	20	50	60	157	1054
Westford	18	55	55	140	1100
Medicina	32	45	110	362	846
Onsala	20	30	80	94	2343
Hartebeesthoek	26	21	53	112	1320

In the following chapters, new low budget feed systems for the 15-m SEST (Swedish-ESO Sub-millimeter Telescope) antenna and the Onsala 20-m antenna, will be described and evaluated.

2. NEW DUAL FREQUENCY FEED SYSTEMS FOR SEST AND ONSALA

High quality radio astronomical antennas used in the mm/submillimeter wavelength regime are mostly of Cassegrain type with a movable subreflector of low weight. The secondary focus cabin is typically crowded with quasioptics and front-end receiver equipment. The restrictions for low frequency operation are thus:

1. No prime focus operation
2. No extra equipment in the secondary focus cabin,

conditions which should be combined with the demand for

3. Fast and easy changeover from radio astronomical observations to geo-VLBI
4. Dual frequency operation
5. 10 % bandwith, and
6. Low cost.

The design shown in Figure 2.1 fullfills all these requirements. It takes advantage of the fact that the subreflectors of both the SEST antenna and the Onsala 20-m antenna are located in the near-field of a feed system at the geo-VLBI frequencies. As the phase center of the near-field is located behind the feed aperture, the optimum position of the feed is in front of the Cassegrain focus.

The system consists of two standard offset parabolic reflectors, one for each frequency, fed by horn antennas. The S-band reflector, 1.2 meter in diameter, is located in front of the smaller X-band reflector, 0.45 meter in diameter. The central part of the S-band reflector is therefore replaced with a dichroic surface, transparant for X-band and reflective for S-band signals.

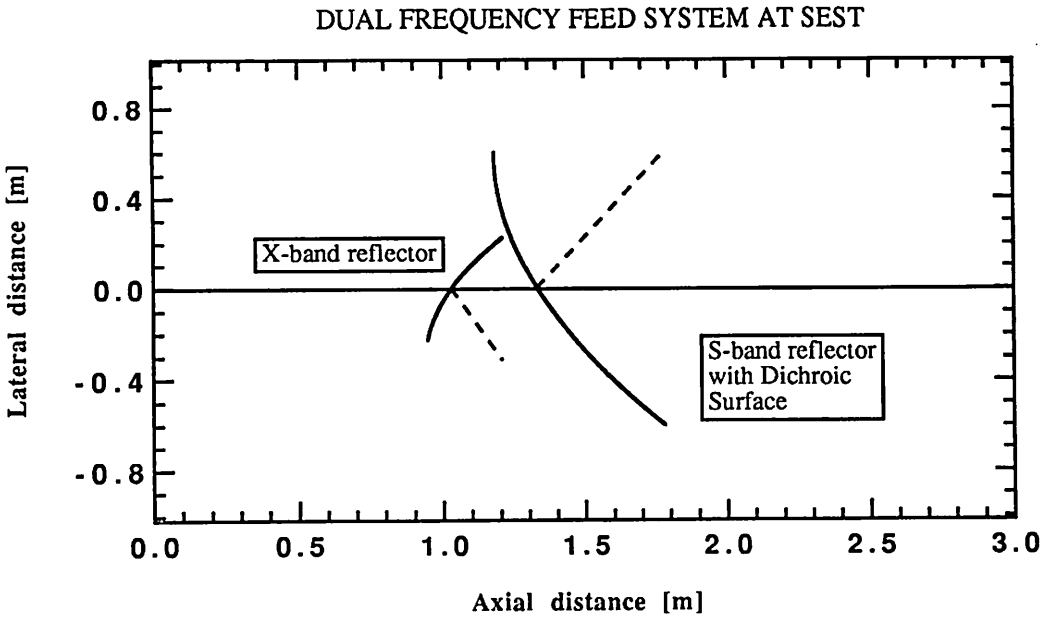

Figure 2.1 Dual frequency feed system at SEST.
The Cassegrain focus is located at (0.0) and the vertex of the main dish at (3.0).

This dichroic surface consists of crossed slots with a thin layer of plastic foam as a supporting sheet. See Figure 2.2.

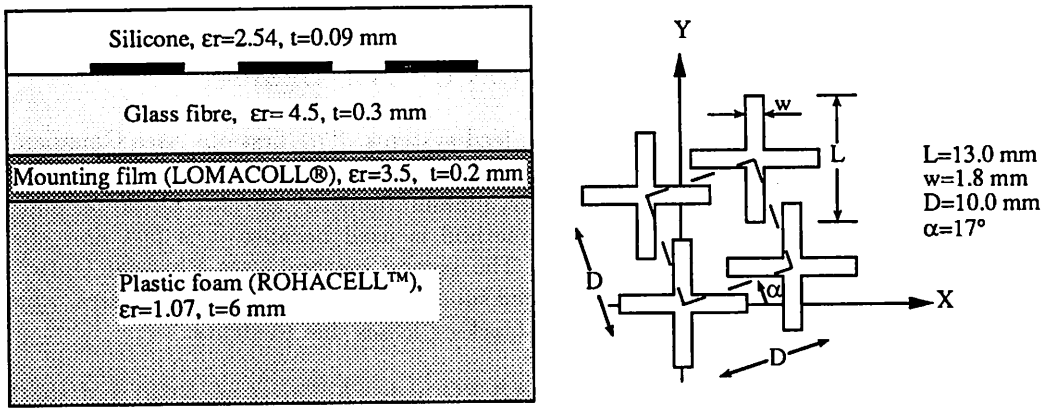

Figure 2.2 The layers (left) of the dichroic surface
using crossed slots (right) (from *Johansson* (1985)).

The surface is designed for a transmission band at 8.0-9.0 GHz and a reflection band at 2.05-2.65 GHz with an angle of incidence of 26.5° (see, *e.g.*, *Johansson* (1985)). The theoretical performance is shown in Figure 2.3.

For simplicity the dichroic surface is plane. Its diameter is fixed and given by the aperture diameter of the X-band reflector located behind. Since it is plane, rather than parabolic, it will introduce phase errors for the reflected field at S-band. However, one can minimize the resulting losses by placing the dichroic surface at the optimum axial position. The optimum position is mentioned in Chapter 4.

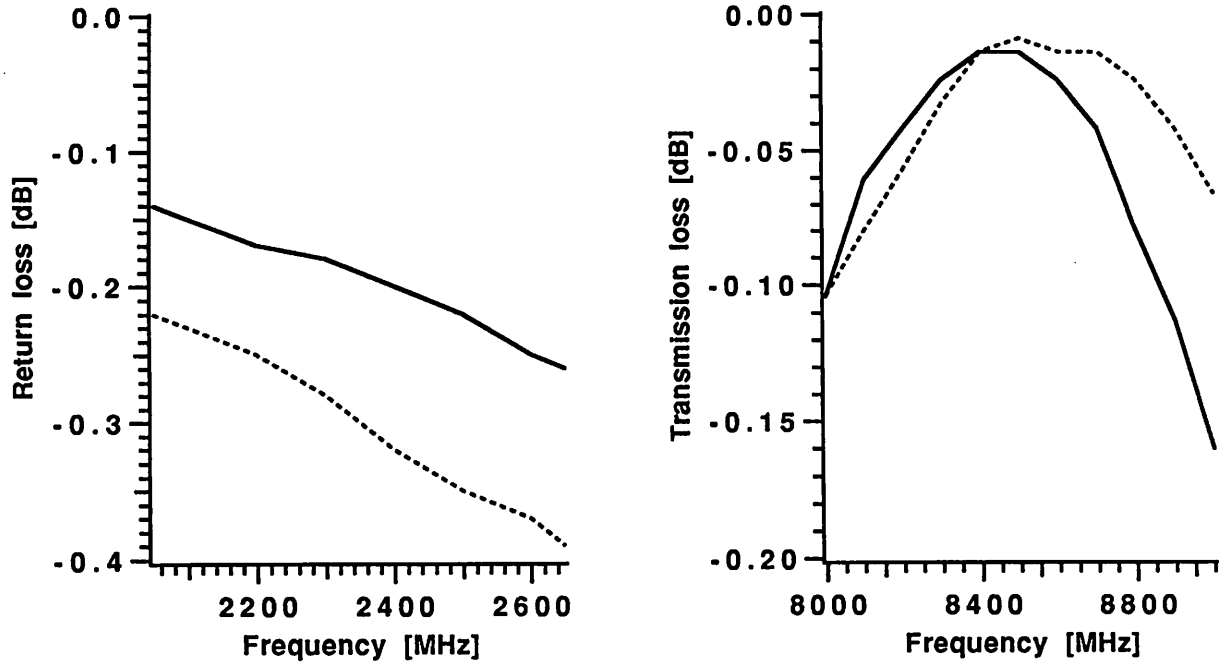

Figure 2.3 Theoretical performance of the dichroic surface. Reflection band to the left and transmission band to the right. Dashed line: TE-polarization, Solid line: TM-polarization.

3. THEORETICAL EVALUATION OF THE DESIGN

Two different methods have been used to analyze the feed systems. The first one uses Gaussian beam optics in order to calculate a first approximate feed configuration for optimum efficiency of the Cassegrain antenna. This method accounts for losses due to spillover, illumination, subreflector blocking, and phase errors (see, *e.g.*, *Saitto* (1981) and *Love* (1979)). The method is used because it is fast and gives the opportunity to test many different feed configurations. The second method uses Physical Optics (PO) integration and accounts, in addition to the above mentioned subefficiencies, for diffraction losses, which can be high at longer wavelengths, for polarization losses and blocking losses due to struts.

The software used for the PO integration is the ELAB PO code (*Kildal et al.* 1989) and the ELAB SAC code (Symmetrical Antenna Code), (*Kildal et al.* 1986), both developed at ELAB-RUNIT, Trondheim, Norway. The software has been implemented on a PC-AT. In order to fit the purposes of this project, some of the software have been modified. New software has also been developed, compatible with the PO and SAC code, by the author in cooperation with Per-Simon Kildal.

The SAC code calculates, among other things, the aperture efficiency of classical rotationally symmetric Cassegrain antennas with a hyperboloidal subreflector and paraboloidal main reflector. The input to the code is the incident co- and crosspolar radiation pattern for $\phi = 45°$ on the subreflector and can be found from the PO code. This means that only the radiation integral over the induced currents of the first reflector, *i.e.*, the reflector feed, has to be evaluated, whereas for the PO code, the radiation integral over the induced currents of all reflectors in the Cassegrain system has to be evaluated. This saves a lot of computer time.

The SAC code requires as input the far-field from the feed. In the case under study, the subreflector is in the near-field of the feed system, at S-band as well as at X-band. However, the SAC code will also work

properly by using an incident near-field, if this has the form of a far-field at the distance of the subreflector. In order to calculate the near-field radiation pattern from the reflector feed by PO integration, the PO code has to be extended, as the original PO code cannot do this. A limitation of the analysis method is that the SAC code cannot handle a possible beam squint, introduced by the reflector feed.

A complete analyze of the feed systems, together with a comparison of the above mentioned methods, will be given in a report, by the author, to be published this autumn. See also *Jaldehag* (1991). In the next chapter a few results will be given.

4. RESULTS FOR THE SEST ANTENNA AND THE ONSALA 20-m ANTENNA

The parameters describing the antenna configurations for the SEST antenna and the Onsala 20-m antenna are given in Table 2 below, where Θ_0 and ψ_0 are the subtended angles from the primary focus to the main reflector, and from the secondary focus to the subreflector, respectively.

TABLE 2. PARAMETERS FOR THE SEST ANTENNA AND THE ONSALA 20-M ANTENNA

	D_{main} [m]	d_{sub} [m]	Θ_0 [deg]	ψ_0 [deg]
SEST	15	1.5	75.1	5.6
Onsala	20	1.8	58.0	6.2

4.1 Theoretical and Measured Results at X-Band

Gaussian beam optics shows that edge taper values of -38 dB at SEST and -33 dB at Onsala, for the 0.45 meter X-band reflector, give the highest possible aperture efficiency. A corrugated horn which gives this illumination would, however, be too large. Instead a horn which gives an edge taper of -20 dB has to be used. This results in a degradation in aperture efficiency of about 0.5 dB compare to the highest possible value. By using these results in the PO and SAC code, it is shown that theoretical values of the total aperture efficiency can be as high as 59 % and 62 %, respectively, in spite of the poor illuminations. In the SEST case the measured efficiency is 50 %.

However, the dichroic surface together with the limited hole in the S-band reflector (in which the former one is attached) will introduce losses. Transmission losses through the dichroic surface is estimated to be less than 5 % over the complete band. Another degradation of the X-band performance is the diffraction and blocking losses due to the limited extent of the hole in the S-band reflector. The measured efficiency, with the complete feed system installed, is 40 % at SEST.

4.2 Theoretical and Measured Results at S-Band

Gaussian beam optics shows, for both the SEST antenna and the Onsala 20-m antenna, that an edge taper of -20 dB for the 1.2 meter S-band reflector gives the highest possible aperture efficiency. By using these results in the PO and SAC code it is shown that theoretical values of the total aperture efficiency can be 62 % for both the SEST antenna and the Onsala 20-m antenna.

Let us now include the plane dichroic surface but neglect the reflection losses at S-band of the surface. These are normally small, of the order of a few percent, for a good design and will therefore not be considered. However, the non-parabolic surface of the dichroic plate will introduce phase errors for the reflected field, which will degrade the aperture efficiency at S-band.

An estimate of the loss of gain due to these phase errors in the reflector aperture is obtained by means of Ruze formula (*Ruze* 1966)

$$\frac{G}{G_0} = \frac{\left| \int_0^{2\pi} \int_0^a f(r,\phi) e^{j\delta(r,\phi)} r dr d\phi \right|^2}{\left| \int_0^{2\pi} \int_0^a f(r,\phi) r dr d\phi \right|^2} \tag{4.1}$$

where G_0 is the gain without phase errors, G is the gain with an arbitrary phase error or abberation $\delta(r,\phi)$, a is the radius of the reflector, and $f(r,\phi)$ is the illumination function in terms of the aperture coordinates r,ϕ. The illumination function used is

$$f(r,\phi) = (1-r^2)^n \tag{4.2}$$

where the edge taper is determined by the value of n.

In *Jaldehag* (1991) this method, to calculate the loss of gain due to the plane dichroic surface, is compared with the results from the modified PO code. The methods show very good agreement.

The theoretical results for the total aperture efficiency with the dichroic surface fixed to the reflector are as low as 10 and 12 % for SEST and Onsala, respectively. However, by moving the dichroic surface to the position where the phase errors are minimized, which is about 2-3 cm behind the S-band reflector, the total aperture efficiency can be increased to 43 and 44 %, respectively.

Another way, in order to minimize the phase errors, is to make use of a parabolic shaped surface. The design and manufacturing of such a surface are, however, complicated and expensive. A compromise is to manufacture the dichroic surface in *several* plane parts, rather than one. This was done for the SEST feed system, resulting in a measured efficiency of 30 %. Another approach is of course to make use of a plane dichroic surface of less diameter. This requires, though, a smaller aperture of the X-band reflector.

5. PRELIMINARY RESULTS OF THE ESTIMATED BASELINE LENGTH BETWEEN SEST AND ONSALA

Figure 5.1 shows the first preliminary results of the estimated baseline length between the SEST antenna and the Onsala 20-m antenna (*Goddard Space Flight Center, Personal communications* 1990). The 24 hour long April experiment (X-GLOBAL) included three stations and the 48 hour long May experiment (GLOBAL) eight stations in USA, Japan, South Africa, Tasmania, Chile and Sweden. The different networks may explain the 7 cm difference in estimated baseline length. The quite high formal 1σ error can be explained by the fact that the effective area of the SEST antenna is small and due to a safety limit of 50° around the sun.

6. CONCLUSIONS

Two feed systems of similar configurations have been studied, one for the SEST antenna and one for the Onsala 20-m antenna. The one at SEST has been manufactured, tested and used at two different geo-VLBI experiments during spring 1990. The preliminary results from these experiments have been discussed.

The choise of a *plane* dichroic surface has shown to be more critical than expected. The losses at S-band due to the plane dichroic surface can, however, be minimized by moving it in axial direction. A few other approaches, in order to decrease these losses, have been discussed.

The conclusion is that feed systems of the type described in this report is a good low budget solution for simultaneous dual frequency observations. The calculations show that aperture efficiencies sufficiently good for geo-VLBI can be obtained. The measured results show a quite good agreement with the theoretical results.

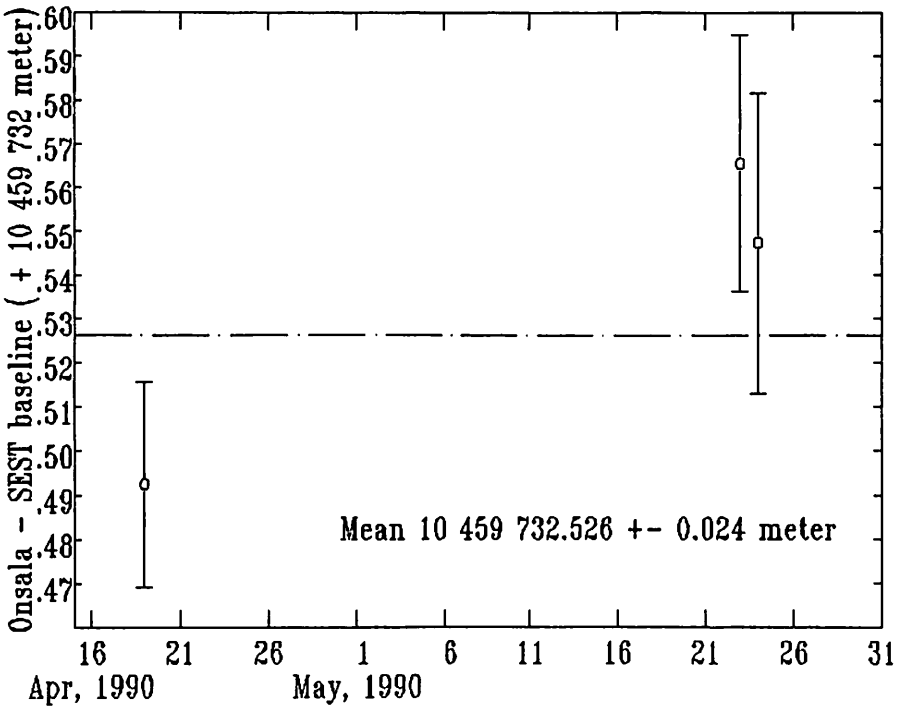

Figure 5.1 Preliminary estimations of the baseline length between SEST and Onsala.

ACKNOWLEDGEMENTS

I wish to thank my supervisor Bernt Rönnäng, who gave me the opportunity to work on this project, as well as Stefan Johansson and Per-Simon Kildal, at the Department of Network Theory, Chalmers University of Technology. Stefan for the design of the dichroic surfaces and Per-Simon for letting me use his antenna software.

REFERENCES

Jaldehag, K., Dual Frequency Feed Systems for Space Geodesy Radio Telescopes, *Proc. of Antenn 91, Gotland, Sweden*, pp. 199-207, 1991.

Johansson, F.S., Analysis and Design of Double-Layer Frequency Selective Surfaces, *IEE Proc. H*, **132**, pp. 319-325, 1985.

Kildal, P-S., Lier, E., Olsen, E., ELAB Symmetrical Antenna Code, *Project Memo*, Norwegian Institute of Technology, 1986.

Kildal, P-S., Kuhnle, J., Documentation of the ELAB PO-Code for Analysis of Reflector Antennas and Beam Waveguides by Phycical Optics Integration, *ESA/ESTEC Contract No. 8035/88/NL/PB*, 1989.

Love, A.W., Quadratic Phase Error Loss in Circular Apertures, *Electronics Letters*, **15**, pp. 276-277, 1979.

Ruze, J., Antenna Tolerance Theory - a Review, *Proc. IEEE*, **54**, pp. 633-640, 1966.

Saitto, A., Gain-Beamwidth Product and Other Reflector-Antenna Relationships, *ESA Journal*, **5**, pp. 249-258, 1981.

Whitington, J.R., Williams, W.F., A Common-Aperture S- and X-Band Four-Function Feedcone, *The 1981 Antenna Application Symposium, University of Illinois*, 1981.

IRIS-S Data Analysis at the Bonn Geodetic Institute

Axel Nothnagel
Geodetic Institute of the University of Bonn
Nussallee 17
D-5300 Bonn 1
Federal Republic of Germany

1. Introduction

Since December 1989 the IRIS-S network (International Radio Interferometric Surveying - South) has been scheduled in monthly intervals to observe polar motion, UT1, and nutation. The standard configuration of the IRIS-S network consists of five stations, i.e. Westford Observatory (Massachusetts, USA), Richmond Observatory (Florida, USA), Mojave Base Station (California, USA), Wetttzell Geodetic Fundamental Station (Bavaria, Federal Republic of Germany) and Hartebeesthoek Radio Astronomy Observatory (South Africa).

The VLBI data is being routinely correlated at the Mark III correlator of the Max-Planck-Institut für Radioastronomie in Bonn, FRG, by members of the VLBI group at the Geodetic Institute of the University of Bonn (GIUB). With 5 playback drives the Mark III correlator presently allows 10 baselines to be correlated simultaneously if the equipment operates smoothly. On average one week per month is used for geodetic correlation (Müskens, this Volume).

The geodetic VLBI data, i.e delays and delay rates, is subsequently analysed at the Geodetic Institute of the University of Bonn where earth orientation parameters are determined and submitted to the International Earth Rotation Service (IERS).

2. Data Analysis

The geometric time delay τ of a plane wave front of white noise arriving at two radio telescopes is to first order a function of the baseline vector $\mathbf{b}$ between the two telescopes and the unit vector in the direction of the radio source $\mathbf{k}$:

$$\tau = -\frac{1}{c}\mathbf{b}\,\mathbf{k} \qquad (1)$$

The negative sign reflects the conventions used in defining τ and $\mathbf{b}$. c is the velocity of light.

For practical reasons the baseline vector **b** is normally expressed in a three dimensional Cartesian coordinate system defined by a number of VLBI radio telescopes while the radio source positions form a quasi inertial reference frame in space at a certain epoch (J2000.0).

In order to express **b** and **k** in the same coordinate system a number of transformations are necessary (e.g. Ma, 1978). These can be applied to either vector. In a unified system eq. (1) is written as:

$$\tau = -\frac{1}{c} \boldsymbol{b}\, \boldsymbol{WSNP}\, \boldsymbol{k} \qquad (2)$$

where **W** is the rotation matrix for polar motion (wobble), **S** is the diurnal spin matrix, **N** is the nutation matrix and **P** is the precession matrix. Any parameters in equation (2) or combination of parameters can be determined depending on the configuration of the VLBI experiment.

The data collected at the Geodetic Institute up to the end of 1990 consists of 12 sessions in monthly intervals. These data sets alone are not sufficient to determine terrestrial and celestial reference frames with adequate accuracies. Therefore, we have chosen to use the results of the global VLBI solution GLB627 (= GSFC 90 R 01) of the VLBI group at the NASA Goddard Space Flight Center which contains all Mark III S/X experiments from 1979 to December 1989 (Ma et al., 1990).

The list of station positions of GLB627 includes continental drift parameters dx/dt, dy/dt, dz/dt for each station which permit the computation of station coordinates for each of the IRIS-S observing dates. The radio source positions are identical to RSC(GSFC) 90 R 01.

All sessions of the IRIS-S campaign are individually reduced using the CALC 7.0/SOLVE software system (Ryan, 1989) which is based on the MERIT standards (Melbourne et al., 1983) and which is consistent with the IAU (1976) Resolution on Astronomical Constants, Time Scales and the Fundamental Reference Frame (Kaplan, 1981). The theoretical delays in the adjustment are calculated according to the Shapiro model (Ryan, 1989) and Hellings (1986) correction for relativistic bending. Horizontal and vertical ocean loading displacement effects Scherneck (1991) are applied to the delay observables. For the tropospheric corrections we use the CfA model (Davis et al., 1985) based on surface meteorological data. The ionospheric refraction is dispersive and can therefore be calibrated by dual frequency observations. Only group delay observables are used in our analyses.

In the least squares adjustments the two polar motion components x_p, y_p, Universal time UT1 - TAI and two nutation offsets ($d\psi$, $d\varepsilon$) relative to the IAU 1980 Theory of Nutation (Wahr, 1981) are estimated as principal parameters. In addition, atmospheric excess path delays in zenith direction and their rates as well as relative offsets, rates and higher order terms of the atomic clocks have to be estimated.

In an attempt to keep the number of unknown parameters at a reasonable level, the parametrisation for the atmospheric excess path delay is chosen to follow the real behaviour of the atmosphere as closely as possible. The only indications of variations are changes in the refraction calculated for the dry and wet component of the atmosphere determined from surface meteorological data, i.e. pressure, relative humidity and temperature. Figures 1 and 2 display the variations in the dry and wet refractivity components of the station HartRAO. The initial parametrization consists of one offset and one rate parameter for the atmospheric excess path delay for each station at the beginning of the experiment. When the refractive behaviour of the atmosphere at one station indicates a significant change, additional rate parameters are introduced starting from the epoch of the change. The arrows in the figures indicate epochs where rate changes are introduced. This method, however, does not account for possible time lags due to advanced or delayed air mass movements at greater heights.

The behaviour of the atomic clocks of the stations are modelled using one initial set of relative offsets, rates and second order terms per station except of one reference station. Additional parameters for modeling the clock behaviour are chosen depending on obvious deviations in the residuals.

The formal errors of the pole coordinates are based on observation weights adjusted so that the Chi-square per degree of freedom ratio

$$\chi^2 = \frac{\sum pvv}{n - u} \qquad (3)$$

is close to unity (p = observation weights, v = post fit residuals, n = number of observations, u = number of unknown parameters). These contributions to the a priori variances should account for unmodelled effects in the data reduction (Herring et al., 1986).

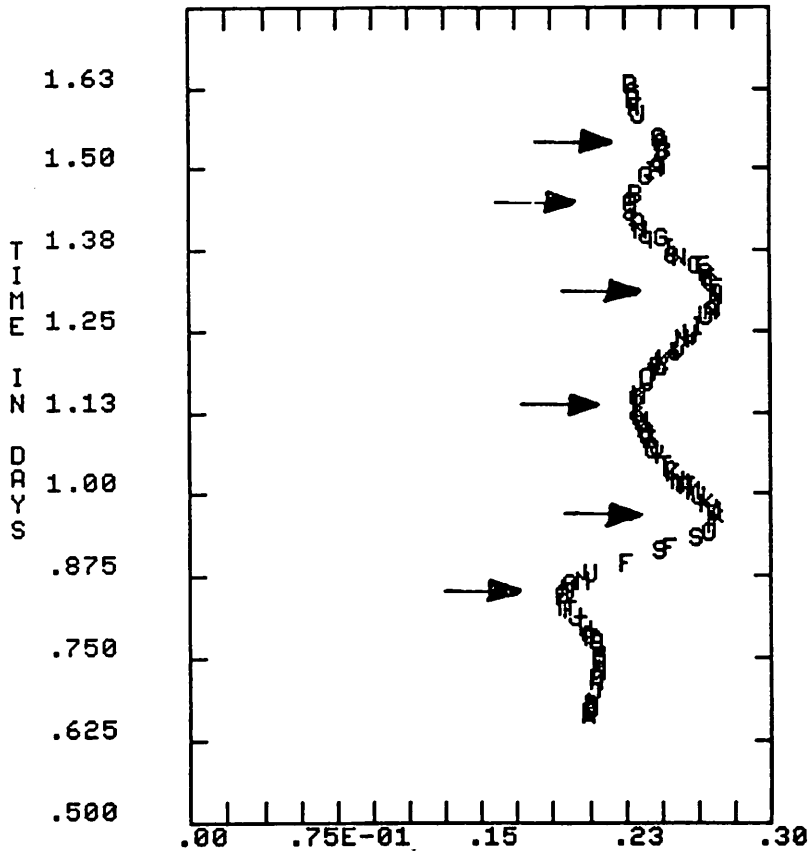

Fig. 1., Wet component at zenith for HartRAO (CfA model) in nsec

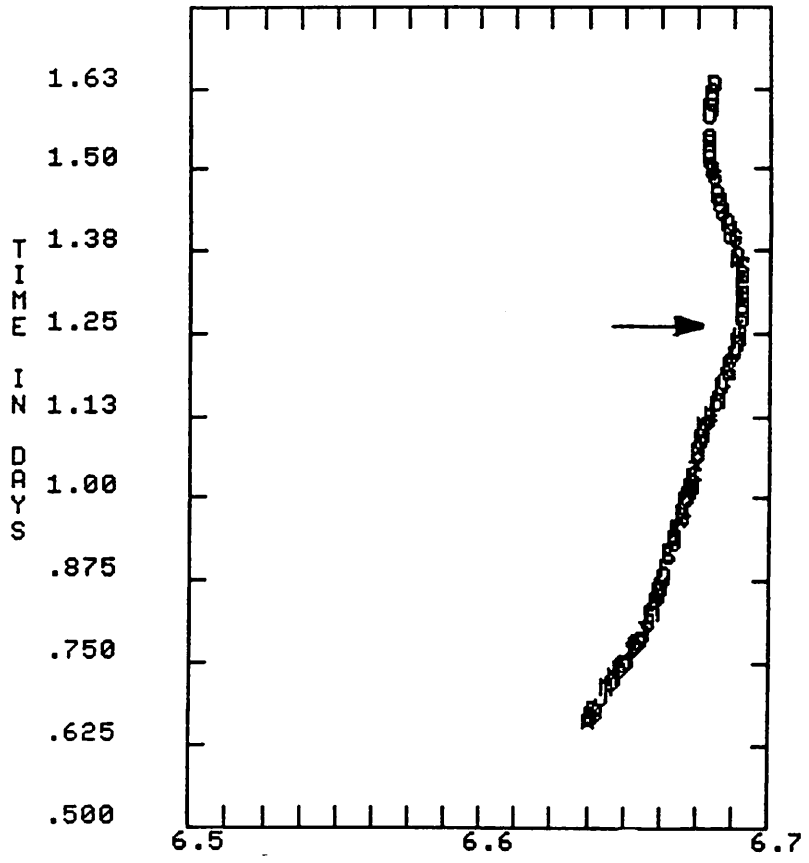

Fig. 2., Dry component at zenith for HartRAO (CfA model) in nsec

3. Results

The average formal errors of the IRIS-S experiments are listed in Table 1 together with average formal errors of the IRIS-A experiments of 1990. Owing to the network geometry with the improved north-south extension, the x and y component of the pole and the two nutation offsets show considerably smaller standard deviations in the IRIS-S experiments as compared to the IRIS-A sessions. Only the UT1 - TAI parameter is better determined with the IRIS-A network. The reason is that in the IRIS-A sessions more observations are scheduled on the east-west baselines which are particularly sensitive to changes in UT1.

EOP	IRIS-S Av. F.E.	IRIS-A Av. F.E.	GIUB - IERS RMS
x_p	0.25 mas	0.27 mas	1.02 mas
y_p	0.16 mas	0.28 mas	0.74 mas
UT1	0.015 ms	0.013 ms	0.062 ms
$d\psi$	0.34 mas	0.58 mas	0.60 mas
$d\varepsilon$	0.15 mas	0.21 mas	0.63 mas

Table 1, Average formal errors of IRIS-S and IRIS-A experiments and RMS differences between IERS evaluation and GIUB solutions

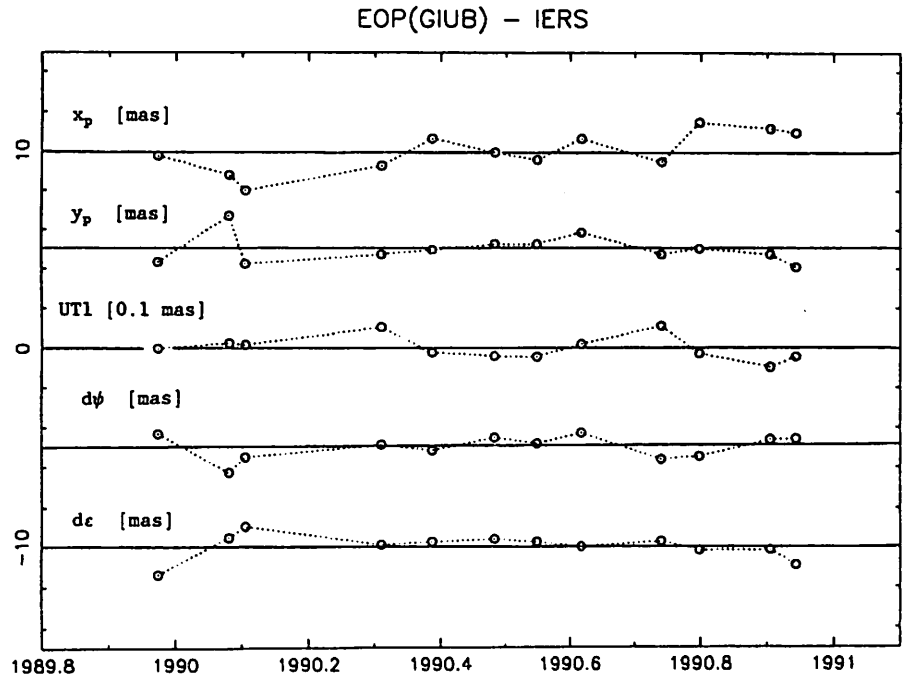

Fig. 3, Differences between GIUB and IERS evaluation after an offset and a linear trend were removed

The accuracy of the IRIS-S series can best be demonstrated displaying a comparison with a preliminary annual evaluation of the International Earth Rotation Service (IERS). Figure 3 depicts the differences in the EOP between the evaluation of the IERS and GIUB after an offset and a linear trend are removed. Offset and trend originate from the different celestial and terrestrial reference frames used in the analyses. The RMS differences are listed in Table 1.

The number of sessions analysed is still comparably small and a single outlier does affect the overall results. Special attention will be given to the sessions with larger deviations, for example the January 1990 session, in order to investigate the reasons for the differences. Nevertheless, the RMS differences between the two series show very good agreement and may be improved even further. Right now a study is underway which should provide some information about the backgrounds of the offsets and trends between the IRIS-S and other EOP series.

References

Davis, J.L. et al., Radio Science, 20, p. 1593; 1985
Hellings, R.W., Astron. J., 91, 1446, 1986
Herring, T.A. et al., JGR, 91, No. B8, p. 8341, 1986
Kaplan, G.H., USNO Circular No. 163; Washington D.C.; 1981
Ma, C., Ph.D. Thesis; NASA Technical Memorandum 79582; Greenbelt, USA, 1978
Ma et al., IERS Technical Note 5, Paris 1990
Melbourne, W. et al., USNO Circular No. 167, Washington D.C., 1983
Ryan J.W., CALC-7 Release Document, GSFC, 1989
Scherneck H.G., A Parameterised Solid Earth Tide Model and Tide Loading Effects for Global Geodetic Baseline Measurements, accepted by Geophys. Journ. Int., 1991
Wahr, J.M., Geoph. Journ. of Royal Astron. Society, 64, p. 705, 1981

PRELIMINARY RESULTS OF THE 1989 MOBILE VLBI

EUROPEAN CAMPAIGN

N.REBAI : IGN 2 avenue Pasteur 94160 Saint-Mandé
G.PETIT : BIPM Pavillon de Breteuil 92312 Sèvres Cedex

8th Woorking Meeting on European VLBI for Geodesy and Astrometry Dwingeloo 13-14 June 19991

A mobile VLBI campaign was done in Europe in 1989 with the goal of establishing a high precision geodetic network. Once established, this network will be used as a fiducial network for other studies (geodynamics, oceanography...) and for the determination of a global terrestrial reference system. The experiment uses the current standard of geodetic VLBI technique (acquisition system MARKIII, double frequency receiver S and X with Hydrogen maser clock). This VLBI system allows to obtain in one day of observations a geodetic precision of a few centimeters on the baseline components between antennas. The data lasts 26 days, staggered on four months, with four to five days of observations by station. This experiment includes nine IRIS sessions.

The VLBI data processing includes three steps. Correlation of the data recorded on tapes, determination of delays and delay rates (measured quantities), adjustment of geometric parameters (the vector joining the two radio-telescopes) to the mesured quantities.

The first two stages have been done by the US National Geodetic Survey who gave us the VLBI measures. We use the VLBI adjustment software MODEST of "Jet Propulsion Laboratory".

The data analysis requires a preliminary study adjustment, during which we estimate the troposphere and clock, session by session, while excluding bad observations. The only parameters determined are, for each station, excepting WETTZELL taken as reference, the geodetic coordinates, with a vertical tropospheric delay and an average of two to four linear segments representing the clocks. All the other parameters of a priori models have been fixed.

A first global solution has been produced with all the stations coordinates, a vertical troposphere delay by session and by station and the same segments of clocks as in the preliminary treatment.

The residuals after adjustment of the model on the measures have a normal distribution and a quadratic average of 100 ps for the delays and 70 fs/s for the delay rates. The comparison of coordinates determined by our global solution with the ITRF90 solution of the IERS allows us to conclude on the precision of our results to be about 2 cm (1σ) on the station coordinates.

The 1989 mobile VLBI european campaign

Common effort of	Germany	Hohenbuenstorf	21–26 Jun
	Finland	Metsahovi	5–11 Jul
	Norway	Tromso	30 Jul–2 Aug
	UK	Carnoustie	18–22 Aug
	France	Brest	30 Aug–4 Sep
		Grasse	12–16 Sep

4–5 days of observations at each station.
Total of 26 days, including 9 IRIS sessions.
"Fixed" VLBI stations: Wettzell, Noto, Onsala, Westford, Richmond, Mojave.

Characteristics of the VLBI solution

Software

MODEST from JPL.
Clock and tropospheric parameters estimated over a given interval.

A priori model

Station coordinates: ITRF89 system
Solid Earth tides: Quadrupole response, K1 correction
Ocean loading: Turned off
Antenna terms: Axis offset from station info

Source coordinates: IERS Celestial Reference Frame
Source structure: none

Earth orientation: IAU precession and nutation
UT1, polar motion, celestial pole offsets from IERS

Troposphere: Vertical delay from Saastamoinen model
Lanyi mapping function

Relativity gamma: 1.

Preliminary analysis

One session at a time.

Wettzell reference station (x, y, z, clock)

Solve for: station coordinates
1 troposphere vertical delay
2–4 linear segments (clock)

RMS of residuals (typical): 100 ps
70 fs/s

Repeatability of 1–day solutions:

Station	#days	RMS (mm) East	North	Vertical
Hohen.	5	5	5	22
Metsahovi	5	14	18	86
Tromso	4	14	20	47
Carnoustie	4	3	5	56
Brest	4	16	4	86
Grasse	4	10	6	56

Test global consistency
Solve for : (All) station coordinates
1 troposphere vertical delay/day/st.
Clock parameters (same intervals as preliminary solutions)

- Comparaison of the solution with ITRF 90
- Parameters transformation and standard deviation.

	Seven parameters of transformation between the two sets						
	TRANSLATION (m)			SCALE	ROTATION (mas)		
DESIGNATION	TX SIGMA TX	TY SIGMA TY	TZ SIGMA TZ	D(10^{-8}) SIGMA D	RX SIGMA RX	RY SIGMA RY	RZ SIGMA RZ
VLBI MOBILE	0.124 0.025	0.032 0.018	0.054 0.020	-2.18 0.20	0.90 0.80	0.10 0.10	-1.8 0.5
ITRF 90 SIGMA NORMAL	0.000 0.000	0.000 0.000	0.000 0.000	0.000 0.000	0.000 0.000	0.000 0.000	0.000 0.000

Agreement at the level of 2 cm
Largest residual : Brest vertical 5 cm

Analysis of Recent European VLBI Experiments

Hayo Hase
Geodätisches Institut der Universität Bonn
Nußallee 17, D-5300 Bonn 1

Vincenza Tornatore
Istituto di Radioastronomia - Consiglio Nazionale delle Ricerche
Via Irnerio 46, I-40126 Bologna

Abstract: Following the December 1990 earthquake near Noto (Sicily), a preliminary analysis of the European VLBI-experiment was carried out in order to find possible earthquake-related displacements. So far, no significant baseline changes could be detected, but baseline repeatability of 1 cm confirms the accuracy level of European experiments.

1 Introduction

During the last three years the number of European VLBI stations increased from two (Wettzell, Onsala) to six (Medicina, Madrid, Noto, Matera), Campbell [1989]. The observations in the expanded European VLBI network began with the East-Atlantic experiments of the NASA Crustal Dynamics Project (CDP) in 1988 and 1989, in which the US stations Westford and Richmond still took part. Since 1990 a pure European VLBI network consisting of the six station mentioned above is being observed. This series is called EUROPE. Today the data of the observation period of almost three years is available.
For the comparison of the results we have to introduce a common reference system and the same strategy of post-processing should be used. For this presentation we focussed our attention on experiments containing baselines to Noto station because of the occurence of an earthquake close to Noto on December 12th, 1990. In addition we used some IRIS-A experiments in which Noto took part as tagged along station.
For this presentation a short overview of the results concerning the baselines to Noto is given. (Results of the European network are in preparation.)
The Mediterranean area is a tectonically instable region, as shown by its seismicity and vulcanism. This area represents the zone of collision between the Eurasian and the African Plate. According to some geodynamic modellings this area is subdivided in several microplates, Geis, Drewes [1987], Campbell [1987]. A model based on the study of Besse et al. [1984] shows a northward motion of the Sicilian plate; while the model by Jongsma et al. [1987] shows an eastward motion. In this scenario Noto station appears to be situated on the Sicilian Plate.

2 Data Analysis

2.1 Experiments with Noto

The following table gives an overview of the experiments that have been processed in this analysis.

Experiment	Name	Stations WETT-ONSA-MEDI-MADR-NOTO-MATE WEST-RICH-MOJA
@89JUN03	E.ATL-2	WETT-ONSA- MADR-NOTO WEST
@89JUN21XE	IRIS-A	WETT- NOTO WEST-RICH-MOJA
@89JUN26XE	IRIS-A	WETT- NOTO WEST-RICH-MOJA
@89AUG30XE	IRIS-A	WETT- NOTO WEST-RICH-MOJA
@89SEP04	IRIS-A	WETT-ONSA- NOTO WEST- MOJA
@89SEP29	IRIS-A	WETT- NOTO WEST-RICH-MOJA
@90JAN26XG	EUROPE-1	WETT-ONSA-MEDI-MADR-NOTO
@90SEP05XA	EUROPE-2	WETT-ONSA-MEDI-MADR-NOTO-MATE
@90DEC18XT	IRIS-A	WETT-ONSA- NOTO WEST-RICH-MOJA
@90DEC20XA	EUROPE-3	WETT-ONSA-MEDI-MADR-NOTO-MATE

2.2 Data Analysis

The correlation was done at Washington and Bonn. The geodetic software used was CALC 7.0 and SOLVE for standard Mark III experiments. The software runs on the HP 1000-F of the Geodetic Institute.

In the SOLVE program we followed two principles for the parametrization:

1. Use of significant parameters for modelling the reality during observation.
2. Use of consistent reference systems for a priori values.

In the procedure to realize the principles we followed six steps:

1. Consistent systems are derived from the CDP global solution 627. The corresponding changes were made with the mapping functions for stations, sources, earth orientation and nutation parameters.
2. The translations of the coordinate system were fixed at Wettzell as reference station. The rotations were fixed in the the IRIS experiments using Westford and Richmond or Mojave, in the EUROPE experiments using the IRIS earth orientation parameters.
3. For the calibration of the atmosphere we used the CfA model. The atmosphere parameters were introduced according to the local weather conditions.
4. The clock behaviour was modelled by visual inspection of the residual plots.
5. We examined outlyers for low elevation (stronger influenced by the atmosphere), signal to noise ratio and the quality factor of the correlation process.
6. The baselines were reweighted.

As results we obtained the coordinates of the new stations and sometimes in addition coordinates of those sources that did not form part of the standard catalog.

2.3 Results

The following tables give an overview of the baseline lenghts and their errors. The EUROPE-2 and EUROPE-3 experiment of 1990 were split into two 12hour-experiments because of the limitation of the capacity of the HP 1000-F. (In these experiments short scans were used, which means more than 3000 observations in 24 hours.)

Experiment	Name	Stations WETT-ONSA-MEDI-MADR-NOTO-MATE WEST-RICH-MOJA	Observations Total	Used	Number of Parameter	WRMS [ps]
@89JUN03	E.ATL-2	WETT-ONSA- MADR-NOTO WEST	863	725	54	44
@89JUN21XE	IRIS-A	WETT- NOTO WEST-RICH-MOJA	540	467	106	52
@89JUN26XE	IRIS-A	WETT- NOTO WEST-RICH-MOJA	602	553	76	67
@89AUG30XE	IRIS-A	WETT- NOTO WEST-RICH-MOJA	511	420	65	101
@89SEP04	IRIS-A	WETT-ONSA- NOTO WEST- MOJA	604	462	60	58
@89SEP29	IRIS-A	WETT- NOTO WEST-RICH-MOJA	750	532	55	57
@90JAN26XG	EUROPE-1	WETT-ONSA-MEDI-MADR-NOTO	1664	1531	70	64
@90SEP05XA	EUROPE-2	WETT-ONSA-MEDI-MADR-NOTO-MATE	1790	1486	64	69
@90SEP06XA	EUROPE-2	WETT-ONSA-MEDI-MADR-NOTO-MATE	1683	1392	79	70
@90DEC18XT	IRIS-A	WETT-ONSA- NOTO WEST-RICH-MOJA	1398	1321	64	67
@90DEC20XA	EUROPE-3	WETT-ONSA-MEDI-MADR-NOTO-MATE	1641	1079	75	50
@90DEC20XB	EUROPE-3	WETT-ONSA-MEDI-MADR-NOTO-MATE	1490	1097	68	63

Experiment	Name	Wettzell - Noto 1371100,000 [m]	Onsala - Noto 2280150,000 [m]	Madrid - Noto 1711830,000 [m]	Medicina - Noto 893720,000 [m]	Matera - Noto 444530,000 [m]
89JUN03	E.ATL-2	+1,056 ± 0,003	+4,885 ± 0,003	+2,917 ± 0,003		
89JUN21XE	IRIS-A	+1,058 ± 0,004				
89JUN26XE	IRIS-A	+1,062 ± 0,006				
89AUG30XE	IRIS-A	+1,055 ± 0,006				
89SEP04	IRIS-A	+1,056 ± 0,004	+4,898 ± 0,005			
89SEP29	IRIS-A	+1,067 ± 0,004				
90JAN26XG	EUROPE-1	+1,056 ± 0,002	+4,876 ± 0,003	+2,908 ± 0,002	+4,232 ± 0,002	
90SEP05XA	EUROPE-2	+1,043 ± 0,003	+4,874 ± 0,003	+2,908 ± 0,003	+4,221 ± 0,002	+2,979 ± 0,003
90SEP06XA	EUROPE-2	+1,050 ± 0,003	+4,877 ± 0,003	+2,900 ± 0,003	+4,227 ± 0,003	+2,992 ± 0,003
90DEC12	Mag. 5.1 earthquake at 37.2°N, 15.2°E, depth 10 km					
90DEC18XT	IRIS-A	+1,035 ± 0,005	+4,856 ± 0,006			
90DEC20XA	EUROPE-3	+1,053 ± 0,003	+4,885 ± 0,003	+2,908 ± 0,003	+4,221 ± 0,002	+2,983 ± 0,003
90DEC20XB	EUROPE-3	+1,046 ± 0,003	+4,896 ± 0,003	+2,911 ± 0,003	+4,222 ± 0,002	+2,980 ± 0,003

Although the number of experiments on the European baselines is still rather small, it is possible in some cases to see first signs of a trend in the length evolution, but no estimates shall be given at this stage of the analysis.
As a good example a plot of the baseline Wettzell-Noto which contains 10 experiments over a time span of nearly two years is shown below.

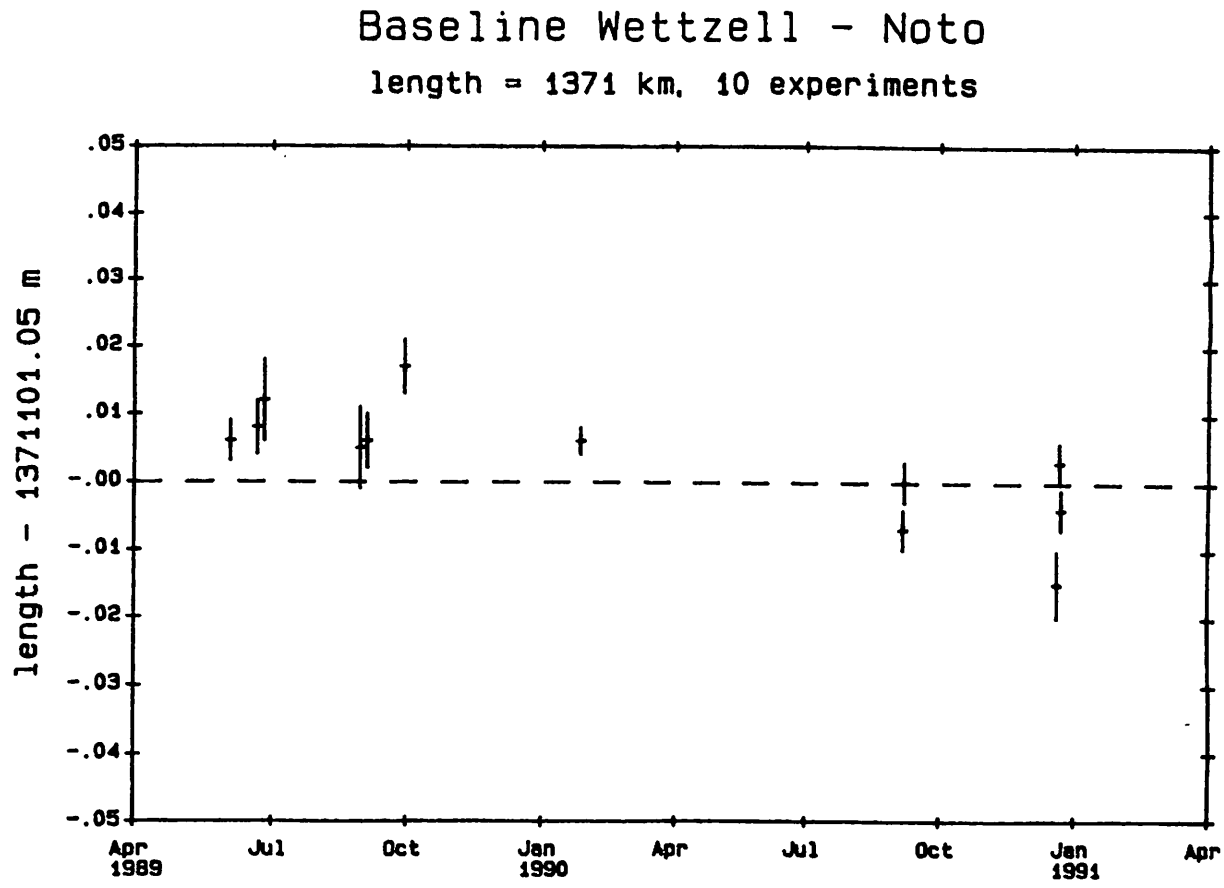

The WRMS scatter about the mean is ± 9 mm, which shows an excellent baseline repeatibility over a distance of 1371 km. There is at present no sign of any significant earthquake-related displacement at 1cm-level. A refined analysis with more experiments to come will have the potential to reveal even smaller displacements.

3 Acknowledgement

The authors would like to thank in particular the Consiglio Nazionale delle Ricerche (Institute for Radioastronomy in Bologna) which has actively supported this work.

4 References

Besse, J., Pozzi, J.P., Masche, G., Feinberg, H.: Paleomagnetic Study of Sicily: Consequences for the Deformation of Italian and African Margins Over the Last 100 Million Years. Earth Planet Sci. Lett. (67) 377-390, 1984

Campbell, J.: European VLBI for Geodynamic, Proc. of the 3rd intern. conf. on the WEGENER/MEDLAS project, 361-374, Bologna, 1987

Campbell, J.: Status Report on Global and European Geodetic VLBI, Proc. of the 7th work. meet. on European VLBI for Geodesy and Astrometry, 1-7, Madrid, 1989

Geiß, E., Drewes, H.: The Calbrian Arc Project and its Application for Continuum Mechanics Modelling, Proc. of the 3rd intern. conf. on the WEGENER/MEDLAS project, 147-179, Bologna, 1987

Jongsma, D., Woodside, J.M., King, G.C.P., van Hinte, J.E.: The Medina Wrench: a key to the kinematics of central and eastern Mediterranean over the past 5 Ma. Earth Planet Sci. Lett. (82), 87-106, 1987

Tomasi, P.: VLBI in Southern Europe, Proc. of the 7th work. meet. on European VLBI for Geodesy and Astrometry, 39-42, Madrid, 1989

SESSION 3

astrometry

VLBI OBSERVATIONS OF MILLISECOND PULSARS

G. Petit, BIPM, 92312 Sèvres CEDEX, France
J-F. Lestrade, Obs. Meudon/DERAD, 92195 Meudon CEDEX, France
T. Fayard, CNES, 18 Av Ed. Belin, 31055 Toulouse, France
A. Rius, IAG (CSIC-UCM), 28040 Madrid, Spain

ABSTRACT

Millisecond pulsars provide a direct way to link the extragalactic celestial reference frame with the dynamical reference frame of the solar system, by comparing astrometric positions obtained with VLBI and timing observations. We present an observing and processing procedure to obtain VLBI positions of millisecond pulsars, and preliminary results of a first experiment designed to validate the method.

1. INTRODUCTION

Linking to one another the different realizations of celestial reference systems is a major task of present astrometry. A survey of this field can be found in [Dickey 1989]. In this respect, millisecond pulsars can be used to provide a direct link between the extragalactic reference frame of the quasars, observed by VLBI, and the dynamical frame of the Solar System. Indeed timing observations provide the astrometric position of the pulsars in the latter frame with sub-milliarcsecond precision. VLBI observations of the pulsars could provide milliarcsecond VLBI positions in the former frame thus the link would be determined provided several pulsars, well distributed over the sky, can be observed.

Noting that the signals from millisecond pulsars are regularly spaced in time and dispersed by the interstellar medium, it is possible to gain significant Signal to Noise Ratio (SNR) by gating and dedispersing the VLBI data before correlation [Petit et al. 1990]. Noting that the Phase Reference Tracking (PRT) technique allows to obtain VLBI position of even very weak objects relative to a reference [Lestrade et al. 1990], we started a project whose goal is to obtain VLBI positions of millisecond pulsars relative to nearby quasars. A system is being developed that will allow to gate, dedisperse and correlate VLBI data. It is initially based on the MarkII acquisition system, but could be adapted to other systems in the future.

A first experiment in March 1990 has acquired MarkII data on PSR1937+214 and two nearby quasars. We report here preliminary results based on the quasar data that allow to validate the processing scheme and observation procedure.

2. KEY POINTS OF THE PROCESSING

The basic observation scheme is to acquire data alternately on the reference source and on the program source (here the pulsar). The PRT technique gives a position accuracy that is basically proportional to the uncertainty on the phase difference (program minus reference) of one observation, and inversely proportional to the (square root of the) number of observations for which the reference phase can be unambiguously connected. The procedure must thus fulfill two goals: Allow to connect unambiguously the reference phase and minimize the uncertainty on the phase difference.

The first point is mainly related to the knowledge of the physical model: The best it is known, the farthest apart the phase connection can be realized. We will assume observations at 1.6 GHz (1 cycle = 0.6 ns, 1 cycle/10 min = 10^{-12}), with baselines not exceeding 2000 km and H-masers clocks at the stations. In these conditions, the errors due to the geometry and to the clock random behavior can be neglected for intervals of up to 15-30 minutes. The limitations will be from the troposphere and mainly from the ionosphere.

The uncertainty on the phase difference contains two parts: The measurement noise and the error in the model of the phase difference. The first part is linked to the SNR while the second is, again, a problem of propagation linked to the spatial separation of the reference and program sources and to the separation in time of the observations.

In the following section, we will address these points, using the quasar observations of our preliminary experiment.

3. PHASE-REFERENCED TRACKING QUASAR-QUASAR

The experiment included the 100-meter antenna at Effelsberg, the 70-meter DSS63 antenna near Madrid and the 34-meter antenna at Medicina. The observing sequence was 10 to 10.5 minutes long with 3-minute scans on two quasars (1923+210 and 1929+226) and on PSR1937+214. 1929+226 is a quasar which has been identified for this experiment and whose precise position is not known. As a test of the procedure, we will determine its position with respect to 1923+210 using PRT.

3.1. Phase connection

For each baseline, we try to connect the residual phases of the consecutive scans on 1923+210 using the residual phase rates for each scan. We do not describe here the exact algorithm that is used, but just want to enhance the main result: Although it cannot be proved at this stage that the connection is correct or not (this can be done in the next step, in our case where the program source is strong), it is clear that, under moderate ionospheric conditions (i.e. until some time between 9H and 10H UT), the connection can be performed adequately over a 10-minute interval (Figure 1).

3.2. Estimation of the phase difference

After connection, the residual phase of the reference is estimated at the times of observation of the program source, and a total reference phase is reconstructed by adding back the correlator model. The total phase of the program source is also computed and the differenced total phases are formed.

The PRT technique does not require that these differenced phases are connected but, as the program source (1929+226) was powerful enough, it was possible to obtain connected differenced phases. One check was then to form the closure phase for the times where the three stations were recording simultaneously (unfortunately only 1.5 hour). Figure 2 shows that the closure condition is fulfilled with uncertainties of 0.04 cycle for the phases and 0.9 mHz for the rates.

It should be noted that this merely checks the quality of the phase connection: Large biases (from propagation) could remain in the differenced phases on each baselines, which would bias the astrometric solution without showing up in the closure.

3.3. PRT position of the new quasar

We then estimate the differenced propagation phase (troposphere from in situ meteorological measurements and ionosphere from GPS dual frequency measurements at Madrid and Paris). We substract it from the differenced total phase to obtain estimates of the differenced geometrical phase, which are input to the mapping routine [x]. Figure 3 is an example of dirty map obtained from this data. We can make the following comments:

*The dynamic is not so good, with a second peak at about 70% of the main. This is due to a weak geometry after the loss of some data. However, in similar configurations, the a-priori position of the pulsar (obtained from the timing position) should be good enough to discriminate the peak.

*The RMS of the phase residuals is at the level of 0.16 cycle which is much more than expected from system noise for those two quasars. Thus the main source of error is the ionosphere, and it should be about the same for the pair quasar-pulsar.

*Propagation mismodelling can cause a large bias in the astrometric position. For example when it is assumed that ionosphere has no effect (figure 4), the obtained position differs by more than 50 mas from that with an estimation for ionosphere (figure 3). This stresses the importance of minimizing the ionospheric error.

4. CONCLUSIONS

A 1.6 GHz MarkII Phase Reference Tracking experiment has been conducted. Preliminary analysis of the data provides the following indications:

*It is possible to connect the reference phases up to 10 minutes apart under moderate ionospheric conditions, thus allowing to spend about 60% of the time on the program source.

*The uncertainty on the position will probably be limited by the ionosphere, if system noise phase error is lower than 0.1 cycle. For a 12-hour experiment with 3 baselines of the order of 1000 km, it will result in a position uncertainty of a few mas.

*Ionospheric error being probably the limiting factor on the position accuracy, one possibility is to measure the ionospheric effect at the stations, for example with dual frequency GPS receivers. Another approach would be to have two or more reference sources in order to more closely monitor the phase variations due to ionosphere fluctuations in space and time.

5. ACKNOLEDGEMENTS

We thank the staff at each observatory (Effelsberg, DSS63, Medicina) who participated in the experiment. We are indebted to Dr D. Graham and Dr W. Sherwood (MPIfR) for fringe search and correlation of the data.

6. REFERENCES

Dickey, J.O.: 1989, in Reference Frames in Astronomy and Geophysics, J. Kovalevsky, I.I. Mueller, B. Kolaczek eds, Kluwer Academic Pub. p.305

Lestrade, J-F., Rogers, A.E.E., Whitney, A.R., Niell, A.E., Phillips, R.B., Preston, R.A.: 1990, A. J. 99, 1663

Petit,G., Fayard, T.,Lestrade, J-F.: 1990, Astron. Astrophys. 231, 581

FIGURE CAPTIONS

Figure 1: Connected residual phases for the quasar 1923+210 on the baseline Effelsberg-Medicina. The segment at each point indicates the phase rate.

Figure 2: Sum of the phase differences (1929+226 minus 1923+210) for the triangle Effelsberg-DSS63-Medicina.

Figures 3-4: Dirty map of 1929+226 from the phase differences with 1923+210, with (fig. 3) and without (fig. 4) ionosphere correction. The origin of the coordinates is arbitrary.

FIGURE 1

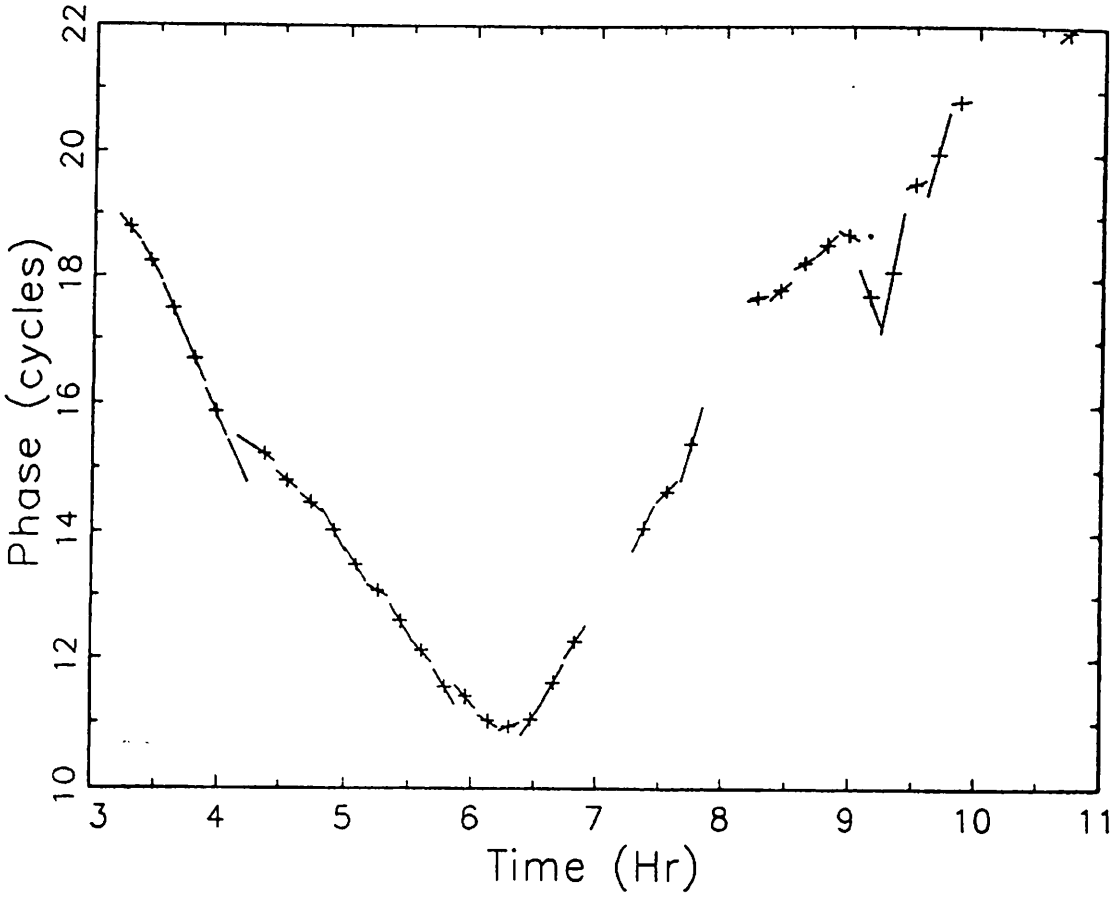

FIGURE 2

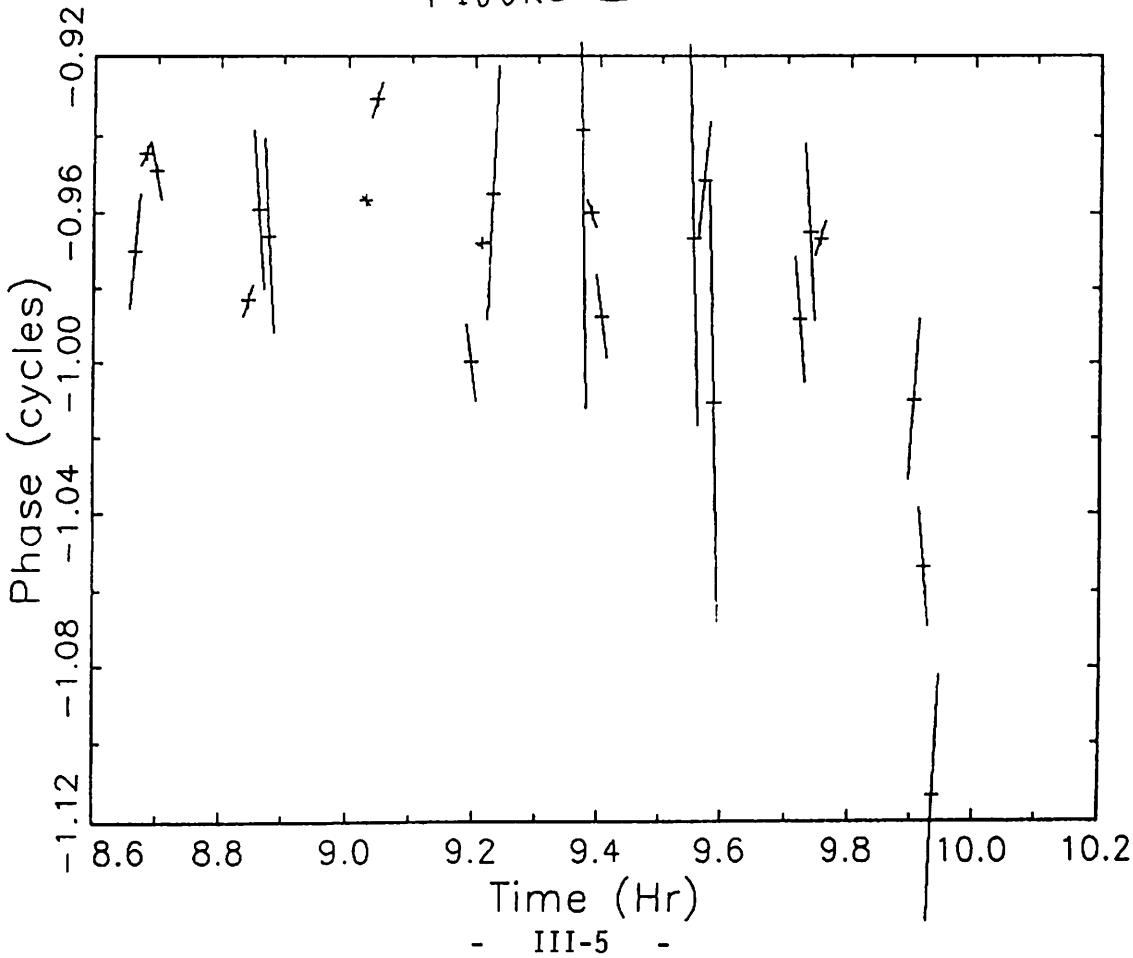

FIGURE 3

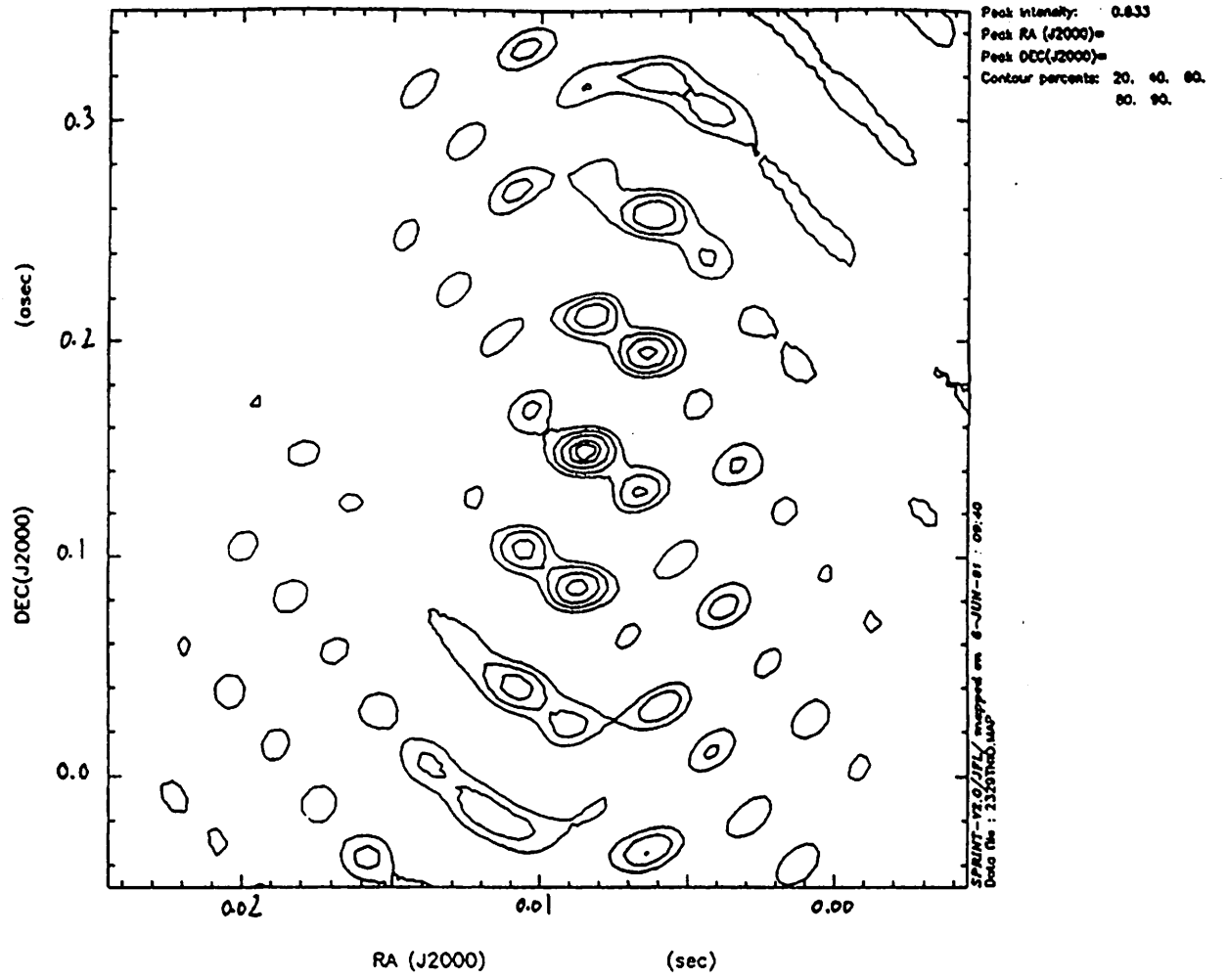

FIGURE 4

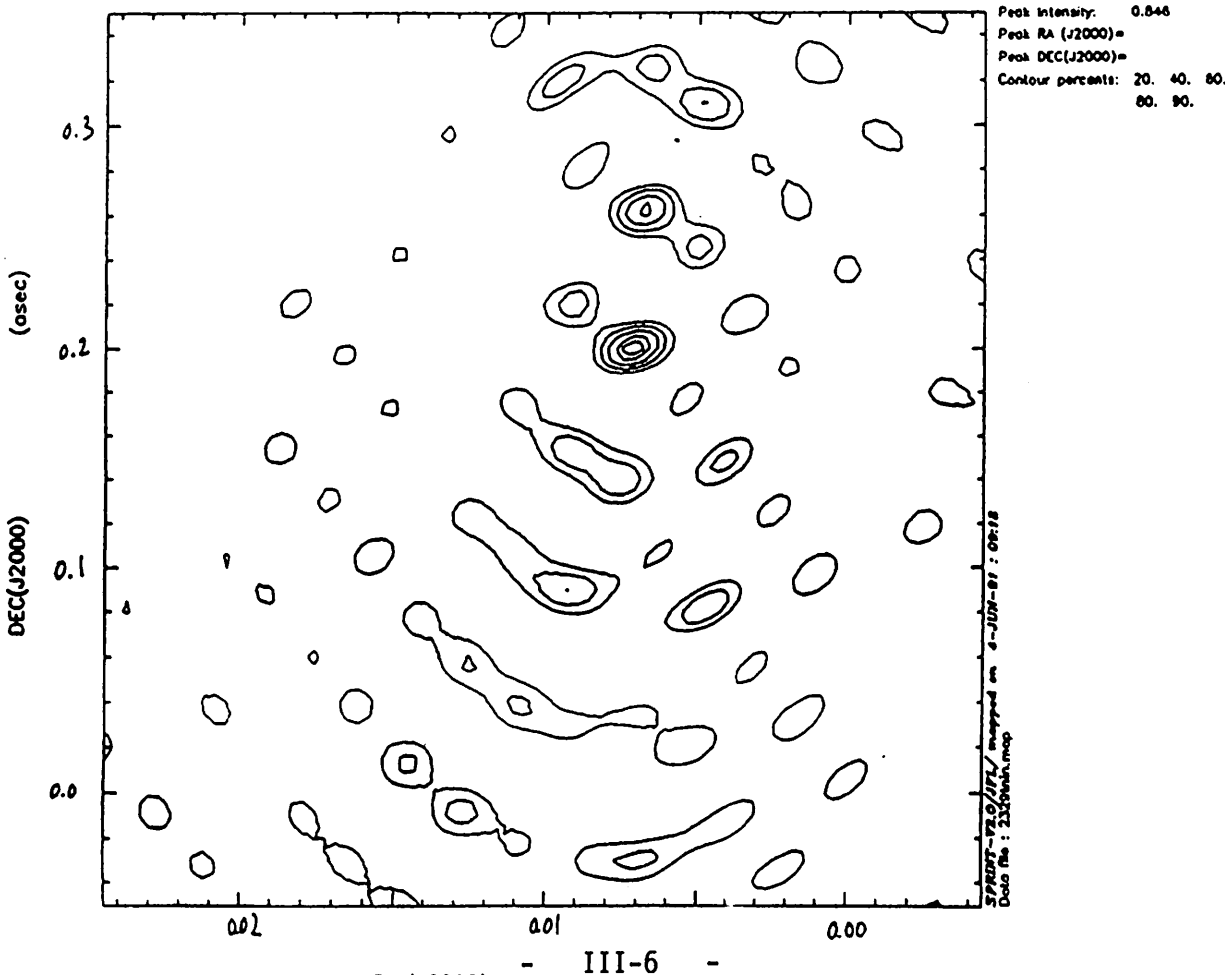

VLBI OBSERVATIONS OF THE HIPPARCOS RADIO STAR LSI+61°303

J. M. Paredes[1], M. Massi[2], R. Estalella[1,3], M. Felli[2]

[1]Departament d'Astronomia i Meteorologia, Universitat de Barcelona, Av. Diagonal 647, E-08028 Barcelona, Spain
[2]Osservatorio Astrofisico di Arcetri, Largo E. Fermi 5, 50125 Firenze, Italy
[3]Laboratori d'Astrofísica, Societat Catalana de Física (IEC), Spain

Abstract. An hybrid map of the radio star LSI+61°303 has been obtained from VLBI observations, at 6 cm wavelength. The map of the source reveals two components separated by 0.9 mas and aligned along a position angle of 45°. The size of the source, at a contour level of 50% of peak intensity, is approximately 1.6 mas.

1. Introduction

Radio stars are suitable objects for linking the Hipparcos reference frame to extragalactic objects through VLBI observations. An observational program monitoring the flux density of selected radio stars has been carried out during the last years. From a preliminary list of radio stars with optical characteristics suitable for Hipparcos observation, objects with good characteristics for VLBI observation have been selected. Here we report VLBI observations of one of these stars, LSI+61°303. The radio emission from LSI+61°303 exhibits periodic behavior with a period of 26.5 d (Taylor & Gregory 1982, 1984). In addition, the peak radio flux density is modulated on a time scale of approximately 4 yr (Gregory et al. 1989; Paredes et al. 1990). An optical modulation, with a period of about 26.5 d has been reported by Mendelson & Mazeh (1989). Radial velocity observations are consistent with the radio period and give support to the presence of a companion (Gregory et al. 1979; Hutchings & Crampton 1981). The system has also been identified as an X-ray source (Bignami et al. 1981) and a probable γ-ray source (Pollock et al. 1981). All these characteristics place LSI+61°303 in the class of X-ray binaries with associated variable radio emission, which includes SS 433, Cyg X-3, Sco X-1, and Cir X-1.

LSI+61°303 has been already observed with VLBI techniques (Lestrade et al. 1985) during its quiescent state (25 mJy) at 1.6 GHz, yielding a source size of 4 mas entirely due to interstellar scattering. The extrapolation of the 1.6 GHz measurements gives a size, due to interstellar scattering, of only 0.4 mas at 5 GHz.

2. Observations

The observations were made with the Mark III VLBI system in the standard A mode (56 MHz) on 6 June 1990, at 6 cm wavelength. The antennas used were Effelsberg, Westerbork, Medicina, Onsala and the VLA. The calibrator source 0224+67 was observed three times, during 3 minutes each time, along the 14 hours observing run.

Our observation was carried out at an orbital phase $\phi = 0.7$, that is, approximately two days after the predicted maximum of the 26.5 d periodicity, and two months after the predicted maximum of the long term (4 yr) periodicity (Paredes et al. 1990).

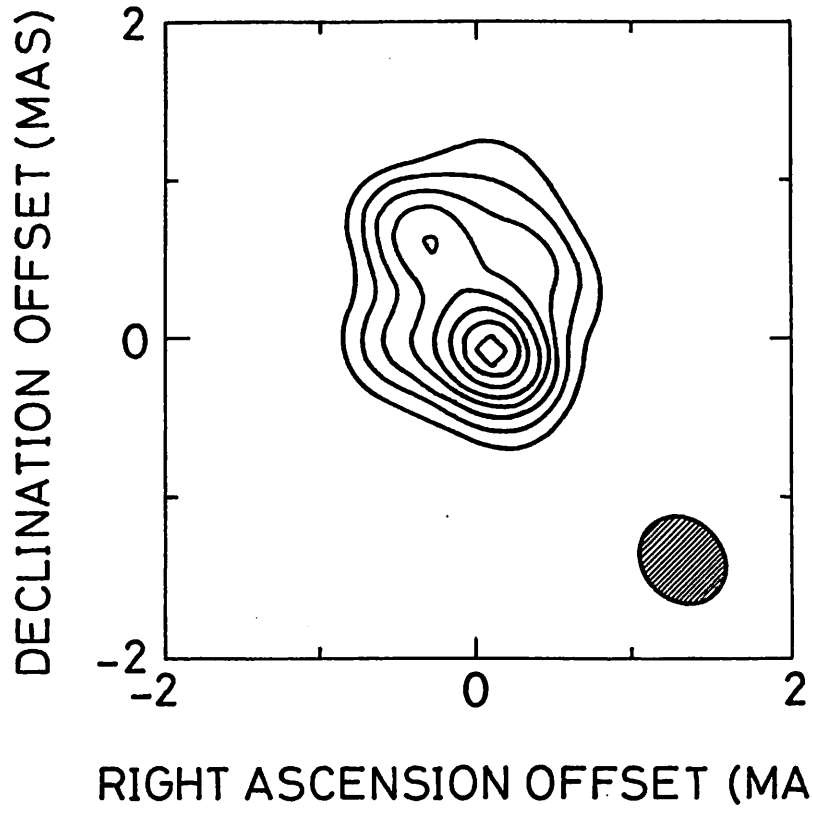

Figure 1: Map of LSI+61°303. The peak flux density is 36 mJy beam^{-1}. The lowest contour level is 25 % of the peak and the increment is 10% of the peak. The half power contour of the restoring beam is shown as a hatched ellipse.

The radio star was detected at all baselines, with a SNR above 7. The source correlated flux density was 220 mJy.

3. Results

The hybrid map of the source was obtained with the Caltech VLBI package. Figure 1 shows the final map obtained with a HPBW of 0.6×0.5 mas (P.A. = 45°). Two components, separated by 0.9 mas, can be seen in the map. The southern component is approximately two times stronger than the northern component. The overall size of the source, at a level of 50% of peak intensity, is 1.6×1.0 mas, which corresponds to a linear size of $5.5\,10^{13} \times 3.4\,10^{13}$ cm for a source distance of 2.3 kpc. The total flux density in the VLBI map is 200 mJy.

4. Discussion

From our results, we estimate the brightness temperature to be $5.5\,10^{9}$ K. This value confirms the non-thermal nature of LSI+61°303. Assuming an spectral index of -0.2, which is the value observed by Taylor & Gregory (1982, 1984) in previous multifrequency observations for an orbital phase $\phi = 0.7$, and equipartition of high-energy particles and magnetic energy, we can evaluate (Pacholzyk 1970) the minimum energy content $E_{min} = 4.2\,10^{39}$ erg, and the magnetic equipartition field $B_{eq} = 0.7$ G. In addition, assuming that the observed radio outburst started 4 days before our observation and that both components expand away from a common center,

we can estimate the projected expansion velocity to be $4.4\,10^7$ cm s^{-1}. The values derived from the data for the expansion velocity, magnetic field and energy content are consistent with an adiabatic expansion model of a synchrotron emittig source with prolonged injection of energetic particles (Paredes et al. 1991).

The estimated total size of the source, less than 2 mas, seems to indicate that this radio star is a good candidate to be included in the final group of stars to be used for the connection of the Hipparcos reference system to the VLBI extragalactic reference system (Froeschlé & Kovalevsky 1982).

Acknowledgements. We wish to thank G. Comoretto, D. Graham, and W. Alef for their help during the data reduction. R. E. and J. M. P. acknowledge partial finantial support from CICYT (Spain) contract ESP88-0731

References

Bignami, G. F., Caraveo, P. A., Lamb, R. C., Markert, T. H., Paul, J. A. 1981, ApJ 247, L85

Froeschlé, M., Kovalevsky, J. 1982, A&A 116, 89

Gregory, P. C., Taylor, A. R., Crampton, D., Hutchings, J. B., Hjellming, R. M., Hogg, D., Hvatum, H., Gottlieb, E. W., Feldman, P. A., Kwok, S. 1979, AJ 84, 1030

Gregory, P. C., Huang-Jian Xu, Backhouse, C. J., Reid, A. 1989, ApJ 339, 1054

Hutchings, J. B., Crampton, D. 1981, PASP 93, 486

Lestrade, J. F., Mutel, R. L., Preston, R. A., Phillips, R. B. 1985, in: Radio Stars, eds. R. M. Hjellming & D. M. Gibson, Reidel, Dordrecht, p. 275

Mendelson, H., Mazeh, T. 1989, MNRAS 239, 733

Pacholczyk, A. G. 1970, Radio Astrophysics, Freeman, San Francisco

Paredes, J. M., Estalella, R., Rius, A. 1990, A&A 232, 377

Paredes, J. M., Martí, J., Estalella, R., Sarrate, J. 1991, A&A in press

Pollock, A. M., Bignami, G. F., Hermsen, W., Kanback, G., Lichti, G. G., Masnou, J. L., Swanenburg, B. N., Wills, R. D. 1981, A&A 94, 116

Taylor, A. R., Gregory, P. C. 1982, ApJ 255, 210

Taylor, A. R., Gregory, P. C. 1984, ApJ 283, 273

Third epoch of the Pair of Quasars 1038+528 A,B: Preliminary results.

M. J. Rioja[1], P. Elósegui[1], and J.M. Marcaide[1,2]
[1]Instituto de Astrofísica de Andalucía
[2]Universitat de Valencia

ABSTRACT

We have determined, from the third epoch VLBI observations on the pair of quasars 1038+528 A and B, their relative separation at λ=3.6cm. We have measured, at the μas level, a variation over the time domain of the quasar 1038+528 A with respect to 1038+528 B. This preliminary result entails a new constraint to any interpretation of their relative kinematics.

I. Introduction

Astrometry is the branch of astronomy concerned with measurements of positions of sources on the sky. These positions are routinely determined with milliarcsecond precision (Ma *et al.* 1990) under several VLBI (Very Long Baseline Interferometry) observation programs. This precision is a direct consequence of the contamination of the purely geometric information in our observables with other contributions and the imperfection in the modelling of the latter ones.

For a given interferometer the interferometric phase observable can be written as a sum of several terms:

$$\Phi_{total} = \Phi_{geo} + \Phi_{str} + \Phi_{pm} + \Phi_{inst} + 2\pi n$$

where $\Phi_{geo} = \vec{D}.\hat{s}/c$ depends only on the relative position of the constant vector towards the observed source ($\hat{s}$) with respect to the baseline vector joining the two telescopes ($\vec{D}$); Φ_{str} is the contribution to the phase due to the extended structure

Proceedings of the 8th Working Meeting on European VLBI for Geodesy and Astrometry (page III-10 - III-16)

of the source; Φ_{pm} reflects the effect caused by the propagation medium which a given wavefront crosses before reaching the two ends of a baseline; Φ_{inst} accounts for instrumentation effects (telescope or baseline based); and $2\pi n$ reflects the inherent ambiguity of a phase.

Differential VLBI astrometry of pairs of radio sources with small angular separations bypass the majority of the latter limitations by using a differential observable (obtained by subtraction of the observables estimated for each source at a given time). The contaminating terms (Φ_{pm}, Φ_{inst}) to the phase observable mostly cancel out in the difference. The degree of cancellation improves as the angular separation decreases. For close pairs of radio sources the differential astrometric technique provides relative positions of radio sources with precisions well under a milliarcsecond.
The differential interferometric phase observable for two sources (namely A and B) is defined as follows:

$$\Delta\Phi_{total} \equiv \Phi^A_{total} - \Phi^B_{total} = (\Phi^A_{geo} - \Phi^B_{geo}) + (\Phi^A_{str} - \Phi^B_{str}) + (\Phi^A_{pm} - \Phi^B_{pm}) + (\Phi^A_{inst} - \Phi^B_{inst}) + 2\pi(n^A - n^B)$$

II. Observations

On 18-19 June 1990 we observed simultaneously the pair of quasars 1038+528 A, B at λ=3.6/13cm with the Mark III VLBI system (Rogers *et al.* 1983). An array of eight telescopes (Wettzell, Medicina, Effelsberg, DSS63, Haystack, Green Bank, Pie Town, and Owens Valley) participated for about ten hours in the observations. The recorded bandwidth was 28 MHz for each frequency at each telescope except for Pie Town, where a VLBA data acquisition terminal limited the synthesized band at λ=3.6cm to 16 MHz and at λ=13cm to 12 MHz. The recording was made in right-circular polarization.

The recorded data were cross-correlated with the Mark III processor (Rogers *et al.* 1983) at the MPIfR, Bonn, to obtain the fringe amplitude, group delay, (ambiguous) phase delay, and phase delay rate observables for each 11 minute observation.

Marcaide *et al.* (1985) and Elósegui (1991) have reported of similar observations from epochs 1981.2 and 1983.4, respectively. The experimental conditions under which the two prior observations were carried out were reproduced to a maximum extent to allow reliable intercomparison among the results.

III. 1038+528 A, B

If two radio sources are sufficiently close in angular separation that they can even be observed simultaneously because they lie within the main beam of each telescope, antenna-time dependent effects affect nearly in the same way to the interferometric phase derived for both sources ($\Phi^A_{pm} \sim \Phi^B_{pm}, \Phi^A_{inst} \sim \Phi^B_{inst}$). Then, the differential interferometric phase observable, ($\Delta\Phi_{total}$), reduces to:

$$\Delta\Phi_{total} \approx \Delta\Phi_{geo} + \Delta\Phi_{str} + 2\pi(n^A - n^B)$$

and contains only contributions from the relative geometry, the structures, which can be estimated, and the differential number of ambiguities which can also be resolved.

The pair of quasars 1038+528 A, B fulfills this condition. Given that their angular separation is of about 33 arcsecond ($\Delta\alpha \approx 19''$, $\Delta\delta \approx 27''$, 1038+528 B North-East with respect to 1038+528 A) the uncancelled atmospheric contribution $\Delta\Phi_{pm}$, at λ=3.6cm, should be no more than 0.1 μas (Elósegui, 1991). On the other hand, the number of ambiguities to have the differential phases connected is easily estimated once they were found for one epoch (Marcaide and Shapiro, 1983).

Given two sources with coordinates (α, δ) and $(\alpha + \Delta\alpha, \delta + \Delta\delta)$, and a baseline $\vec{D}$, the dependence of the geometric part of the differential phase delay observable with respect to their coordinates is given by the following expression,

$$\Delta\tau_{ph,geo} = \Delta\tau_{ph,geo}(\mathrm{GST} \equiv \mathrm{t,D,}\alpha,\delta,\Delta\alpha,\ \Delta\delta)$$

$$\Delta\tau_{ph,geo} = \frac{D_e.\cos\delta.\cos(D_\lambda + GST - \alpha)}{c} - \frac{D_e.\cos(\delta+\Delta\delta).\cos(D_\lambda + GST - (\alpha+\Delta\alpha))}{c} + \\ + \frac{D_z.\sin\delta}{c} - \frac{D_z.\sin(\delta+\Delta\delta)}{c}$$

where GST (Greenwich Sidereal Time) stands for a measure of time, $\vec{D} = (D_e, D_z, D_\lambda)$ refers to the baseline vector with components: projection on the equatorial plane, projection onto the Earth rotation axis (both in units of length), and angular distance to Greenwich meridian. The maximum sensitivities of the geometric part of the delay observable to changes (or errors) in the source coordinates ($\alpha, \delta, \Delta\alpha$, or $\Delta\delta$) are given by:

$$\left(\frac{\partial(\Delta\tau_{geo})}{\partial(\Delta\alpha)}\right)_{t=t_\alpha} = \frac{D_e.\cos(\delta+\Delta\delta).\cos(\Delta\alpha)}{c} \qquad (1)$$

$$\left(\frac{\partial(\Delta\tau_{geo})}{\partial(\Delta\delta)}\right)_{t=t_\delta} = -\frac{D_e.\sin(\delta+\Delta\delta).\cos(\Delta\alpha)}{c} - \frac{D_z.\cos(\delta+\Delta\delta)}{c} \qquad (2)$$

$$(\frac{\partial(\Delta\tau_{geo})}{\partial\alpha})_{t=t_\alpha} = -\frac{D_e.\cos\delta}{c} + \frac{D_e.\cos(\delta+\Delta\delta).\cos(\Delta\alpha)}{c} \quad (3$$

$$(\frac{\partial(\Delta\tau_{geo})}{\partial\delta})_{t=t_\delta} = -\frac{D_e.\sin\delta}{c} + \frac{D_e.\sin(\delta+\Delta\delta).\cos(\Delta\alpha)}{c} + \frac{D_z.\cos\delta}{c} - \frac{D_z.\cos(\delta+\Delta\delta)}{c} \quad (4$$

The maximum sensitivity to right ascension takes place at a time t_α such that: $\mathrm{GST}(t_\alpha) + D_\lambda = \alpha \pm 90$ deg, that is, when the source vector is perpendicular to the baseline vector. The maximum sensitivity to declination takes place at a time t_δ such that: $\mathrm{GST}(t_\delta) + D_\lambda = \alpha$, or $\mathrm{GST}(t_\delta) + D_\lambda = \alpha \pm 180$ deg.

For the particular case of 1038+528 A, B, given their small angular separation, a first order approximation of the formulas (1) to (4) is good enough. A representative baseline of our June 1990 observations can be $D_e = 5000$ Km and $D_z = 600$ Km (similar to the Effelsberg-Haystack baseline). An error of 20 μas in $\Delta\alpha$ (or $\Delta\delta$) would cause an extra sinusoidal variation (or a constant offset due to the component D_z of the baseline plus a sinusoidal variation) with time on the differential phase delay of an amplitude of about 1picosecond (ps). On the other hand, an error of 1mas (1mas=$50 * 20\mu$as) in α or δ will cause an extra sinusoidal variation with time of an amplitude of about 0.01 ps, which represents a systematic error of about 0.2μas in the relative separation determination of 1038+528 A and B.

IV. Data Analysis

The angular distance between the pair of quasars corresponds to the relative separation between two well-defined reference positions within their structures (one in each of the two sources). For each source, the contribution of the structure with respect to the reference position is subtracted from the total phase delay.

In order to obtain the structures one needs to use the information contained in Φ_{str}. In VLBI is not possible to isolate this contribution from Φ_{total}, as mentioned above, but there exist several ways to estimate Φ_{str} subject to the phase-closure condition (Rogers *et al.* 1974). The fine calibration of the visibility amplitudes was carried out using a self-calibration method (Cornwell and Wilkinson, 1981) after a standard calibration based on measured system temperatures and antenna sensitivities. We performed the imaging using the Caltech software package (kindly made available by T.J. Pearson). In Figure 1 we present the VLBI brightness distributions of the quasars 1038+528 A and B at λ=3.6cm. The sources 1038+528 A and B have not undergone any significant change in their structures compared to the maps from the epoch 1983.4 (Elósegui, 1991) at the same wavelength.

In order that the comparison of astrometric solutions from different epochs to make sense, a common celestial reference system (J2000.0) and origin for the time-dependent Earth-orientation parameters (UT1 and pole position) must be used for every epoch, as well as common phase reference positions within the extended structure of each source. These reference positions must be properly chosen (easily recognizable over time and frequency) to define (and permit comparison from epoch to epoch) the relative separation of both sources.

The relative astrometric parameters have been estimated from the geometric contribution to the phase delay $\Delta\tau_{ph,geo}$ using global weighted-least-squares adjustment techniques. We have used the latest version of the program VLBI3 (Robertson, 1975), which also models other effects (e.g., propagation medium and instrumental effects) which leave a signature in the differential interferometric phase delay observable, and the Goddard Space Flight Center (GSFC) CDP VLBI Global Solution GLB718 Earth Orientation Parameters (EOP) values (Ma, private communication). In Figure 2 we present the astrometric solutions, at λ=3.6cm, from the epochs 1981.2 and 1983.4, and the preliminary result from the epoch 1990.5.

V. Discussion

The position of the quasar 1038+528 A, as appears in Figure 2, does not agree with the scenarios proposed after the analysis of the first two epochs of this pair of radio sources (Marcaide, Elósegui, and Shapiro, 1990). Subtle problems may still be plaguing our preliminary results. The phase-connection we have based our solution on appears good but tests to ascertain it are still underway. It appears that some structure effects cannot be responsible of the present disagreement.

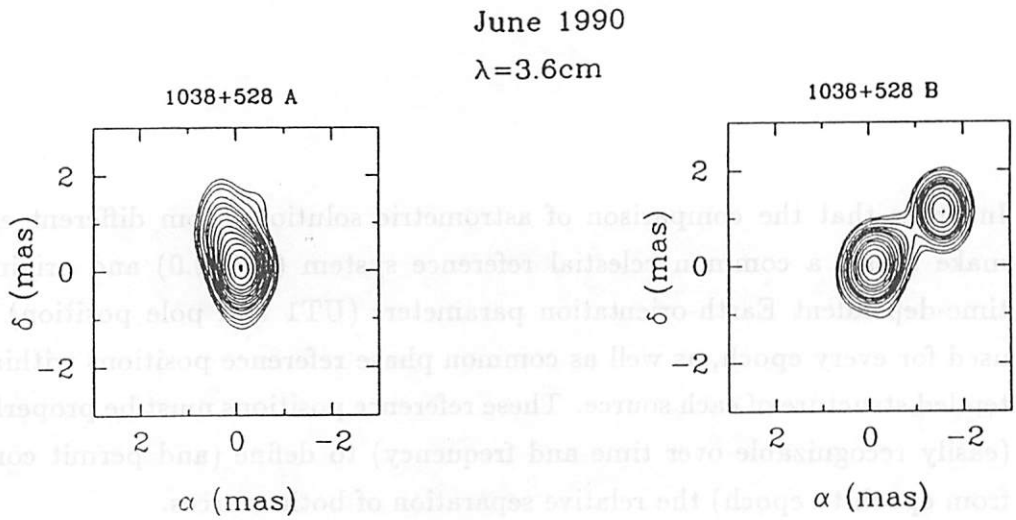

Figure 1: Maps for the quasars 1038+528 A and B at $\lambda = 3.6$ cm for the epoch June 1990. The contours correspond to -2,2,4,6,10,15,20,25, 30,35,40,45,50,60,80,95 % and -3,3,5,6,10,15,20,25,30, 40,50,60,80,95 % of the peak of brightness in their respective maps. A Gaussian beam of 0.8 * 0.6 mas in P.A. -2^0 has been used to restore the images.

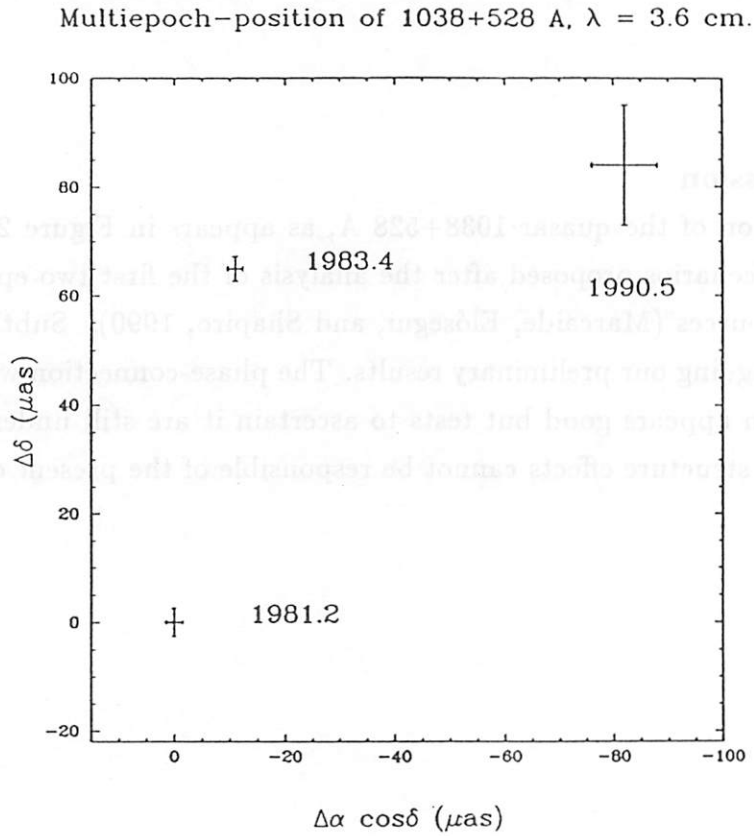

Figure 2: Estimates of the position of the quasar 1038+528 A at $\lambda = 3.6$ cm relative to 1038+528 B at epochs 1981.2, 1983.4, and 1990.5 (with 1981.2 offsets subtracted).

References

Cornwell, T.J. and Wilkinson, P.N., *M.N.R.A.S*, **196**, 1067 (1981).

Elósegui, P., *Ph.D. thesis, Universidad de Granada* (1991).

Ma, C., Shaffer, D.B., de Vegt, C., Johnston, K.J., and Russell, J.L., *Astron. J.*, **99**, 1284 (1990).

Marcaide, J.M. and Shapiro, I.I., *Astron. J.*, **88**, 1133 (1983).

Marcaide, J.M., Shapiro, I.I., Corey, B.E., Cotton, W.D., Gorenstein, M.V., Rogers, A.E.E., Romney, J.D., Schild, R.E., Bååth, L., Bartel, N., Cohen, N.L., Clark, T.A., Preston, R.A., Ratner, M.I., and Whitney, A.R., *Astron. Astrophys.*, **142**, 71-84 (1985).

Marcaide, J.M., Elósegui, P., and Shapiro, I.I., in *Parsec Scale Radio Jets*, ed. J.A. Zensus and T.J. Pearson, Cambridge University Press, p.43. (1990)

Robertson, D.S., *Ph.D. thesis, Massachusetts Institute of Technology* (1975).

Rogers, A.E.E., Hinteregger, H.F., Whitney, A.R., Counselman, C.C., Shapiro, I.I., Wittels, J.J., Klemperer, W.K., Warnock, W.W., Clark, T.A., Hutton, L.K., Marandino, G.E., Rönnäng, B.O., Rydbeck, O.E.H., and Niell, A.E., *Ap. J.*, **193**, 293 (1974).

Rogers, A.E.E., Cappallo, R.J., Hinteregger, H.F., Levine, J.I., Nesman, E.F., Webber, J.C., Whitney, A.R., Clark, T.A, Ma, C., Ryan, J., Corey, B.E., Counselman, C.C., Herring, T.A., Shapiro, I.I., Knight, C.A., Shaffer, D.B., Vandenberg, N.R., Lacasse, R., Mauzy, R., Rayhrer, B., Schupler, B.R., and Pigg, J.C., *Science*, **219**, 51 (1983).

Shapiro, I.I., Wittels, J.J., Counselman, C.C., Robertson, D.S., Whitney, A.R., Hinteregger, H.F., Knight, C.A., Rogers, A.E.E., Clark, T.A., Hutton, L.K., and Niell, A.E., *Astron. J.*, **84**, 1459 (1979).

SESSION 4

computing methods in geodetic VLBI

KALMAN ANALYSIS OF GEODETIC VLBI OBSERVABLES

E. Sardón, A. Rius and N. Zarraoa
Instituto de Astronomía y Geodesia, C.S.I.C.-U.C.M.
Madrid, Spain

ABSTRACT

This paper describes our application of the Kalman filtering technique to the analysis of VLBI data. We present a brief description of the Kalman theory and its implementation in the software that we use for the estimation of parameters of geodetic interest. We have chosen stochastic models for the stochastic parameters and we have studied their influence on the final estimates.

1.- INTRODUCTION

From the analysis of VLBI observables (group delay and phase delay rate), it is possible to estimate geodetic parameters like station coordinates, source coordinates, earth rotation parameters, Love numbers, nutation coefficients, etc (deterministic parameters) as well as stochastic parameters related to unmodeled effects in the propagation trough the atmosphere, uncalibrated delays across the interferometer and non-ideal behavior of the station clocks.

In some software packages the method used for analyzing individual VLBI experiments is based on a standard (not sequential) least squares adjustment. In this case, the stochastic parameters are modelled using several low-order polynomials. Therefore, the set of parameters to be estimated should be augmented by the corresponding coefficients.

The Kalman filtering technique is a recursive extension of the standard least squares method, in which the stochastic parameters are described in terms of stochastic models. In each step we have a new estimate of the stochastic parameters and an improved estimate of the deterministic parameters. In this case, the matrices involved are smaller than the corresponding ones in the standard mode, therefore many experiments can be combined in a relatively small computer.

2.- SUMMARY OF THE KALMAN THEORY

We will assume that the relation between the collected data y_2 and the parameters x_2 at the epoch t_2 has been linearized:

$$y_2 = G*x_2 + e \qquad (1)$$

where e is the vector of measurement noise, with zero mean and covariance matrix C_D and G is the differential of the model computed in an a suitable point. (See figure 1)

Some or all the elements in the parameters vector can be time dependent, so we need a dynamic model for representing this time variation:

$$x_2 = T*x_1 + u \qquad (2)$$

where x_1 represents the parameters for the instant t_1, and T is a transition matrix (dynamic model). The stochastic vector u contains the unmodeled effects on the prediction and we assume that has zero mean and covariance Q (stochastic model). Of course, in the case of deterministic parameters the corresponding elements of Q are set to zero.

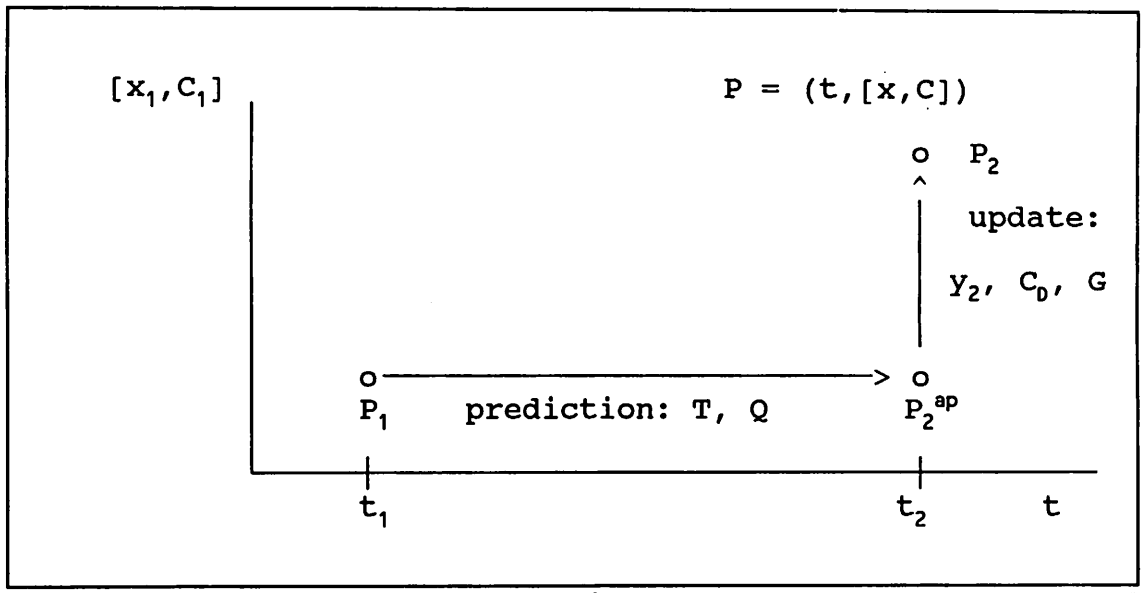

Figure 1: P_i represents the estimate of the parameters x_i and their covariance C_i at t_i. P_2^{ap} represents the predicted value at t_2.

The Kalman filtering technique consists in the iteration of the following two steps:

1) Prediction: given x_1 and its covariance C_1, the equation (2) allows to predict a priori values x_2^{ap} at t_2 and, using and the law of propagation of the covariances, C_2^{ap}:

$$x_2^{ap} = T*x_1$$
$$C_2^{ap} = T*C_1*T^t + Q \qquad (3)$$

This part does not depend on the data we have collected at t_2. Only depends on the dynamic and stochastic models we have chosen.

2) Update: applying a least squares procedure to the model given by equation (1) with a priori values x_2^{ap} and C_2^{ap}, we get the estimated values x_2 and C_2 at t_2 (Tarantola, 1987; see also Herring et al 1990):

$$x_2 = x_2^{ap} + C_2*G^t*C_D^{-1}*(y_2 - G*x_2^{ap})$$
$$C_2 = [(C_2^{ap})^{-1} + G^t*C_D^{-1}*G]^{-1} \qquad (4)$$

In this step, the data gathered and their covariances take part in the process. The measurement y_2 is compared to its predicted value $G*x_2^{ap}$ and the "observation minus calculus" is multiplied by the weight matrix $K=C_2*G^t*C_D^{-1}$.

The equations in (4) are recursive, so they could provide the estimate of the parameter vector for the step n based on all the measurements up to the step t_{n-1} without the necessity of storing these data. This information is contained in x_{n-1} and C_{n-1}.

3.- APPLICATION OF THE KALMAN FILTERING TO THE ANALYSIS OF VLBI EXPERIMENTS

We have included the capability of modeling deterministic (i.e.: station coordinates, source coordinates), white noise (i.e.: variation in the EOP between experiments) and random walk (i.e.: clocks and troposphere) processes.

For each parameter we have chosen the corresponding components of T and Q according to the table 1, where PSD is the power spectral density of the associate white noise and dt is t_2-t_1.

In the present implementation we assume that the covariance matrix of the data C_D is a diagonal matrix and each element of the diagonal is given by

$$C_D^i = (data\ noise)_i^2 + (experiment\ noise)^2 \qquad (5)$$

where "experiment noise" is a constant that we add, if necessary, depending on the result of a statistical test that we perform after the process of a complete experiment.

	Deterministic	White noise	Random walk
T	I	0	I
Q	0	PSD	PSD*dt

Table 1. Dynamic and stochastic models implemented in the software

We test if

$$\frac{\chi^2}{m} \approx 1 \qquad (6)$$

where

$$\chi^2 = (G*x_2-y_2)^t*C_D^{-1}*(G*x_2-y_2) + (x_2-x_1)^t*Q^{-1}*(x_2-x_1) \qquad (7)$$

and m is the number of observations.

Information on possible "clock breaks" at different stations, the initial estimates of the different clock offsets as well as estimates of the PSD are obtained with a previous run of OCCAM (see Zarraoa et al,1989) and added to the input data base.

4.- REPEATABILITY

In order to study the influence that the selection of the PSD of the stochastic processes involved can have in the estimation of the geodetic parameters, we have processed the data of the 1990 EUROPE-1 experiment using different values for the PSD of the stochastic parameters.

In figure 2, each box shows the repeatability of baseline lengths in meters, with respect to the power spectral density of the zenith tropospheric correction parameter. For each bar a factor of 10^{-2}, 1, 10^2, 10^4 has been applied to the PSD values derived from OCCAM estimations. We can see that only the last factor has produced significative changes in the lengths. Then, our PSD estimation could change two orders of magnitude without noticeable influence in the results.

We have obtained the same repeatability when a similar comparison has been done with respect to the PSD of the clocks.

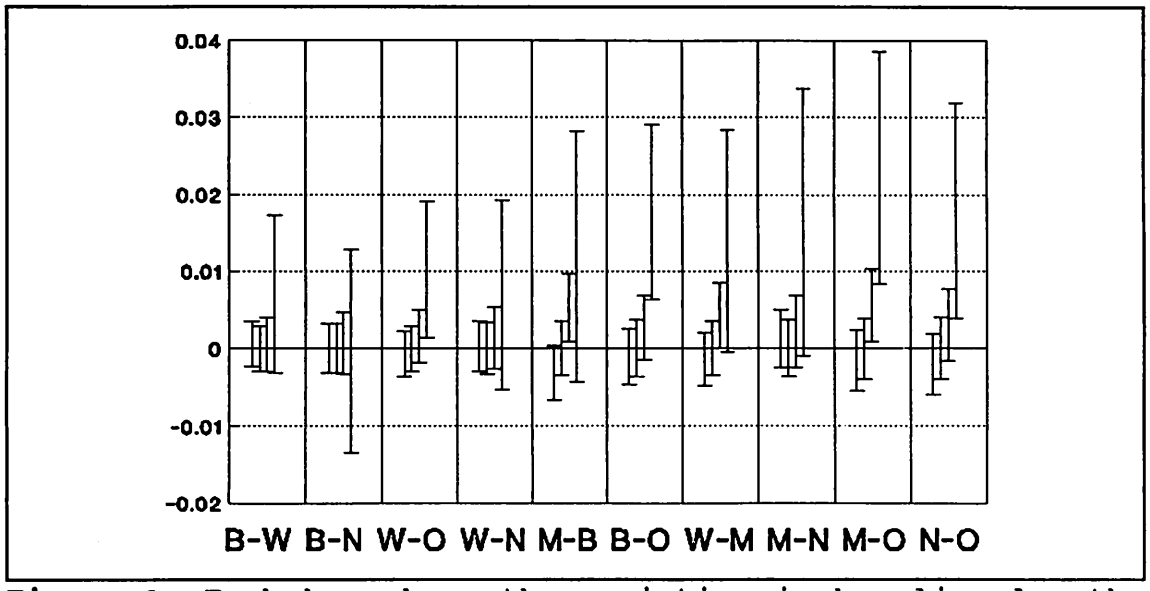

Figure 3: Each box shows the variation in baseline lengths (m) when the estimated PSD for the tropospheric path delay is multiply by $10^{-2},1,10^{2},10^{4}$. B.- Medicina, M.- Matera, O.- Onsala, W.- Wettzell, N.- Noto.

6.-CONCLUSIONS

- There is a good flexibility in the choice of the stochastic models for the stochastic parameters, in the sense that the estimates of the geodetic parameters are not affected if the PSD is changed in two orders of magnitude.

- The solution obtained with this method is in good agreement with that obtained with a standard least squares adjustment and does not require more computing time.

- The combination of several experiments is possible with not special requirements on the computer resources.

7.- REFERENCES

Herring, T., Davis, J.L., Shapiro, I.I.: "Geodesy by Radio Interferometry: The Application of Kalman Filtering to the Analysis of Very Long Baseline Interferometry Data", Journal of Geophysical Research, Vol 95, No. B8, Pag 12561-12581, 1990.

Tarantola, A. : "Inverse Problem Theory. Methods for Data Fitting and Model Parameter Estimation". Ed: Elsevier, 1987.

Zarraoa, N., Rius, A., Sardón, E., Schuh,H., Vierbuchen, J. "OCCAM: a Compact and Transportable Tool for the Analysis of VLBI Experiments", Proceedings of the 7th Working Meeting on European VLBI for Geodesy and Astrometry, 1989.

Variations in the Wet Path Delay

G. Elgered, J.M. Johansson, B.O. Rönnäng
Onsala Space Observatory
Chalmers University of Technology
S–43900 Onsala, Sweden
phone +46 300 60650, fax +46 300 62621, e-mail geo@oden.oso.chalmers.se

Abstract. Water-Vapor Radiometer (WVR) data have been used to study wet path-delay variations at four sites. Most of the data were from the Onsala Space Observatory located on the Swedish west coast. As expected, the size of the variations is dependent on season and site. We also find a good correlation between the largest variations and passages of weather fronts at the Onsala site. We have found no corresponding correlation at the other three sites.

1. Introduction

The error in the delay introduced by the "wet" atmosphere continues to be an important source of error for geodetic very-long-baseline interferometry (VLBI). We have used radiometer data obtained at (1) the Onsala Space Observatory on the Swedish west coast, (2) Mojave at the Goldstone complex in the Mojave desert in California, (3) Fort Davis in the semi-arid climate of Texas, and (4) Kokee Park on the west side of the Kauai island of Hawaii in order to study and characterize variations of the wet delay [*Elgered et al.*, 1990].

Here we present statistical information on the measured equivalent zenith wet delay and its variation with time for the different sites. In addition, the time gradients with the largest absolute values estimated from one hour long data blocks are studied in detail by searching for features in the meteorological conditions using synoptic weather maps.

Instead of the rather expensive method of microwave radiometry one can use Kalman filter techniques to estimate the wet delay from the VLBI data themselves [*Herring et al.*, 1990; *Sardon*, 1991 (these proceedings)]. The idea of using the delay rate residuals obtained for the different baselines in each experiment to determine the size of the wet delay variations at each site rely on the assumption that the delay rate residuals are dominated by variations in the wet delay [*Herring et al.*, 1990]. This assumption is tested by comparing the wet delay variations obtained from the delay rate residuals with those inferred from microwave radiometer measurements for the different months.

2. Site Descriptions and Water-Vapor Radiometer (WVR) Data

Onsala

The Onsala WVR site has the approximate coordinates 11.9°E and 57.4°N and the height above sea level is only about 10 m. It is located on the Swedish west coast in a temperate climate dominated by polar westerlies.

A description of the radiometer can be found in *Elgered and Lundh* [1983]. All the data used for the Onsala site were divided into 203 data sets, in total approximately 11500 hours. Radiation from the sun and radiation due to rain degrade the accuracy of the estimated wet delays. These effects can be significant sources of error for studies of variations in the wet delay since they change quickly. Therefore, the affected observations must be removed from the wet delay data sets. All data taken closer than 20° from the sun were, therefore, deleted. The algorithm

used to infer the wet delay from the WVR data assumes that the attenuation due to liquid water is proportional to the square of the frequency. This is true when the sizes of the liquid water drops are much smaller than the wavelength of the attenuated signal [*Staelin*, 1966] (*i.e.* $\ll$10 mm). Here we discard all wet delay estimates made when the simultaneous estimate of the zenith liquid water content is larger than 0.3 mm. This is a very conservative limit if all the observed liquid water is in the atmosphere [*Westwater*, 1978; *Westwater and Guiraud*, 1980]. Liquid water may, however, also form on the covers of the feed horns of the radiometer. Experience has shown that when liquid water contents are inferred to be less than 0.3 mm there are no water drops on the feed system. A more detailed discussion on this problem and references can be found in *Elgered et al.* [1990].

Mojave, California

The microwave radiometer (R07) was located at: longitude 243.1°E, latitude 35.2°N, and altitude 900 m. The site is in the Mojave desert in California. The local climate is dry and it rarely rains at the site. The R-series radiometer is described by *Resch et al.* [1985]. The wet delay data used were taken during geodetic very-long-baseline interferometry (VLBI) experiments and have been used previously in the analysis of such experiments [*Kuehn et al.*, 1987].

We discarded all data sets with long gaps in the estimated time series of the wet delays. Thereafter, we selected the two data sets per month containing the most data points. The resulting data covers 792 hours.

Fort Davis, Texas

The microwave radiometer (JR9) is located at: longitude 253.7°E, latitude 31.4°N, and altitude 1600 m. The site is in a semi-arid climate. The amount of water vapor in the atmosphere above the site is further reduced by the high altitude of the site. The JR9 radiometer is the same type of R-series instrument as is used at Mojave. The main difference is that is was upgraded using the same type of data acquisition electronics as is used in the J-series radiometers [*Janssen et al.*, 1985]. Radiometer data were available from June, 1988, to January, 1989. Also these data are taken during VLBI experiments and have already been carefully analyzed and used in studies of these experiments [*Kuehn et al.*, 1991]. We selected 24 data sets distributed as evenly as possible over this period. The number of hours covered were in total 964.

Kokee Park, Kauai, Hawaii

The microwave radiometer (R05) was located at: longitude 200.3°E, latitude 22.1°N, and altitude 1160 m. The site is in the Kokee State Park on the west side of the island Kauai. The weather is dominated by the easterly trade winds and the local weather is similar to that in a tropical rain forest with almost daily rainfall. The climate on the Hawaii islands is very different compared to the three other sites. For example the mean diurnal range of temperature variations is significantly larger then is the mean annual range [*Handbook of Geophysics and the Space Environment*, 1985]. The amount of precipitation show large variations depending on the location because of the high mountains.

The radiometer data were available for the whole year of 1989. However, they have not been analyzed previously. Instrumental corrections are, however, calculated "on-line" even if it is often necessary to perform a more advanced analysis of the instrument stability afterwards. Since the time was limited for this study we chose a different approach. The on-line instrumental corrections were studied for the first 7 days of each month. Thereafter, we selected the approximately two best days of these seven in terms of instrumental stability. The number of hours covered were in total 722.

3. Statistics of Wet Delay Variations

All of the microwave radiometer data have been used in order to estimate time gradients in the equivalent zenith wet delay. We estimated linear gradients for blocks of data. The time windows of the blocks used are $\frac{1}{2}$, 1, 2, and 4 hours. (Due to lower resolution of the data sampling at the US sites 1, 2, and 4 hours were used with these data.) Systematic variations in the size estimated time gradients over the year was investigated. The RMS of the estimated linear gradients for each month and the different sites are shown in Figures 1–4. The seasonal dependence is clear at Onsala, Mojave, and Fort Davis. For these sites we also find a clear correlation between the value of the zenith wet delay and the size of the estimated linear gradient. The result for Kauai is more complicated. We know that the annual variations in temperature are significantly smaller for this site. However, Figure 4 clearly indicate that there are some variations over the year but more data are needed to justify a general conclusion.

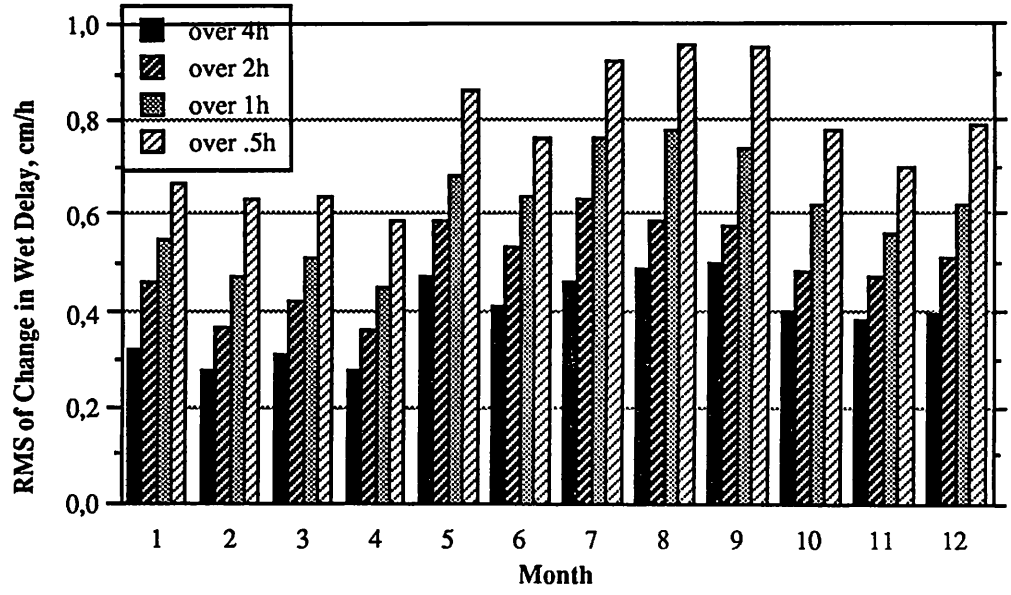

Figure 1. The RMS value of the estimated linear time gradients in the wet delay for the different months at the Onsala site.

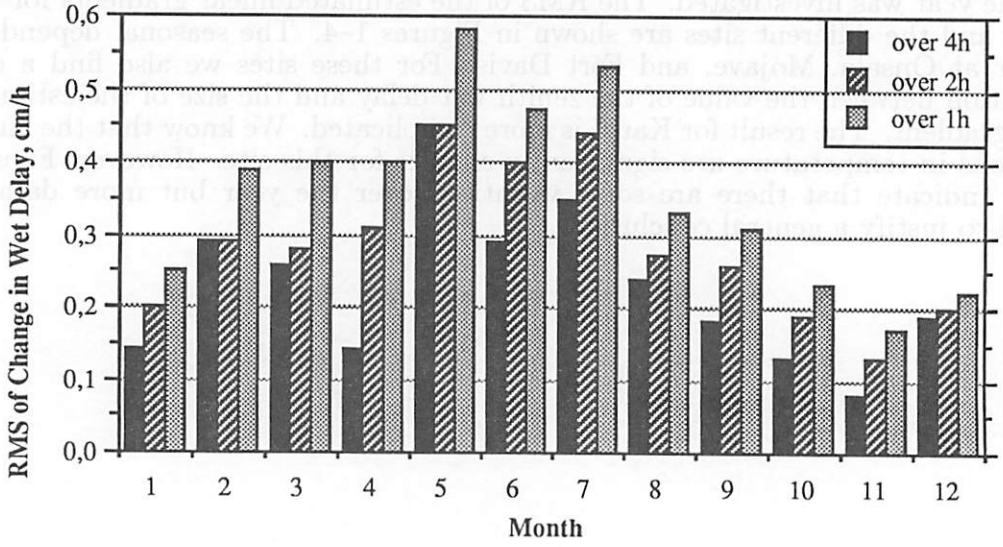

Figure 2. The RMS value of the estimated linear time gradients in the wet delay for the different months at the Mojave site.

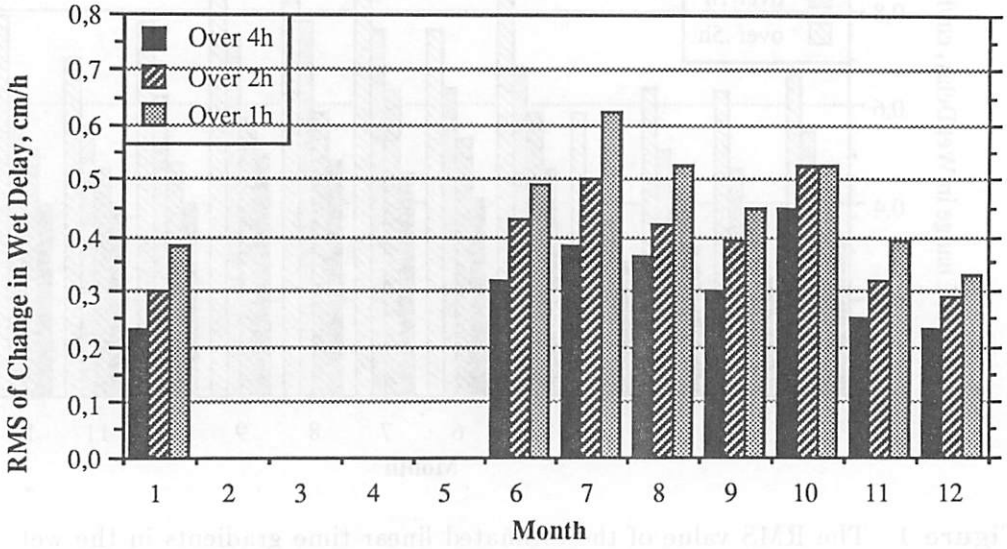

Figure 3. The RMS value of the estimated linear time gradients in the wet delay for the different months at the Fort Davis site.

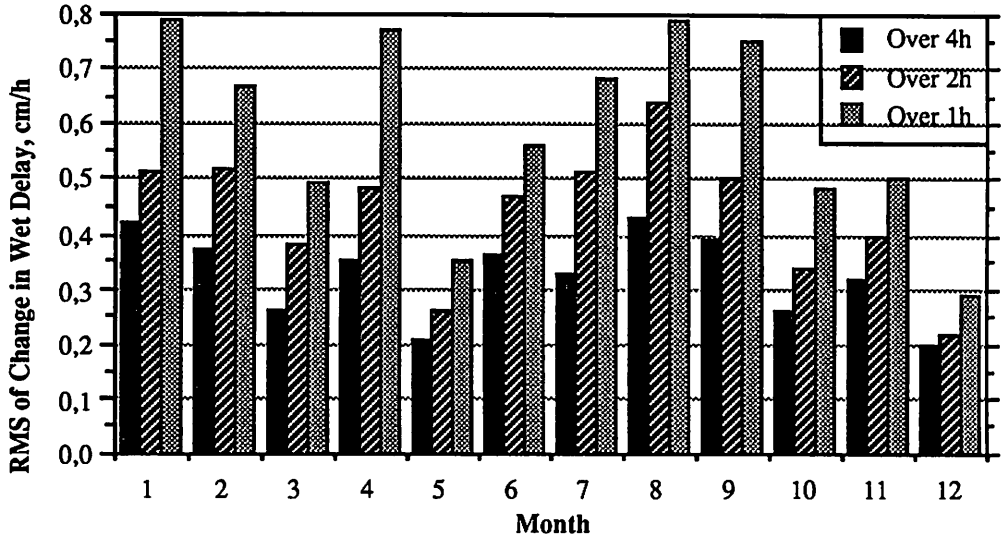

Figure 4. The RMS value of the estimated linear time gradients in the wet delay for the different months at the Kauai site.

The RMS values of the estimated linear gradients for all the sites are presented in Table 1. We conclude that the short time variations (over hours) do not correlate well with the mean wet delay when different sites are compared. This is contradictory to the result above, where the expected short time variation increased with an increasing value of the wet delay itself for a specific site.

Table 1. Statistics of linear time gradients of the equivalent zenith wet delay estimated using data blocks of different time length for the four sites.

Site	Wet Delay		Estimated Linear Gradient Over			
	Mean cm	S.D.[1] cm	$\frac{1}{2}$ h cm/h	1 h cm/h	2 h cm/h	4 h cm/h
Mojave	5.7	3.0	-	0.40	0.32	0.26
Fort Davis	9.8	5.0	-	0.47	0.39	0.31
Kauai	9.0	3.3	-	0.63	0.46	0.34
Onsala	8.6	4.2	0.78	0.63	0.51	0.41

[1] Standard Deviation

The monthly RMS values obtained at the Onsala site for the $\frac{1}{2}$ hour long data blocks have been compared with the average values inferred from the delay rate residuals in geodetic VLBI experiments from 1980 to 1987. The result is shown in Figure 5 where we have assumed that the wet-delay variations are described by a random walk process. Since the VLBI observations are typically obtained every 10–15 minutes we have also included RMS values obtained from 15 minute data blocks for some of the months during 1988 where we have radiometer data sampled with a sufficient resolution. Note that the values inferred from the different time blocks of WVR data should be the same if the wet delay variations are correctly characterized as a random walk process. A seasonal dependence is clearly seen in the variances obtained using the two different methods. Such seasonal dependence in the wet delay variance estimated from the delay rate residuals has also been reported for the Westford site [*MacMillan and Ray*, 1991]. In general the VLBI data show larger variances indicating that the delay rate residuals includes contributions also from other sources than the atmosphere. This is to some extent supported by the fact that the average VLBI value for the month of July is based on two experiments in 1980 only. These were two of the first geodesy VLBI experiments using the Mark III equipment at Onsala and for the example the hydrogen maser at Onsala were not in a temperature stable environment at that time. The other monthly averages are typically based on about 10 experiments spread over the time period 1980–1987.

Another possibility to explain the difference between VLBI and WVR data (especially during the summer period) is that we have been ignoring WVR data implying a zenith liquid content > 0.3 mm. Airplane measurements have shown that cumulus clouds contain not only liquid water but also an excess amount of water vapor (see *e.g. Radke and Hobbs*, [1991]). Large cumulus clouds (with a lot of liquid water) are common during the Swedish summer. It is likely that large variations in the wet delay are undetected when WVR data implying large liquid water contents are discarded.

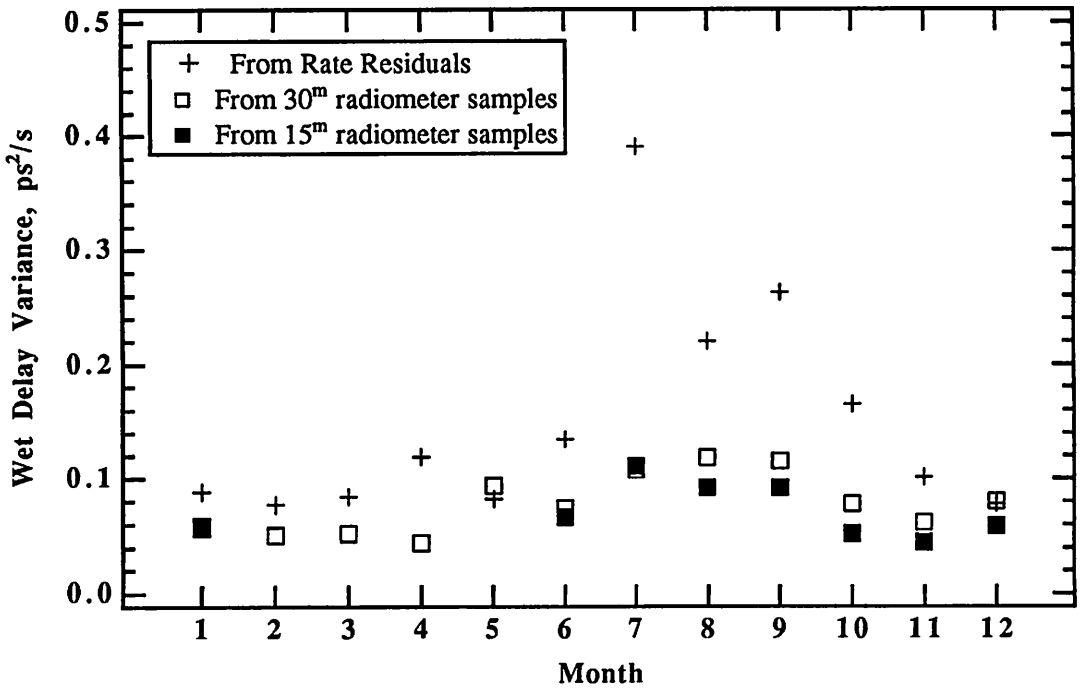

Figure 5. Variances of wet delay variations obtained from WVR data and VLBI rate residuals assuming that the variations are described by a random walk process.

4. On the Correlation Between Large Wet Delay Variations and Weather Map Features

The existence of moving warm and cold air masses in the atmosphere is well known. The often well defined border between different air masses is called a weather front. Since the saturation vapor pressure increases rapidly with increasing temperature a passing weather front may cause a significant change in the observed wet delay. In this Section we investigate this possibility by using weather maps produced for forecasting purposes. A good general description on the different types of weather fronts can be found in *Hsu* (1988).

The weather maps needed for the Onsala data were obtained from the Swedish Meteorological and Hydrological Institute (SMHI). The Climate Analysis Center, NOAA, Washington D.C., USA, supplied the weather maps for the US sites. The location of the fronts, on the ground surface, has an uncertainty smaller than 10 km. For each large change in the wet delay we studied these maps and tried to identify features that could be evidence for rapid variations in the atmospheric water-vapor content. For the Onsala site we found 105 linear time gradients estimated over one hour periods which had absolute values greater than 2.4 cm/h, *i.e.* 1% of all the data. In order to get similar data sets for the US sites we used the approximately 10 one hour periods with the greatest absolute value of the estimated time gradients. We present the result for each site separately.

Onsala

We found that the passage of weather fronts is a very important factor in order to explain the largest time variations in the wet delay. If the front passage on the ground occurs within 6 hours of the time epoch of the detected large change in the wet delay we assume that the front is the cause of the rapid change. A front passage normally implies precipitation. If, however, an epoch is not an obvious front passage we have searched for other possible reasons (such as different types of precipitation) in order to explain the measured change in the wet delay.

We found that 83% of the gradients were associated with the passage of weather fronts. One such an example is shown in Figure 6 (microwave radiometer data) and Figure 7 (the corresponding wether maps). Another 13% of the epochs were associated with thunder and/or showers and changes in cloud coverage. The last 4% of all the epochs could not be explained using weather maps only. Two of these epochs seem to involve a rapidly sinking inversion layer with cold and dry air above (subsidence).

Mojave, California

We find 8 one hour periods with an absolute value of the time gradient greater than 1.3 cm/h. Four of these occasions (all during the same day) seems to be associated with the passage of a cold front. For the other four occasions the weather maps show mainly that there are clouds and rain in the area.

Fort Davis, Texas

We find 10 one hour periods when the estimated linear gradient is greater than 1.5 cm/h. Two of these (one hour apart) occurs when a cold/warm front is located some 300 km south of the site. During another three cases (two of them one hour apart) there are indications on the weather map that a front is starting to build up just north of Fort Davis. In one of these cases there are thunder in the area. In three other cases there are cloud activity. For the last two cases there are no evidence for large changes in the wet delay on the weather maps.

Kauai, Hawaii

We find eight cases when the estimated gradients over one hour periods are larger than 1.8 cm/h. All cases seems to depend on local phenomena. The radiometer site is on the west side of the mountain peak on the island Kauai. The area is described as a "tropical rain forest" with rain showers almost every day. It is therefore likely that the variations in the wet delay are local features.

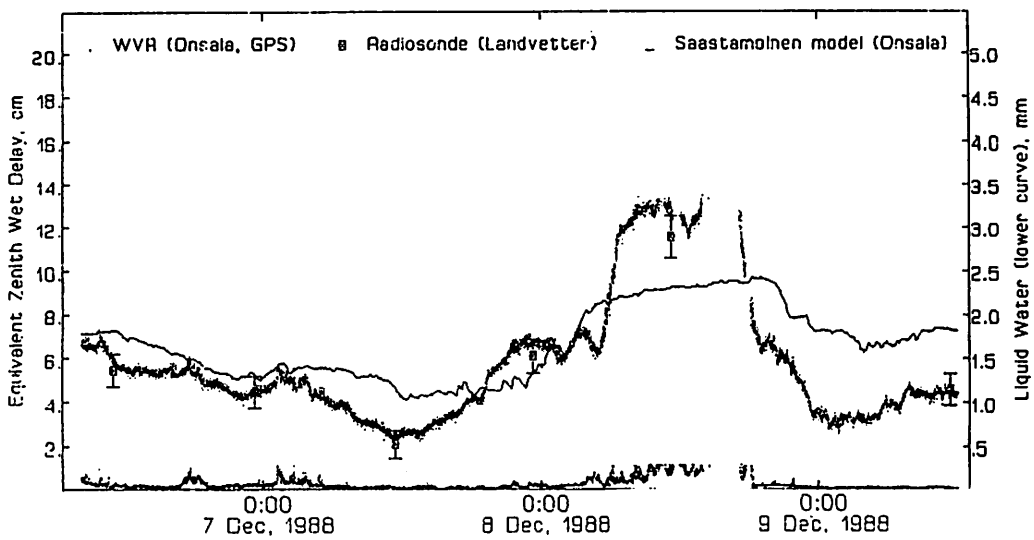

Figure 6. The equivalent zenith wet delay (left scale) measured with the microwave radiometer is shown as a point (.). Also denoted with a point is the integrated amount of liquid water inferred from the radiometer data (right scale in mm). However, the liquid water points will always appear in the lower part of the plot since all measurements implying a liquid-water content larger than 0.3 mm are discarded from the data set. The gaps in the radiometer data on Dec. 8 indicates rain. Also shown is the wet delay calculated from radiosonde launches made at Göteborg-Landvetter Airport at 11:20 and 23:20 UT every day. These wet delays have an error bar which shows the expected one sigma of the *combined* measurement errors of the radiosonde and the radiometer according to a simple error model presented by *Elgered et al.* [1990]. Finally, the wet delay obtained from a ground based model [*Saastamoinen*, 1972] is plotted as a line.

(a) (b)

Figure 7. Weather maps at 9 UT (a), and 18 UT (b), December 8, 1988 (see Figure 6). The shaded area denotes rain and the triangles denotes showers. The warm front passage in the early morning implies a large increase in the wet delay. The warm and cold fronts located in west Norway in the morning arrives at Onsala around 18 UT. The cold front has now reached the warm front and the warm air is lifted off the ground (occluded front). When the rain stopped the wet delay show a large decrease.

Conclusions

Variations in the wet delay are known to be site dependent. This is also clearly shown in this paper. For a given site, larger values of the wet delay increases the probability for larger variations in the wet delay. This is, however, not necessarily true when different sites are compared. We have also seen that large variations in the wet delay often are caused by passing weather fronts at the high latitude Onsala site whereas the variations measured at the Kauai island seem to be driven by local effects.

Acknowledgements

This work was supported in part by, ESA Contract 8128/88/ NL/BI(SC), the Swedish Natural Science Research Council, and the Hasselblad Foundation.

References

Elgered, G. and P. Lundh, A Dual Channel Water Vapor Radiometer System, *Res. Rept. No. 145*, Onsala Space Observatory, Chalmers Univ. of Tech., 1983.

Elgered, G., J.M. Johansson, and B.O. Rönnäng, Characterizing Atmospheric Water Vapour Fluctuations Using Ground Based Microwave Radiometry, ESTEC Contract No 8128/88/ NL/BI(SC) Report, *Res. Rept. No. 165*, Onsala Space Observatory, Chalmers University of Technology, 1990.

Handbook of Geophysics and the Space Environment, Ed. A.S. Jursa, U. S. Air Force Geophysics Laboratory, Chapter 15, 1985.

Herring, T.A., Davis, J.L., & Shapiro, I.I., Geodesy by radio interferometry: The application of Kalman filtering to the analysis of very long baseline interferometry data, *J. Geophys. Res.*, **95**, 12,561–12,581, 1990

Hsu, S.A., *Coastal Meteorology*, Academic Press, San Diego, pp. 47–52, 1988.

Janssen, M.A., A New Instrument for the Determination of Radio Path Delay Variations due to Atmospheric Water Vapor, *IEEE Trans. on Geoscience and Remote Sensing*, **GE-23**, pp. 485–490, 1985.

Kuehn, C.E., M.W. Hayes, G.L. Lundqvist, J.R. Ray, T.A. Clark, Results of WVR Analysis Using VLBI data, *EOS*, **68**, p. 1239, 1987.

Kuehn, C.E., W.E. Himwich, and T.A. Clark, An Evaluation of Water Vapor Radiometer Data for Calibration of the Wet Path Delay in VLBI Experiments, accepted for publ. in *Radio Science*, 1991.

MacMillan, D.S., and J.R. Ray, Current Precision of VLBI Vertical Determinations, *Proc. AGU Chapman Conf. on Geodetic VLBI: Monitoring Global Change*, Washington D.C., 22–26 April, 1991.

Radke, L.F., and P.V. Hobbs, Humidity and Particle Fields Around Some Small Cumulus Clouds, *J. Atmos. Sci.*, **48**, 1991.

Resch, G.M., M.C. Chavez, N.I. Yamane, K.M. Barbier, R.C. Chandlee, Water Vapor Radiometry Research and Development Phase Final Report, *JPL Publication 85-14*, Jet Propulsion Laboratory, Pasadena, California, 1985.

Sardon, E., Kalman Analysis of Geodetic VLBI Observables, *Proc. of the 8th Working Meeting on European VLBI for Geodesy and Astrometry*, this volume, 1991.

Staelin, D.H., Measurements and Interpretation of the Microwave Spectrum of Terrestrial Atmosphere near 1-Centimeter Wavelength, Journal of Geophysical Research, **71**, pp. 2875–2881, 1966.

Saastamoinen, J., Atmospheric correction for the troposphere and stratosphere in radio ranging of satellites, in *The Use of Artificial Satellites for Geodesy, Geophys. Monogr. Ser.*, **15**, edited by S.W. Henriksen *et al.*, pp. 247–251, American Geophysical Union, Washington, D.C., 1972.

Westwater, E.R., The Accuracy of Water Vapor and Cloud Liquid Determination by Dual-Frequency Ground-Based Microwave Radiometry, *Radio Science*, **13**, pp. 677–685, 1978.

Westwater, E.R., and F.O. Guiraud, Ground-Based Microwave Radiometric Retrieval of Precipitable Water Vapor in Presence of Clouds with High Liquid Content, *Radio Science*, **15**, pp. 947–957, 1980.

Source structure enhanced MK III Data Analysis Software

Guenter Zeppenfeld
Geodetic Institute
University of Bonn
Nußallee 17
D-5300 Bonn 1
Germany

Abstract

A source structure analysis software has been developed as an enhancement of the MK III data analysis software CALC/SOLVE in order to correct VLBI observations automatically for source structure effects. A preliminary version is presently operational and first results are presented. The next step is to complete the mapping of all (except two or three) sources in the IRIS/CDP schedule and to study the effects on a set of experiments. We also plan to expand the MK III data flow in order to include the structure data.

Motivation

Today the philosophy in considering source structure effects in geodetic VLBI is to delete all bad sources from the observed source catalogue, i.e. not to use those sources which tend to show significant structure. This may be a good approximation to avoid large structure effects in the actual observation schedule. But there are still some problems, if we go into details. First of all we have to consider the fact that the ideal point source does not exist, i.e. that all known sources show more or less extended structure on the scale of milliarcseconds. As an example, the hybrid map of the source 4C39.25 from the E-ATL 5 experiment in 1988 (fig. 1) shows a very compact brightness distribution at 8.4 GHz.

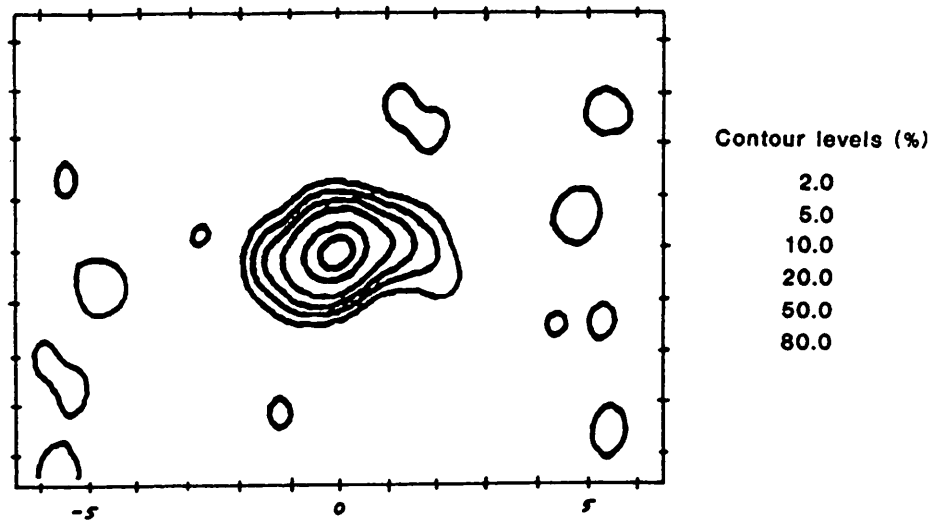

figure 1: CLEAN map of source 4C39.25 at 8.4 GHz

Usually we assume such a source to be a pointlike source. But if we compute delay corrections due to structure effects (figure 2) we obtain results on the order of 50 [psec]. This is a level which must be considered if we wish to improve the accuracy of VLBI.

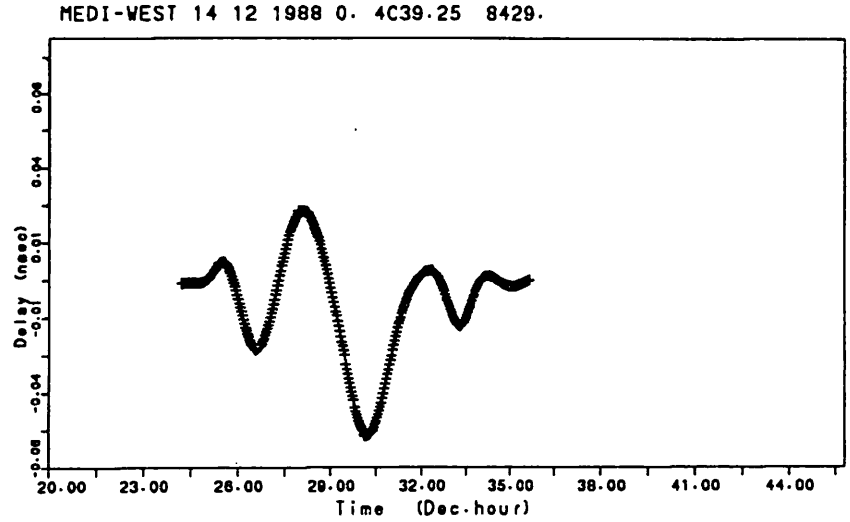

figure 2: group delay corrections due to source structure

A second effect which we cannot neglect is the variation of source structure with time. This structure variation proceeds more or less rapidly and is different for each source. So it could be possible that some sources which appear compact now will show significant structure in the future and must then be deleted from the source catalogue. In this case we will not able to achieve a standard observing source catalogue and a stable celestial reference frame. Structure variation with time is also the reason why we must monitor and map sources continously to be able to determine this effect for each source separately.

In VLBI we obtain the source and station coordinates together with other informations as a result of a global solution. This means that about once a year a solution will be computed which contains all VLBI observations carried out until that date, including all the observations of "bad" sources. To obtain a homogeneous solution all bad observations should be corrected for structure effects. As a consequence we need a suitable software system to compute such effects routinely.

With the ongoing development, the VLBI technique becomes more and more sensitive. If we don't want that the models become the limiting factor we must improve them by adding such model components as source structure software modules.

Against the background of these arguments we believe that the better way to consider source structure effects is to make the effort of creating the structure maps for each source and to routinely correct the observations for these effects.

New modules for MK III data analysis software

A preliminary version of the source structure software developed in Bonn is presently operational and includes two new modules SOURCE MAPPING and STRUC. These modules run parallel to CALC/SOLVE to limit the runtime of the whole analysis system. The advantage of separating the new modules from CALC/SOLVE is, that in this case we are able to run CALC/SOLVE in the usual way and independently from SOURCE MAPPING and STRUC. So one can map and calibrate sources parallel to the geodetic data analysis of the experiment. Only in one of the last steps in SOLVE just before producing final results STRUC will be started to compute source structure effects. These corrections can then be taken into account in SOLVE.

The SOURCE MAPPING algorithm (described by SCHALINSKI et. al., this report) uses B-Tapes to load the observed data. Together with the information about system temperature and antenna gain-curves (calibration data) mapping and calibration can be done. The most important part of the results of the mapping algorithm are the DELTA-MAPS. These data are used as an input to STRUC. Presently we are able to map sources only on the basis of B-Tapes. To use the full advantage of the VLBI Data-Base archives and to make monitoring easier we prefer to use DATA-BASES as mapping input.

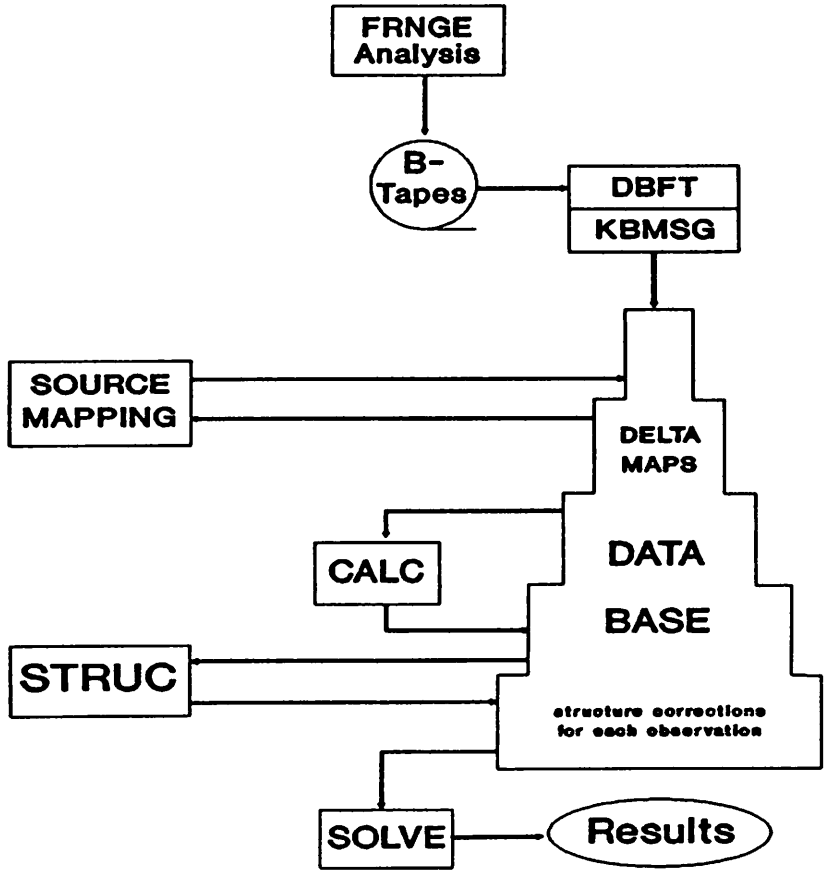

Fig. 3: New modules in the VLBI data flow

In addition to the structure information (delta-maps) STRUC needs information about the real observation schedule from the DATA-BASE to compute source structure corrections. Real observation schedule means that all available observations are stored in the DATA-BASE and used by SOLVE. The structure corrections will then be saved in the DATA-BASE. With the help of a new observation dependent SOLVE option all observations can be corrected for source structure effects. Detailed descriptions of the theoretical background of STRUC have been presented at the previous working meeting held in Madrid (ZEPPENFELD 1989).

Figure 3 shows the FINAL VERSION of our project enhancing the VLBI data analysis software to include source structure corrections. On the condition that all necessary data have been measured and are saved in the DATA-BASE the SOURCE MAPPING module can use the DATA-BASE in the FINAL VERSION directly to obtain all the information needed (antenna and observation information). The results of SOURCE MAPPING, the delta-maps, should also be saved in the DATA-BASE to make source monitoring easier and to guarantee that all further computations use the same map. If the delta-maps are saved in the DATA-BASE, all information will be available to run STRUC without having to rely on any other data sources.

First results

For the first tests we have tried to correct the X-Band observations of source 4C39.25 of the E-ATL 5 experiment (hybrid map see fig.1) for structure effects. Other sources will be dealt with in the near future.

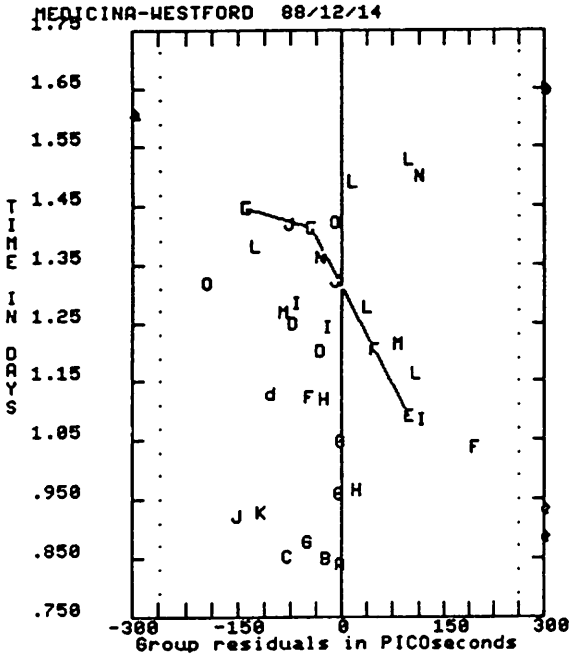

figure 4: (uncorrected)

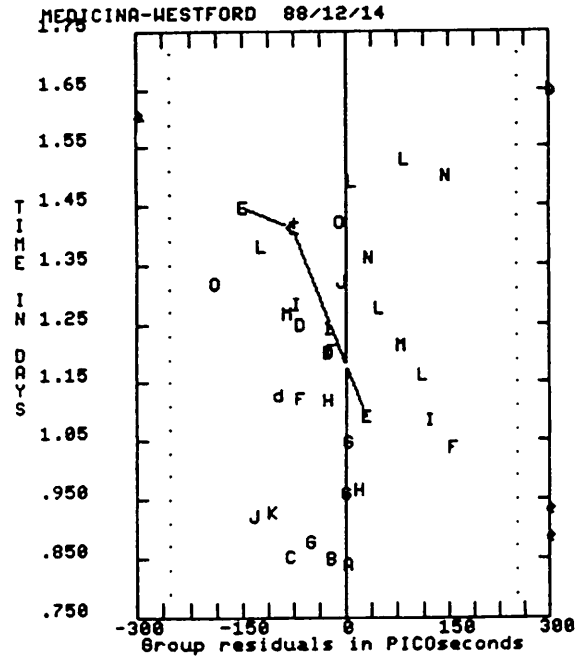

figure 5: (corrected)

The corrected residual plot (figure 5) for the baseline Medicina - Westford shows the corresponding changes. The postfit RMS delay decreases from 87 [psec] to 84 [psec]. As we can see here the effect is very small. If we wish to get any degree of significance we must do more testing with more sources on a larger set of VLBI-experiments.

Remaining Problems

There are two fundamental problems which have not yet been addressed in this paper. The first problem concerns the definition of a reference point for each source. This point must have a stable absolute position near or within the source, because brightness distribution varies with time. This would then be the point to which the computed corrections refer. Due to the fact, that our structure software STRUC uses delta maps, which describe the features of the brightness distribution of a source in terms of relative coordinates, we are able to use any of these features as reference point. This is another advantage of our software.

The second problem is related to the significance of the features represented in a given source map. According to the fact, that maps can be produced with a limited accuracy we have to assess the true structure and the noise level in a source image in order to separate "reality" from artefacts produced by the mapping software due to the scarcity of the data. This problem can be better explained with the help of the following example. If we compute source structure effects for 4C39.25 with all structure data available (figure 1) for the baseline Medicina - Westford we obtain unsmoothed delay corrections (figure 6) with a high noise level:

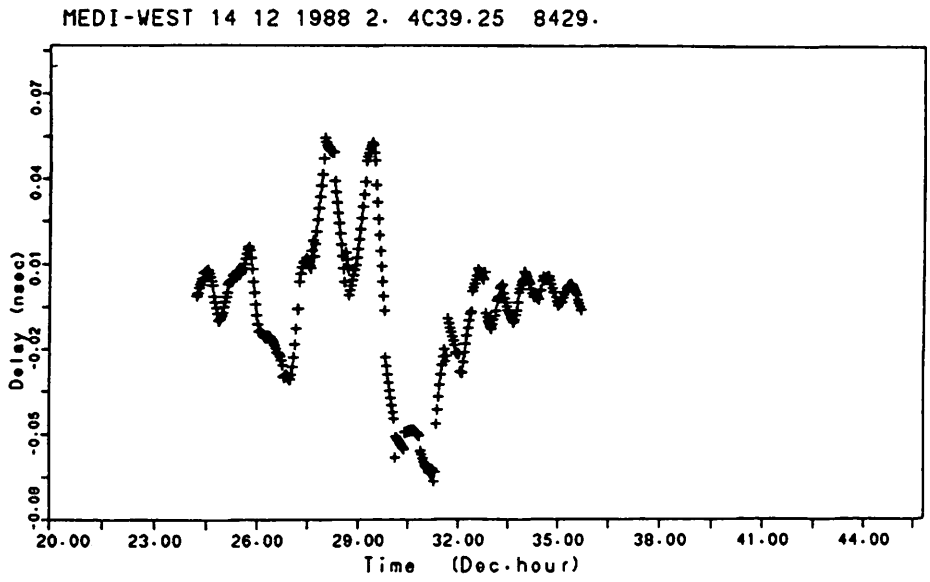

figure 6: (raw data)

But if we neglect all the more distant features seen in fig. 1 while assuming an accuracy (dynamic range) of 1:50 for the central part of the map (see SCHALINSKI et.al. this report) we obtain a smoothed curve (fig. 7) for the source structure effects on the order of 50 [psec].

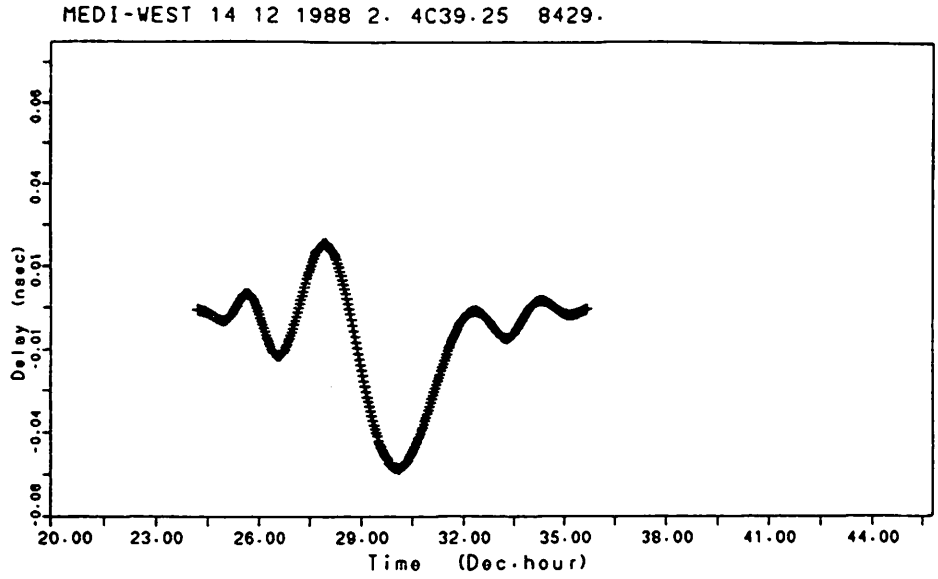

figure 7: (smoothed data)

This curve is only produced by the structure of the source itself. With this rather brutal procedure we plan to study each source in detail in order to place improved constraints on the structure effects. The fact that computation of group delay corrections involves the second derivative of the intensity distribution requires a high degree of smoothing at the level of the image data. This may still prove to be a critical stumbling block of the whole process.

Conclusions and Outlook

Due to the fact that all data are saved in the Data-Base mapping and monitoring are available for all sources and the computation of source structure effects for each source (pointlike or extended) is possible. The new modules run parallel to CALC/SOLVE. So the extension of the runtime of the whole data analysis system can be limited. The computation of source structure corrections means an important step in creating a new radio reference system that is independent from source structure variability and very close to an inertial reference frame.

As a next step we plan to complete the mapping of all (except two or three) sources in the IRIS/CDP schedule to study the effect of source structure on a set of VLBI experiments. Furthermore we want to determine the best strategy for creating a radio reference system independent from source structure variability.

References

Charlot, P. 1990: Radio-Source Structure in Astrometric and Geodetic Very Long Baseline Interferometry, Astrophysical Journal Vol. 99, Nr. 4, p. 1309-1326

Zeppenfeld, G. 1989: Testing the computation of source structure delay. In: Proceedings of the 7 th Working Meeting on European VLBI for Geodesy and Astrometry edited by A. Rius, Madrid 1989, p. 126-131

AUTOSKED-Automatic creation of optimized VLBI observing schedules

Heinz Steufmehl
Geodetic Institute of the University of Bonn

ABSTRACT: With the VLBI scheduling program Sked a skilled operator needs a few days to schedule observations for a 24 hours experiment. He has to select the scans manually and must take care of an optimized solution all the time. This also requires a lot of experience.
The new software Autosked has been developed on the basis of Sked and allows the creation of optimized schedules, which need just a few minutes of preparation time. The scans are no longer selected by the operator, but the automatic selection is made to optimize any one or group of unknowns, such as polar motion, station coordinates etc. Optionally, the program takes care of a good distribution of observing points over the sky or the minimization of telescope slewing time or tape waste. The optimization is done on the basis of the formal errors of the solve-for parameters. Comparisons with "hand-made" schedules have shown Autosked to produce similar or mostly better results as regards the optimization intentions.
In this presentation the optimization process is explained and examples of Autosked schedules for the IRIS-S network are given. These are compared with an original Sked schedule, made at the National Geodetic Survey in the USA.

1. THE OPTIMIZATION PROCESS

A more detailed description about what is going on in Autosked can be given using figure 1 and 2. The first steps (fig.1) are the same as in Sked. The operator has to introduce the starting date and time of the planned experiment. Then he has to select the participating stations and a set of sources. These sources should be well distributed over the sky. Then frequencies are selected and parameters are set.
After this the optimization options are introduced. The solve-for parameters for the subsequent analysis of the experiment must be chosen first. These parameters can be for example Earth orientation parameters, station or source positions, atmospheric or clock polynomial coefficients or any combination of them. The next step consists of the selection of the parameters of major interest, in figure 1 for example Earth orientation parameters. Then the user can select among other secondary optimization features. Besides a best accuracy of the parameters of major interest, also a good local sky coverage with observed sources may be aimed at. Furtheron, it is also possible to minimize tape usage or telescope slewing times.

When these preparations are done, the operator has to introduce a first configuration manually, so that all stations have observed at least once (fig.2). Configuration here means for example one source observed by all stations or two sources observed by different stations.
With the information of the ending date and time, the optimization process can be started. The program will compute a large number of possible configurations for the next observing point of time. These configurations can be regarded as basic components of the whole schedule. For one point of time there can of course only be one configuration selected from this pool of possibilities. For each configuration the contribution matrix to the matrix of normal equations is computed according to the chosen parameterization. These contribution matrices are symbolized by the flat boxes.
The actual optimization algorithm consists of four steps. First, the configurations are tested, if they really can be scheduled. If they pass this test, the contribution matrix will be added to the already existing matrix of normal equations and then the whole matrix will be inverted. The diagonal elements of this matrix represent the formal errors of the unkowns. Among those configurations, which give the best decrement of the errors of the parameters, i.e. the one which fulfills the other optimization features the best, will be selected for scheduling. In figure 2, this configuration is symbolized by the dark box.
When the ending date and time is reached, the optimization process stops and the schedule is ready. If the operator doesn't want an automatic scheduling, he can also have a look at the best configurations and decide by himself, which one to choose for scheduling. An overview gives him all important informations, such as percentual decrease of the errors, sky coverage values or tape usage. At any time he can also have a look at the simulated formal errors of the solve-for parameters or their correlation matrix in order to check the ongoing scheduling process.

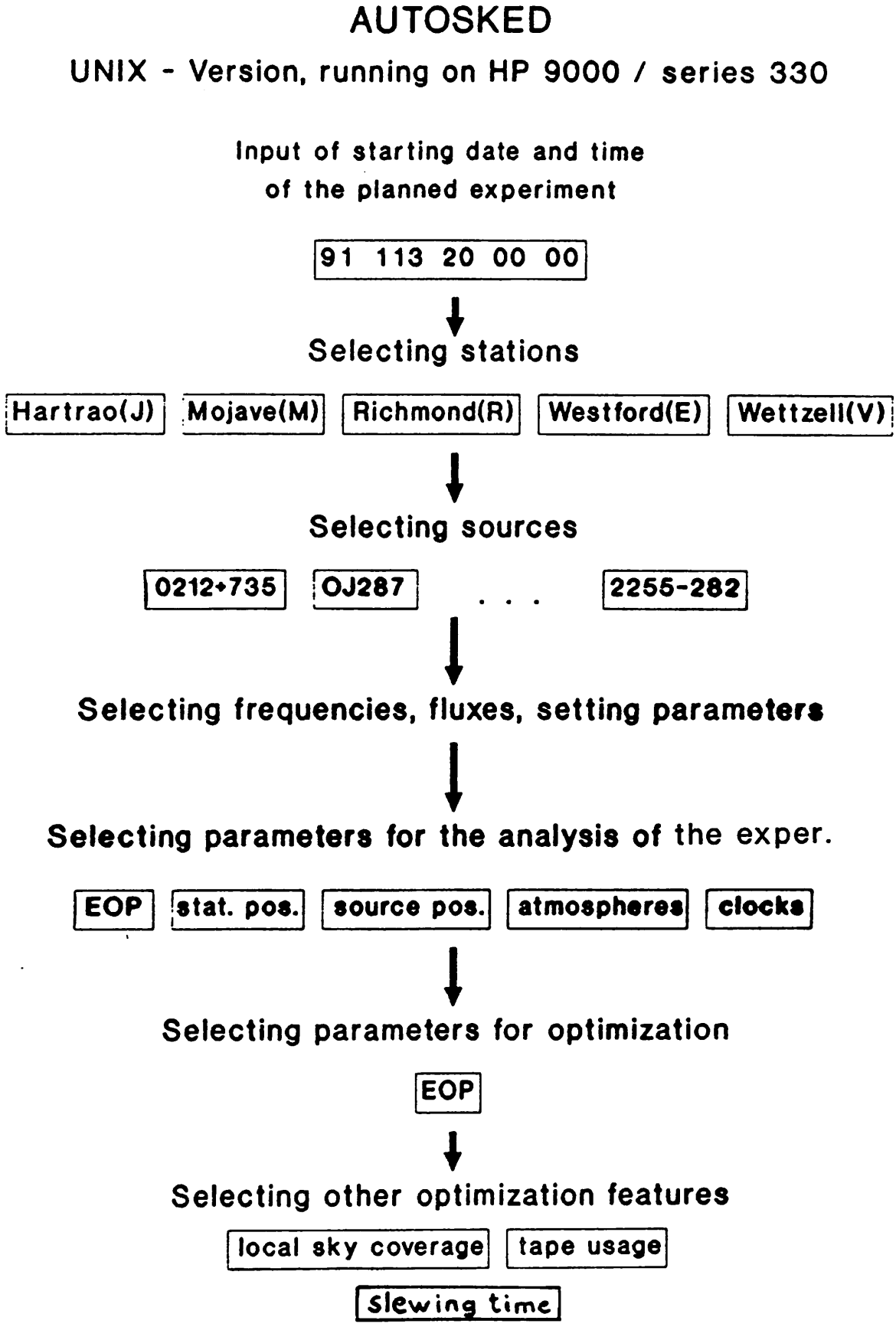

figure 1 : The use of Autosked

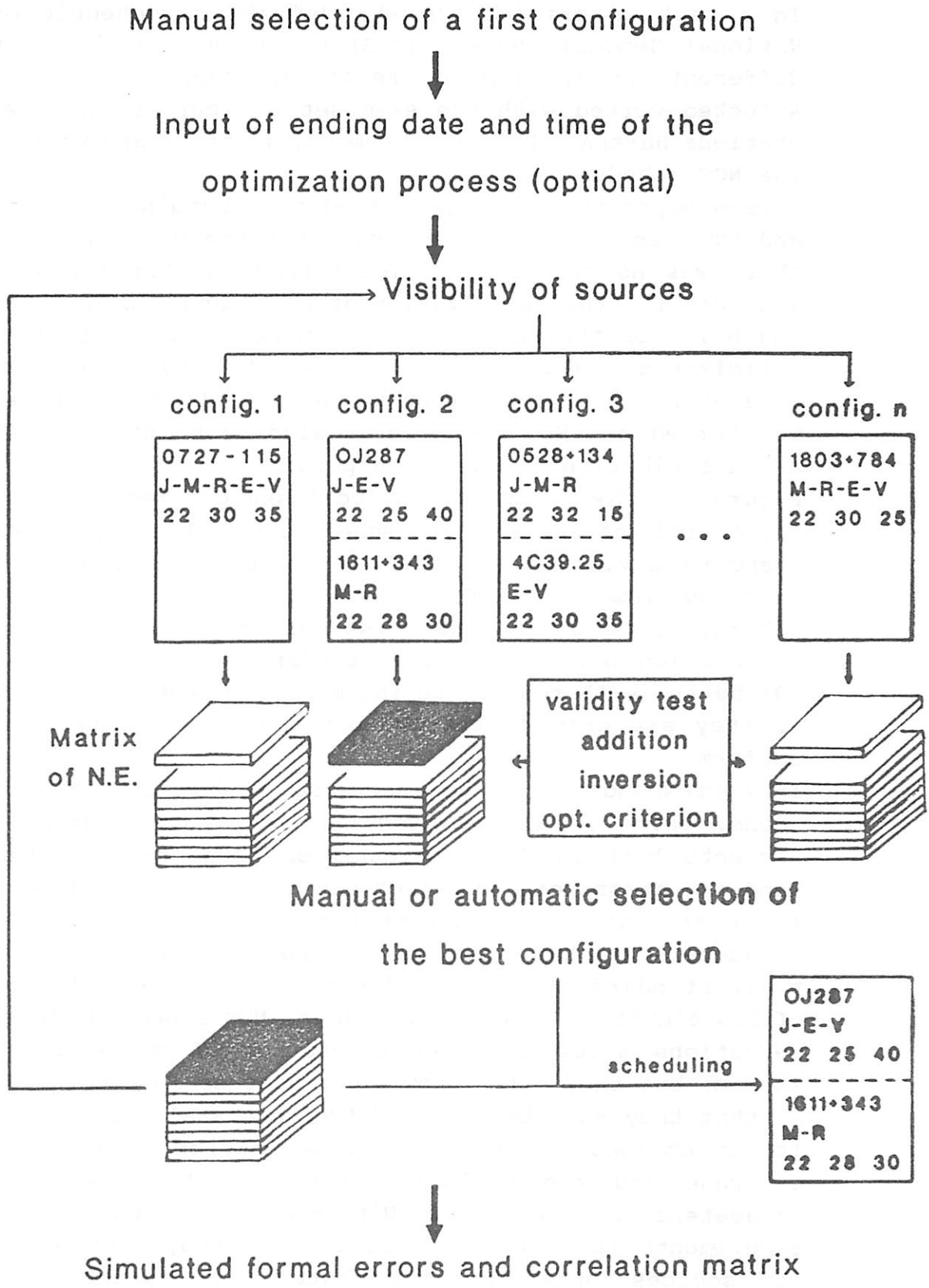

figure 2 : The optimization algorithm

2. Results

In a test an original "hand-made" IRIS-S schedule of the National Geodetic Survey (NGS) has been compared with two different optimized solutions of Autosked.

Autosked worked with the same set of sources and the same stations HartRAO, Mojave, Richmond, Westford and Wettzell as the NGS schedule.

IRIS-S experiments are performed to determine polar motion and UT1. So, for the first run of Autosked (schedule A1), there was no secondary option turned on, but the schedule was done for the optimization of the X and Y pole component and UT1. For the second run of Autosked (schedule A2), the optimization algorithm also selects for these three parameters, but in addition the option "local sky coverage" was turned on. So, the program also took into account the sky distribution of observing points.

Figure 3 shows plots of the local sky coverage of schedule A1, A2 and the original NGS schedule S. Table 1 presents the standard deviations of the unknown parameters due to the Autosked simulation. Schedule A1 is more clumpy than the others, but gives the best accuracy for the earth orientation parameters. The standard deviations are about 10% better with respect to the manual schedule. In schedule A2 they are only 4% better, but the sky coverage is more uniform.

In correspondance to the decrease of the standard deviations, there is also a decrease in the correlation coefficients between Earth orientation parameters on the one hand and atmosphere and clock parameters on the other hand. The correlation coefficients between atmosphere and clock parameters on the stations are however increasing as do their standard deviations. The reason is the higher number of low elevation observations in the NGS schedule. These observations allow a better separation of clock and atmosphere, but they often show wider scatter in the residuals, so that they must be excluded from the analysis.

It is obvious, that there is a compromise between sky coverage and the optimization of the Earth orientation parameters in schedule A2. With the help of data from real experiments the question must be answered, whether or not the sources in A1 are distributed well enough to avoid systematic errors caused by fluctuations in tropospheric wave propagation.

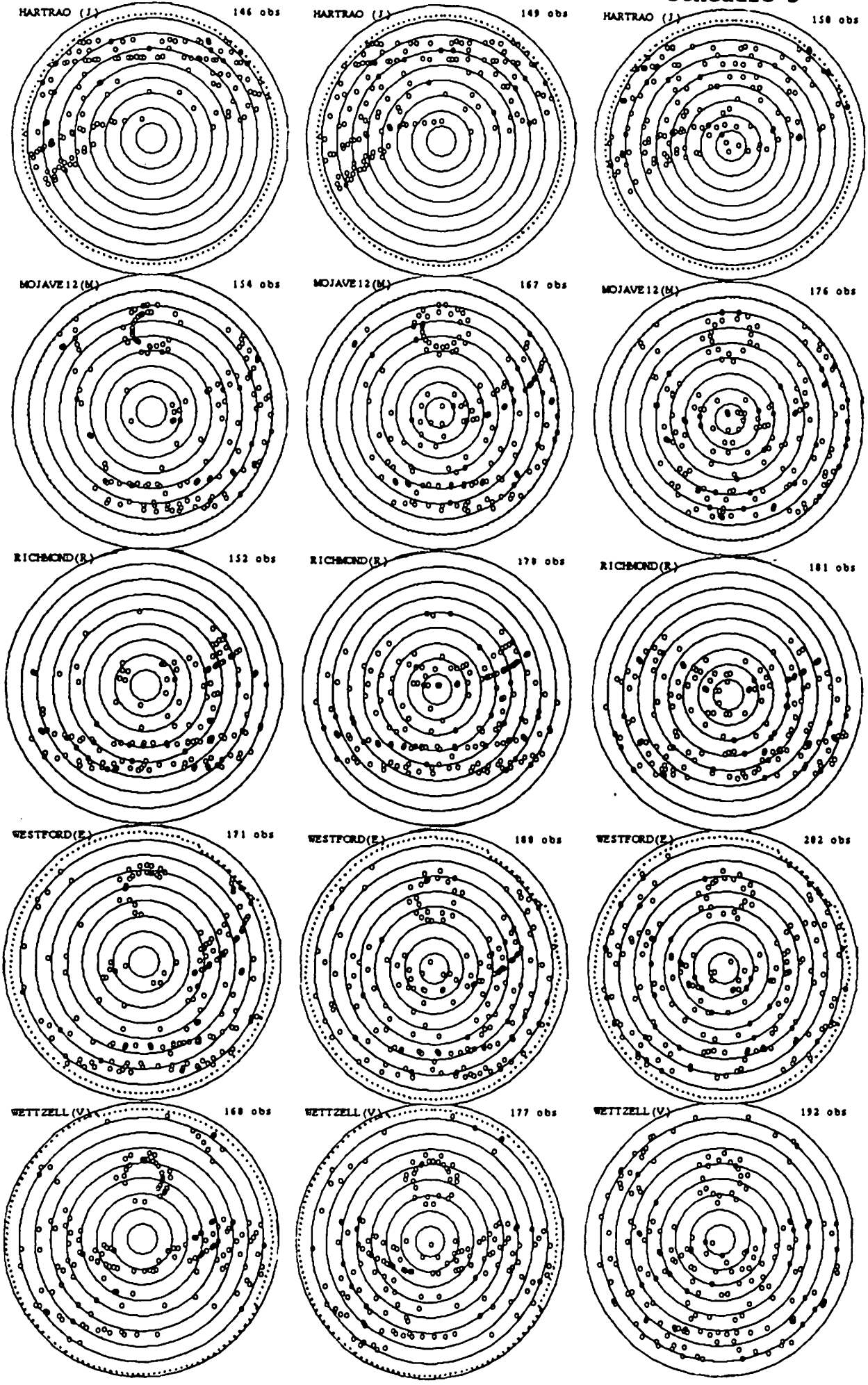
schedule A1
schedule A2
schedule S
HARTRAO (J)
146 obs
149 obs
158 obs
MOJAVE12(M)
154 obs
167 obs
176 obs
RICHMOND(R)
152 obs
170 obs
181 obs
WESTFORD(F)
171 obs
188 obs
202 obs
WETTZELL(V)
160 obs
177 obs
192 obs

	sched. A1	sched. A2	sched. S
number of observations	816	856	989
X pole comp. (asec)	$.1977^{-03}$	$.2069^{-03}$	$.2096^{-03}$
Y pole comp. (asec)	$.1166^{-03}$	$.1221^{-03}$	$.1314^{-03}$
UT1-TAI	$.1255^{-04}$	$.1382^{-04}$	$.1411^{-04}$
Nut. offset in long. (asec)	$.2656^{-03}$	$.2731^{-03}$	$.2857^{-03}$
Nut. offset in obl. (asec)	$.1181^{-03}$	$.1250^{-03}$	$.1216^{-03}$
J atm offset (m)	$.3620^{-02}$	$.3890^{-02}$	$.3945^{-02}$
J atm first rate (m/sec)	$.7529^{-07}$	$.7255^{-07}$	$.7133^{-07}$
M atm offset (m)	$.4340^{-02}$	$.4091^{-02}$	$.3258^{-02}$
M atm first rate (m/sec)	$.8700^{-07}$	$.9300^{-07}$	$.7172^{-07}$
R atm offset (m)	$.5681^{-02}$	$.5147^{-02}$	$.3683^{-02}$
R atm first rate (m/sec)	$.1053^{-06}$	$.9333^{-07}$	$.7413^{-07}$
E atm offset (m)	$.4050^{-02}$	$.3854^{-02}$	$.2709^{-02}$
E atm first rate (m/sec)	$.7142^{-07}$	$.6756^{-07}$	$.5069^{-07}$
V atm offset (m)	$.3036^{-02}$	$.3928^{-02}$	$.2247^{-02}$
V atm first rate (m/sec)	$.6416^{-07}$	$.7241^{-07}$	$.4708^{-07}$
J cl offset (sec)	$.6046^{-10}$	$.6462^{-10}$	$.5734^{-10}$
J cl first rate	$.2156^{-14}$	$.2138^{-14}$	$.2040^{-14}$
J cl second rate (/sec)	$.2127^{-19}$	$.2178^{-19}$	$.2158^{-19}$
M cl offset (sec)	$.6119^{-10}$	$.6078^{-10}$	$.5650^{-10}$
M cl first rate	$.1986^{-14}$	$.2028^{-14}$	$.1890^{-14}$
M cl second rate (/sec)	$.2005^{-19}$	$.2141^{-19}$	$.1932^{-19}$
R cl offset (sec)	$.5533^{-10}$	$.5212^{-10}$	$.4785^{-10}$
R cl first rate	$.1813^{-14}$	$.1655^{-14}$	$.1616^{-14}$
R cl second rate (/sec)	$.1918^{-19}$	$.1891^{-19}$	$.1764^{-19}$
E cl offset (sec)	$.4801^{-10}$	$.4608^{-10}$	$.4134^{-10}$
E cl first rate	$.1674^{-14}$	$.1557^{-14}$	$.1487^{-14}$
E cl second rate (/sec)	$.1814^{-19}$	$.1838^{-19}$	$.1651^{-19}$

table 1 : standard deviations of the unknown parameters from the Autosked simulation

3. Conclusions

Autosked allows to create optimized schedules without great effort. With this software a lot of simulations can be done in order to evaluate networks or test geometric relations. Furtheron, more than one schedule can be created for an experiment and the best one can be selected for the actual run. Although the program needs some hours of computation time, it can run at night without disturbing other users of the computer. Autosked schedules give as good as and often better results than hand-made schedules, but a number of experiments must be performed to decide, whether the clumpiness in the sky coverage does not harm the determination of parameters. A large number of optimization options allows the user to create a schedule best suited for his needs. It is planned to introduce still more optimization features than the three mentioned in this paper.

4. References

Koch, K.R. Parameter Estimation and Hypothesis Testing in Linear Models, Bonn 1987

Vandenberg, N.R. Gregorich, G.A. Sked-Interactive Scheduling Program, Mark III Software Documentation, NASA Goddard Space Flight Center, Greenbelt USA 1990

A Parameterized Solid Earth Tide Model for VLBI: Quality Assessment

Hans-Georg Scherneck

Uppsala University, Dept. of Geophysics, Section of Geodesy, S-755 92 Uppsala, Sweden. E-Mail address: HGIGS@SEUDAC21.BITNET

Summary. A new solid earth tide model for application in precise geodetic measurements has recently been proposed. This contribution summarizes its main features and concepts. Results from a comparison with the currently used module of CALC/SOLV are given.

The model uses recent parameters from tide theory and reliable estimates inferred from observations together with an expansion of the tide generating potential which includes third degree spherical harmonics. It incorporates dynamic effects of the earth mantle and core in closed form and keeps a clear distinction between properties related to the space or the time domain, respectively.

Assuming submillimetre precision and internal consistency of the new model the improvement with respect to tide displacements computed by current software is on the order of five millimeters.

Introduction

A solid earth tide model for precise geodetic methods has recently been presented (Scherneck, 1991). Emphasis has been put on increased accuracy and parameter estimability. Some of its features are described below as a supplement to the report, and a comparison is made to the previous tide model.

The basis of the parameterised solid earth tide model (PSETM) is a decomposition of the tide generating potential in terms of harmonic base functions. This concerns the space domain, where Associated Legendre Polynomials are the set of base functions, as well as the frequency domain, where we have a spectrum of sines and cosines. Recent harmonic tide potential developments have been published by e.g. Buellesfeld, 1985 (Julian date reference 1950), Tamura (1987) and Xi (1987) (both using the J2000.0 system).

Tidal displacements of a site in an instantaneously corotating reference frame depend on the viscoelastic response of the earth and perturbations induced by the liquid core. The transfer function between the signal input into the earth (the tide generating potential) and the output (the observed displacements) connects the two pairs of domains: space and spherical harmonic (SH) degree; time and frequency.

To a good degree of approximation the tide potential is a stationary process, which is the essential basis of harmonic expansion. Explicit time-dependence of earth properties relating to tides does not occur at the present technical level of sensitivity, and transient components in the external tide

Proceedings of the 8th Working Meeting on European VLBI for Geodesy and Astrometry (page IV-30 - IV-38

potential are negligible.

The response of the earth to tides depends primarily on the "wavelength" (SH-degree) of the external potential. The flattening of the earth (and its rotation) is a perturbation from ideal spherical symmetry. As a consequence, the transfer functions depend slightly also on SH-order (which is indicative of orientation). The flattening causes also a coupling of SH as it inflicts on the orthogonality of the base functions.

The earth reacts differently to excitation with different frequencies, resonant and delaying response characteristics being responsible. Hence, the transfer functions are appropriately described by complex valued admittance spectra for single input (SH-degree and order) and multiple output (SH-coupling).

Concepts of the parameterisation

Results from the literature have been adopted for the PSETM as shown in Tab. 1. The term 'parameterised' refers to the way these results are incorporated: Instead of using tables (where frequency would be the entry), frequency-dependent features are described by functions dependent on a minimum of parameters. Forms with a close relation to the underlying physics are preferred. The resonance effects of the liquid core e.g., which occurs when excitation has the near-diurnal frequency ω_{NDR}, are parameterised using the resonance characteristic

$$C_{NDR}(\omega) = \frac{\omega-\omega_{ref}}{\omega-\omega_{NDR}} = C_{NDR}(\omega;\ \omega_{NDR})$$

The key parameter carrying geophysical significance is ω_{NDR}, together with an amplitude coefficient that represents the strength of the resonance. A slightly complex value can be substituted for ω_{NDR} right away, referring to finite quality of the resonance.

An empirical function, however, is more convenient to characterize the viscoelastic admittance spectrum. The reason is that viscoelastic models cover a wide range of frequencies, whereas geodetic methods operate in the narrow slice of daily to yearly periodicities. Much of the structural information about thermally excited relaxation in the earth's mantle is therefore hidden. An asymptotically correct description of the relaxation spectra, tailored for the frequency domain in question, can be given with a few comprehensive key parameters.

The phase spectrum of displacement component ι of the response as computed by Wang (1986) follows roughly

$$\phi^{(\iota)}(\omega) = -\mathrm{sgn}(\omega)\ \Phi_0^{(\iota)}\ |\omega|^{p^{(\iota)}} \qquad 2\pi/(10\ \mathrm{y}) \le \omega \le \infty$$

The attenuation (= log amplitude) spectrum compatible with this phase spectrum is reconstructed using Hilbert transformation,

$$\eta^{(\iota)}(\omega) = \mathcal{H}_{p\to a}\{\phi^{(\iota)}(\omega)\} + \mathrm{const.}$$

$$V^{(\iota)}(\omega) = \exp\{\eta^{(\iota)}(\omega) + i\phi^{(\iota)}(\omega)\} = V^{(\iota)}(\omega;\ \Phi_0^{(\iota)}, p^{(\iota)})$$

referring to the causality of the earth as responding medium. The transform can be obtained analytically (Scherneck, 1991) and contains one parameter in addition to Φ_0 and p, representing the amplitude of the elastic response. The viscoelastic relaxation spectrum is negligible in the case of SH-degree greater than two.

Table 1 Literature references to parameters and submodels. For numeric values and suggested formulas *cf* Scherneck, 1991.

Parameter	Reference
ω_{NDR}	Herring et al, 1986; Neuberg et al., 1987.
Q_{NDR}	Neuberg et al., 1987.
S_{NDR}, solid earth	Wahr, 1981; Wahr & Bergen, 1986.
..., oceanic	Wahr & Sasao, 1981.
Φ_0, p (anelasticity)	Wang, 1986.
H_ν, L_ν, β_n, $\beta_{nm\nu\mu}$	Wahr, 1981; Dehant, 1987; Farrell, 1972.

Relation to tide theory.
In short-hand notation, the input-output relation along the lines of the results of Wahr (1981) can be written

$$\underline{y}(\underline{r}_s,t) = \mathcal{R}e \sum_k \sum_{\nu\mu nm} \underline{\underline{s}}\, \underline{\underline{L}}_{\nu\mu nm}(\omega_k)\, X_{nm}(\omega_k,R)\, \mathcal{Y}_{\nu\mu}(\underline{s}_s)\, \exp\{i\omega_k t\}$$

where the X_{nm}'s are the development coefficients of the external tide potential evaluated at conventional radius R and include phase (astronomical argument at epoch t=0, $X_{nm}\in\mathbb{C}$); $\underline{y}$ are the tide components at the position $\underline{r}_s$ on the earth surface; $\underline{s}_s$ is the projected position on the unit sphere; and $\mathcal{Y}_{nm}$ is a set of spheroidal and toroidal base functions (vector SH's); $\underline{\underline{L}}$ is an array of generalized Love number spectra, including the coupling coefficients between different degrees and orders due to earth ellipticity. Diagonal matrix $\underline{\underline{s}}$ provides dimensional scaling in order to get dimensionless Love parameters ([X] = m^2s^{-2}). Convenient (and in line with Wahr, 1981) for the case of displacements is $s=1/g_e$ and $R=R_e$, i.e. gravity for scaling and radius at the equator for tide potential reference, respectively.

The displacement at time t can be written

$$\underline{u} = \begin{pmatrix} u_r \\ u_\vartheta \\ u_\lambda \end{pmatrix} = \mathcal{R}e \sum_{knm} \underline{\underline{L}}_{\nu\mu nm}(\omega_k) \begin{pmatrix} (\mathcal{Y}_{nm})_r \\ (\mathcal{Y}_{nm})_\vartheta \\ (\mathcal{Y}_{nm})_\lambda \end{pmatrix} X_{nm}(\omega_k)\, \exp\{i\omega_k t\}$$

in a coordinate system r=radial, ϑ=south, λ=east.

The last step is to devise a factorisation scheme for the elements of the L-array to individually represent SH coupling (earth flattening effects), liquid core resonance and viscoelastic mantle relaxation. The result is

$$\underline{\underline{L}}_{\nu\mu nm}(\omega) = \begin{pmatrix} G & 0 & 0 \\ 0 & G & s \\ 0 & s & G \end{pmatrix}, \quad (G = \text{great}, \; s = \text{small term})$$

$$= \begin{pmatrix} H_\nu[1+\beta^{(h)}_{\nu\mu nm}+(S^{(h)}_{NDR}+\sigma^{(h)}_{21n1})C_{NDR}(\omega)\delta_{\nu 2}\delta_{\mu 1})]V^{(h)}_\nu(\omega) & 0 & 0 \\ 0 & & \\ 0 & L_\nu[\underline{1}+\underline{\beta}^{(l)}_{\nu\mu nm}+(\underline{1}S^{(l)}_{NDR}+\underline{\sigma}^{(l)}_{21n1})C_{NDR}(\omega)\delta_{\nu 2}\delta_{\mu 1})]V^{(l)}_\nu(\omega) & \end{pmatrix}$$

where $\beta^{(\ell)}_{\nu\mu nm}$ and $\sigma^{(\ell)}_{21n1}$ are the coefficients for ellipsoidal perturbation and their nearly-diurnal resonance strengths, respectively,

$$C_{NDR}(\omega) = C_{NDR}(\omega;\ \omega_{NDR}) = C(\omega,\ \Omega_{NDR}(1+iQ_{NDR})) \in \mathbb{C}$$

is the nearly-diurnal resonance characteristic,

$$V_v^{(\iota)}(\omega) = V_v^{(\iota)}(\omega;\ p^{(\iota)},\Phi_0^{(\iota)}) \in \mathbb{C}$$

the viscoelastic relaxation spectrum,

$$S_{NDR}^{(\iota)} = S_{SE}^{(\iota)} + S_{OL}^{(\iota)} = \text{const.} \in \mathbb{C}$$

are the solid earth (SE) and ocean loading tide interaction terms describing the strength of the near diurnal resonance, and

$$H_v = \text{const.} \in \mathbb{R},\ L_v = \text{const.} \in \mathbb{R}$$

are so-called basic Love numbers. Since tides at degree $v>2$ are small, one can factor out H_2 and scale the others using $\beta_v = H_v/H_2$ (and equivalently for L_v). The parameters H_2 and L_2 are then primary candidates for estimation from observations.

It is pointed out that the form above differs from the actual equation used in Scherneck (1991), the one above being somewhat clearer for the purpose of demonstration, but less convenient to actually program. (Spherical harmonic coupling can be formulated even simpler. Then, many of the coupling coefficients turn out to be zero or negligibly small.)

It is now straight forward to compute time series of station displacements and partial derivatives with respect to any of the model parameters. Since the influence of Ω_{NDR}, Q_{NDR}, Φ_0 and p is nonlinear, we depend on a good estimate to start from; the respective parameter partial can then safely be derived using a first order divided difference.

The scheme offers access to model parameters and their refinement at the data analysis stage. It should be obvious that their physical basis and relevance is more significant than in the case of the model employed in programs like CALC/SOLV and GEODYNE. Table 2 points out the difference between the previous CALC/SOLV model and the proposed one.

It is also pointed out that the use of SH coupling coefficients is conceptually clearer than an alternative scheme often encountered in analysis of tide gravity measurements, which consists of the use of latitudinally dependent Love numbers and gravity admittance factors with respect to the local tide potential.

Parameter use and interrelations

A number of PSETM parameters can be used by other VLBI program modules. For instance, the rheological model can be extended to the secondary potential by means of the spectrum of Love number k_2. The sources of the secondary potential at SH degree two perturb the moments of inertia and thus are relevant for the tidal part of the ΔUT1 model. Next, the load Love number k_2' can be included which conveys the solid earth part of the polar motion perturbations due to oceanic tides. Finally, the NDR parameters influence the amplitudes of the nutation series.

Further, the following parameters interrelate within global geodynamics: The Chandlerian motion, which is not forward-modelled in CALC, occurs at a frequency affected by the relaxation of Love

number k_2. The parameters S_{OL} relate to ocean tide perturbations of satellite orbits. The NDR frequency is a translation of the free core nutation frequency into the rotating system.

In summary, PSETM attempts to work with a comprehensive set of key parameters, of which several have general importance, be it within the forward models of a VLBI analyzing software package or in terms of interpretation of results.

Accuracy evaluation and discussion

In order to evaluate the level of significance of the proposed model, synthetic tides are computed and compared to a set derived on the basis of the CALC formulation. CALC's solid earth tide model follows largely the GEODYNE code prior to an update by Christodoulidis et al. (1988) and is outlined in the IERS Standards (McCarthy, 1989). Some minor modifications exist, however.

In order to avoid error propagation due to the possible difference between actual lunar-solar ephemeris in CALC and the tide potential used for the test (Buellesfeld, 1985), only the CALC formulas - or, alteratively, the formulas in the IERS Standards - that follow after this stage are considered, assuming that the external potential of tides with degree two is exactly the same in each case.

CALC neglects tides with degree three and four. They turn out to be the major reason for the discrepancy found, which amounts to four millimetres at maximum in my test (*cf* Fig. 1). This is within the accuracy claimed in IERS Standards. A modified formalism actually used in CALC results in a sightly smaller error (*cf* Fig. 2). The modification is that CALC evaluates the ellipsoidal gravity formula at the latitude of the site to scale the tide potential, whereas IERS Standards propose a scaling factor $GM_{trb}r_s^4/(M_eR_{trb}^3)$ (trb = tide raising body, e = earth, s = site). The presently used value of Love number h_2 in CALC differs also slightly from the one documented in IERS Standards, which is identical to Wahr's result if SH coupling is set to zero. However, setting the coupling coefficients to zero does not provide a correct average of an effective h_2 over all latitudes, something which the CALC designers/users might have realized.

PSETM uses the scaling **constant** g_e as given by Wahr (1981) and thus avoids confusion between earth flattening perturbed tide response and latitudinally dependent scaling factors. PSETM's latitudinal dependence is uniquely conveyed through the SH coupling coefficients.

CALC's and GEODYNE's use of ephemeris for the position of earth, moon and sun might seem an advantage at a first glance, expecting higher accuracy for the tide potential computed at the time of observation. However, modern harmonic developments are accurate at a level of one part per ten thousand (Wenzel and Zürn, 1990), translating to 0.03 mm in the vertical component. The disadvantage of ephemeris based processing is, however, that subsequent computation stages remain in the time domain. There, delay properties of the earth are cumbersome to carry out consistently. They require convolution integrals over time, the integral domains being much wider than the time window for an experiment.

CALC utilizes questionable short-cuts to obtain approximations of the effects of NDR and viscoelasticity: A correction is applied on h_2 for the most susceptible partial tide, K_1. The effect on the other diurnal tides and on the horizontal displacements is neglected. The viscoelastic lag of the deformation field (the so-called

tidal bulge, which in reality is time-delayed) is conceived as if the field were rotated in space. CALC/SOLV's lag angle parameter specifies the amount of rotational shift of the positions of the tide raising bodies around the ecliptic pole and is one of the solve-for parameters. The formulation has unfortunate consequences: The zonal, long-period tide phases are hardly affected at all, whereas the effect on semidiurnal terms becomes two times that of the diurnal species. The effect of relaxation on the amplitudes cannot be represented. All displacement components are affected equally; instead, the lag angle becomes dependent on site latitude. Physical reality is rather the contrary: The displacement delay increases towards longer periods and is in the horizontal component six times greater than in the vertical. The admittance amplitude increases towards lower frequencies.

It is more difficult to mimic CALC's treatment of the tide bulge lag without using ephemeris. In order to obtain an approximation, the site position vector in the ecliptic frame is rotated in a clockwise sense, *i.e.*

$$\underline{r}_{s,lag}(t) = \mathcal{R}_3(-\Omega t+h)\mathcal{R}_1(\eta)\mathcal{R}_3(\ell)\mathcal{R}_1(-\eta)\mathcal{R}_3(\Omega t-h)\ \underline{r}_s$$

$$\Delta\underline{r}_{lag}(t) = \underline{r}_{s,lag}(t) - \underline{r}_s$$

with ℓ as the lag angle; η denotes the obliquity of the ecliptic, and h is the argument of the solar longitude. Partial derivatives of displacement time series with respect to eastward and southward shifts of the station, $\Delta\underline{r}_E$ and $\Delta\underline{r}_S$, are computed by divided differences. Then, the CALC simulated displacements result from

$$\underline{u}_{lag}(t) = \underline{u}(\underline{r}_s,t) + \frac{\underline{u}(\underline{r}_s+\Delta\underline{r}_E,t)-\underline{u}(\underline{r}_s,t)}{|\Delta\underline{r}_E|^2}\,\Delta\underline{r}_{s,lag}(t)\cdot\Delta\underline{r}_E +$$

$$+ \frac{\underline{u}(\underline{r}_s+\Delta\underline{r}_S,t)-\underline{u}(\underline{r}_s,t)}{|\Delta\underline{r}_S|^2}\,\Delta\underline{r}_{s,lag}(t)\cdot\Delta\underline{r}_S$$

The discrepancy between $\underline{u}_{lag}$ and a time series computed by PSETM is shown in Fig. 3 and 4. The lag angle ℓ is adjusted such that the phase of the M_2 tide agrees at the start of both time series. For Fig. 3 Love number values according to CALC are used; adjusted values are used in Fig. 4 in order to match the viscoelastic relaxation of the M_2 tide introduced by PSETM. This Love number adjustment is seen to remove a large part of the semidiurnal variations. The remaining diurnal signatures, however, are due only partly to additional viscoelastic relaxation at these lower frequencies; a second source of discrepancy stems from CALC's rough NDR model.

For Fig. 5 the viscoelastic relaxation spectrum is applied on tides from the elastic part of the CALC-simulation and the displacement series is compared with the bulge rotation simulation. This suppresses effects from the NDR model. Long-period tides are now clearly seen and indicate that the bulge rotation method does not treat these species properly.

Conclusions

The proposed model appears more consistent for the part of its formulation and is expected to provide tide predictions at a submillimeter accuracy level. A set of solve-for parameters is offered, of which four represent sensitive gross earth properties:

Basic Love numbers and their relaxation due to mantle rheology. It is computationally more voluminous but is independent of supply with planetary ephemerides.

References

Büllesfeld, F.-J., 1985. Ein Beitrag zur harmonischen Darstellung des gezeitenerzeugenden Potentials, *Dt. Geod. Komm., Reihe C*, 314, Bayer. Akad. Wiss., München.

Christodoulidis, D. C., Smith, D. E., Williamson, R. G. & Klosko, S. M., 1988. Observed tidal braking in the earth/moon/sun system, *J. Geophys. Res.*, 93 B6, 6216-6236.

Dehant, V., 1987. Tidal parameters for an inelastic earth, *Phys. Earth Planet. Inter.*, 49, 97-116.

Farrell, W. E., 1972. Deformation of the earth by surface loads, *Rev. Geophys. Space Phys.*, 10, 761-797.

Herring, T. A., Gwinn, C. R. & Shapiro, I. I., 1986. Geodesy by radio interferometry: Studies of the forced nutations of the earth. 1. Data analysis, *J. Geophys. Res.*, 91, B5, 4745-4754.

McCarthy, D.D. (ed.), 1989. IERS Standards (1989). *IERS Technical Note* 3, Observatoire de Paris, 76pp.

Neuberg, J., Hinderer, J. & Zürn, W., 1987. Stacking gravity tide observations in central Europe for the retrieval of the complex eigenfrequency of the nearly diurnal free-wobble, *Geophys. J. R. astr. Soc.*, 91, 853-868.

Scherneck, H.-G., 1991. A parameterised earth tide observation model and ocean tide loading effects for precise geodetic measurements, *Geophys. J. Int.*, in print, preprint available.

Tamura, Y., 1987. A harmonic development of the tide generating potential, *Bull. d'Inform. Marées Terr.*, 99, 6813-6855.

Wahr, J. M., 1981. Body tides on an elliptical, rotating, elastic and oceanless earth, *Geophys. J. R. astr. Soc.*, 64, 677-704.

Wahr, J. M. & Bergen, Z, 1986. The effects of mantle anelasticity on nutations, earth tides and tidal variations in rotation rate, *Geophys. J. R. astr. Soc.*, 64, 747-766.

Wahr, J. M. & Sasao, T., 1981. A diurnal resonance in the ocean tide and in the earth's load response due to the resonant free 'core nutation', *Geophys. J. R. astr. Soc.*, 64, 747-766.

Wang, R., 1986. Das viskoelastische Verhalten der Erde auf langfristige Gezeitenterme, *Dipl. Thesis*, Mat.-Nat. Fak. Univ. Kiel.

Wenzel, H.-G. & Zürn, W., 1990. Errors of the Cartwright-Tayler-Edden 1973 tidal potential displayed by gravimetric earth tide observations at the BFO Schiltach, *Bull. d'Inform. Mareés Terr.*, 107, 7559-7574.

Xi Qin Wen, 1987. A new complete development of the tide generating potential for the epoch J 2000.0, *Bull. d'Inform. Marées Terr.*, 99, 6813-6855.

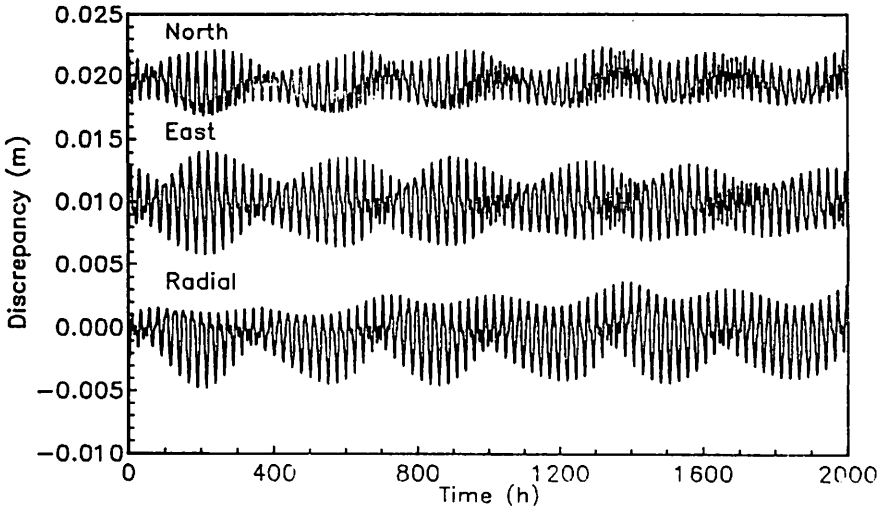

Figure 3 Time series of tidal displacements for a site at 30° colatitude computed with the new model from which the CALC simulated time series have been subtracted. The CALC simulation includes approximation for the viscoelastic delay of the tidal bulge by a small, rigid rotation of the displacment field.

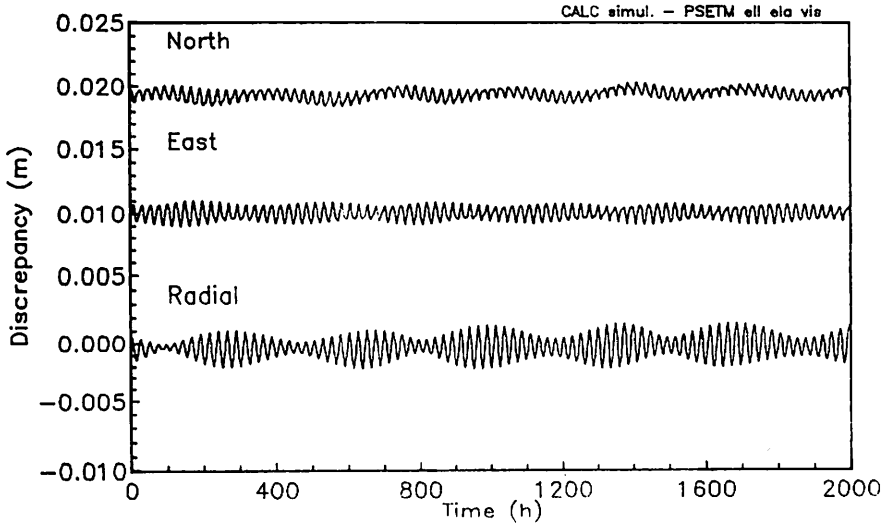

Figure 4 Equivalent Fig.3. Love numbers in the CALC simulation were adjusted in order to yield an exact fit of the two models for the partial tide M_2, however.

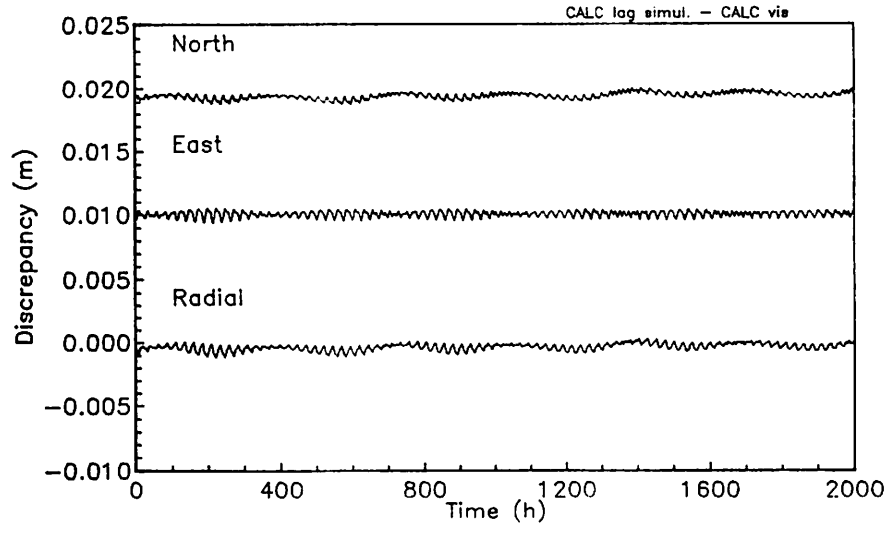

Figure 5 The inconsistency of the bulge rigid rotation concept of CALC is demonstrated by applying the viscoelastic relaxation spectrum of the new model on CALC tides for an elastic earth and comparing the resulting time seriers with those using CALC's bulge rotation method. The difference between the two pairs of time series contains an enhanced fraction of long-period tides.

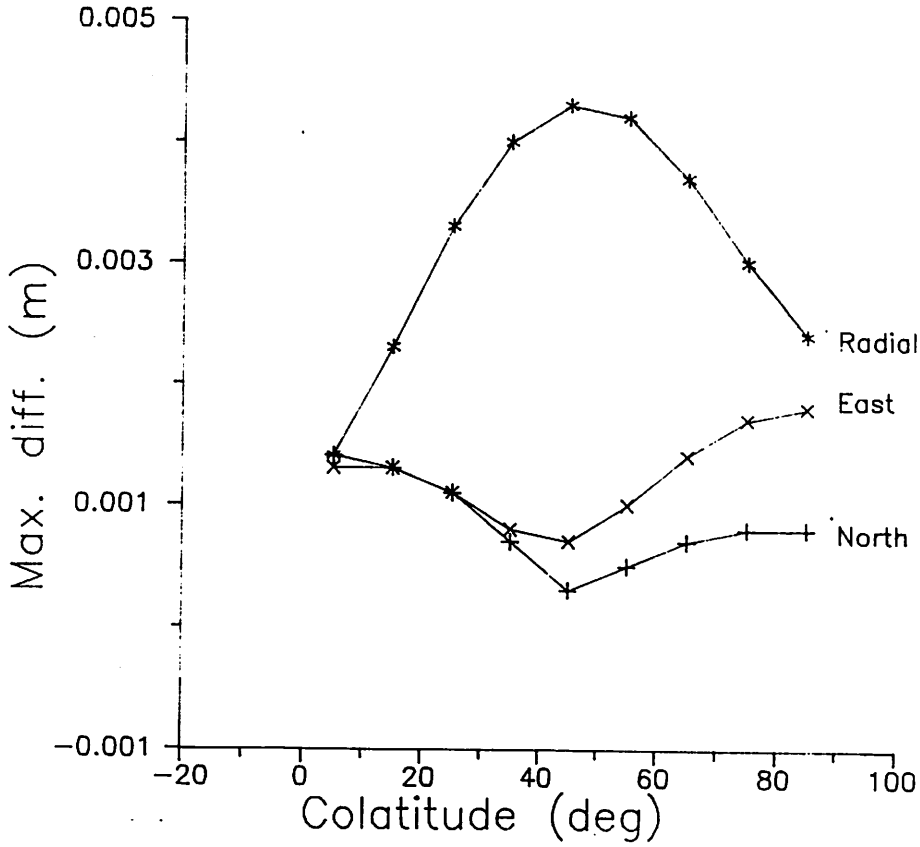

Figure 1 Discrepancy between the old and the proposed tide models as a function of colatitude. The formula as documented in IERS Standards has been employed for the relation between external tide potential and site displacements. Time series with 8000 hourly samples have been used in the analysis.

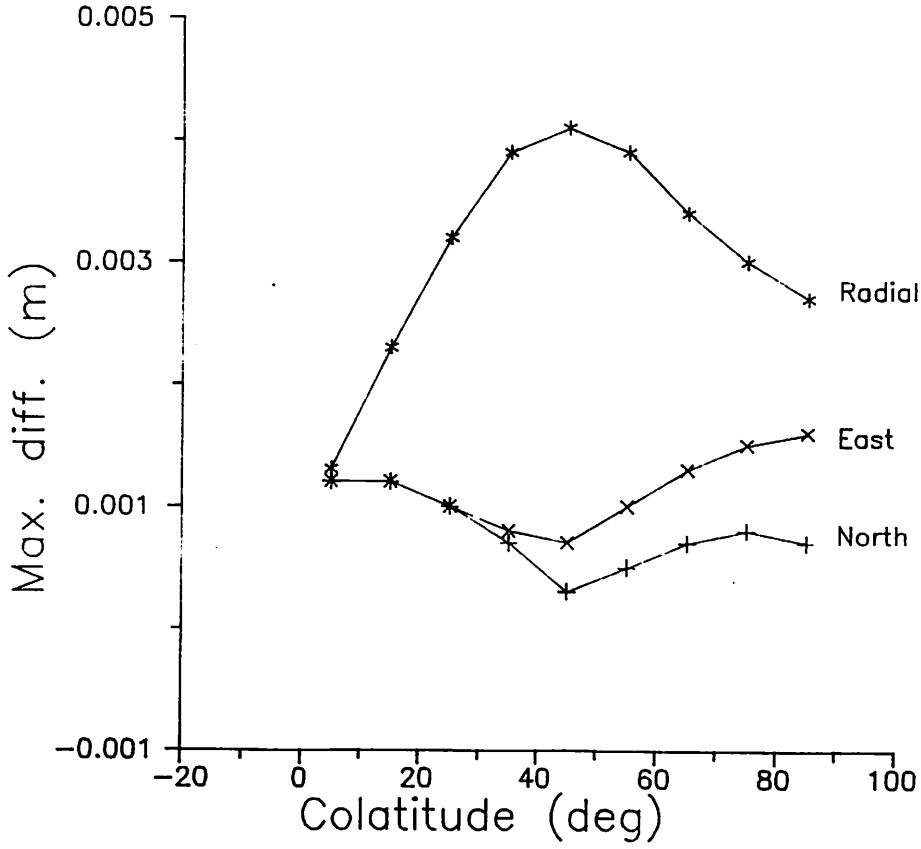

Figure 2 Equivalent Fig. 1. Modifications of CALC as regards scaling (normal gravity) and Love numbers have been employed, however.

FREE NETWORK ADJUSTMENT IN VLBI DATA ANALYSIS

Berthold Plietker
Institute of Photogrammetry
Stuttgart University, Germany

and

Harald Schuh
DLR (German Aerospace Research Establishment)
Cologne, Germany

ABSTRACT: Free network adjustment as a more general way of computing VLBI solutions is introduced. The matrix of constraints which is necessary to compute a pseudoinverse or symmetrical reflexive generalized inverse has been derived analytically. On this basis a software package for VLBI free network adjustment has been developed. Numerical tests confirm the soundness of approach.

1. INTRODUCTION

The datum choice in VLBI solutions usually is made by keeping a sufficient number of parameters fixed so that there is no rank deficiency in the normal equation matrix. For instance, at least one triplet of station coordinates (x,y,z) has to be kept fixed if the station positions or the baseline lengths, respectively, should be solved for. For solutions of single experiments, i. e. VLBI sessions between a few hours and two days usually not only the minimum number of parameters is kept fixed but many more depending on the set of parameters which are to be solved for, e. g. if the analyst is interested in the Earth rotation parameters most of the station coordinates and most of the radio source positions will be kept fixed. A more general approach for the datum choice is the free network adjustment. Here, no parameters are kept fixed but the datum is selected via matrices of constraints keeping the changes of those parameters minimal which are considered decisive for datum definition. In this paper the analytical derivation of such a matrix of constraints is given.

As in the adjustment of classical geodetic networks the fixing of one or a few of the station positions influences the form of the error ellipsoids of the others. For instance, on transatlantic baselines usually the coordinates of WESTFORD, Massachusetts, U.S.A., are kept fixed. This yields relatively big variances of the coordinates of the European stations with respect to the American stations. A free network adjustment on the other hand puts constraints on all participating stations and gives WESTFORD also a variance while those of the European stations are reduced. Thus, the variance/covariance matrix becomes more plausible. Another example is the estimation of radio source positions in a global solution of many VLBI-sessions. Until the end of the last decade, usually the right ascension of one radio source was kept fixed. This makes the coordinate system dependent on that radio source, i. e. any motion of the center of the source, for instance due to source structure effects, will appear as a systematic rotation of the whole system. The application of free network adjustment allows more than one radio source up to all radio sources to be employed for the definition of the datum as successfully applied in recent global VLBI solutions, for instance by Ma et al. (1990).

It has to be kept in mind that free network adjustment does not result in a better accuracy of the network. The application of a datum transformation (Koch, 1988) as a post-processing step after a conventional solution can yield the same results as the free network adjustment. Nevertheless, a datum transformation also depends on the matrix of constraints which will be derived in this paper.

A case where free network adjustment should be applied is the evaluation of the quality of a network

design. Most of the methods in use, as for instance DOP (Dilution of Precision) factors (Plietker and Schuh, 1991, this issue), are based on the inverse of the normal equation matrix. The appearance of the normal equation matrix depends strongly on the datum used. Free network adjustment then delivers a minimum norm solution, i. e. the trace of the variance/covariance matrix becomes a minimal one for the parameters chosen to contribute to the datum.

2. MODEL USED

Usually a Gauss Markov Model with full rank is used for VLBI adjustment while for the free network adjustment the rank of the design matrix is assumed to be smaller or equal to the number of unknown parameters.

As a functional model of the geodetic application of VLBI the equation for the pure geometric time delay is chosen:

$$\Delta\tau = -\frac{1}{c}\vec{b}\cdot\vec{k} \tag{1}$$

with

$$\vec{k} = \vec{k}(\alpha,\delta)\ , \quad \vec{b} = \vec{b}(T,\Delta x,\Delta y,\Delta z)$$

and

$$T = T(\Delta\psi,\Delta\varepsilon,DUT1,x_p,y_p)$$

For the derivation of the matrix of constraints we assume that the velocity of light c, i. e. the scale factor, is a parameter to be estimated as are the station coordinates (x, y, z) and radio source positions (α, δ), respectively, and the transformation parameters T. The latter ones connect the two systems in which the station positions and radio source coordinates are defined. They include the nutation parameters $\Delta\psi$, $\Delta\varepsilon$, the variation of Earth rotation $DUT1$, and polar motion x_p, y_p. All parameters are thought to undergo no changes with time.

3. DATUM PROBLEM

The datum problem is founded in the noninvertibility of the normal equation matrix because of a rank deficiency of the design matrix. The reason for this can be either a critical configuration of the observation network which will not be treated here or a poor definition of the coordinate system. As mentioned above the latter case is normally dealt with by fixing specific parameters to make the normal equation matrix regular. In this paper the computation of a minimum or partial minimum norm solution is proposed. Therefore the pseudo inverse, also called Moore-Penrose inverse, or a symmetrical reflexive generalized inverse ,respectively, is needed.

As seen in the equation for the pseudo inverse

$$(X'X)^{+} = (X'X+E'E)^{-1} - E'(EE'EE')^{-1}E \tag{2}$$

and in the equation of the symmetrical reflexive generalized inverse

$$(X'X)^{-} = (X'X+B'B)^{-1} - E'(EB'BE')^{-1}E \tag{3}$$

the matrices of constraints E and B are required. Those can be determined either by a numerical or an analytical approach. The former has the disadvantage of a much higher numerical effort than the latter since the normal equation matrix has to be reduced twice, once for the derivation of the matrix of constraints and then again for the real inversion. Furthermore, the analytical derivation of the matrix of constraints provides a more general idea how the choice of the datum influences the error distribution. Thus, the analytical approach was chosen and will be described in this paper.

4. ANALYTICAL APPROACH

The approach which is applied is based on the properties of the matrix of constraints E. As one of the main attributes of E the columns of E' are the base of the Null space of the design matrix X, i. e.

$$XE' = 0 \tag{4}$$

Because of (4) the next formula can be given:

$$\vec{y} = X_t\vec{\beta}_t = X\vec{\beta} + XE'\vec{t} \tag{5}$$

with $\vec{y}$ as the vector of the observables, $\vec{\beta}$ as the vector of the unknown parameters and $\vec{t}$ as the vector of the transformation parameters. Thus, in E' all the changes of the unknown parameters are contained which do not alter the observables.

This yields the general approach:

$$\Delta\tau = f(\vec{\beta}_t) = h(\vec{\beta},\vec{t}) , \quad \vec{t} = \vec{0} \tag{6}$$

Because (6) is usually a non-linear formula of the unknown parameters a linearization has to be carried out, which leads to

$$d\Delta\tau = \frac{\partial f}{\partial\vec{\beta}_t}d\vec{\beta}_t = \frac{\partial h}{\partial\vec{\beta}}d\vec{\beta} + \frac{\partial h}{\partial\vec{t}}d\vec{t} \tag{7}$$

After substituting $\frac{\partial f}{\partial\vec{\beta}} = \frac{\partial h}{\partial\vec{\beta}} = \vec{x}'$ and $\frac{\partial h}{\partial\vec{t}} = \frac{\partial h}{\partial\vec{\beta}}\cdot\frac{\partial\vec{\beta}}{\partial\vec{t}} = \vec{x}'\cdot A'$ formula (7) can be rewritten:

$$d\Delta\tau = \vec{x}_t'd\vec{\beta}_t = \vec{x}'d\vec{\beta} + \vec{x}'A'd\vec{t} \tag{8}$$

The vector $\vec{x}'$ contains the derivatives of the observable $\Delta\tau$ for the unknown parameters and, hence, is the respective column of the design matrix. A' is the matrix of the derivatives of the unknown parameters for the transformation parameters. Thus, due to the identical structure of equations (5) and (8) from A' the matrix of constraints E' can be derived.

Since an infinitesimal transformation is assumed the following expression can be obtained from equation (8) by comparison of the coefficients:

$$d\vec{\beta}_t = d\vec{\beta} + A'd\vec{t} \tag{9}$$

which forms a basic set of equations.

As a special approach for $h(\vec{\beta},\vec{t})$ a concatenated infinitesimal similarity transformation is chosen. However, this causes a problem: $\vec{x}'A' \neq \vec{0}$ because A' does not contain the null space of the design matrix which was the main property of the matrix of constraints E'. This problem can be solved by splitting the matrix into two submatrices $A' = A'_1 + A'_2$ with $\vec{x}'A'_1 = \vec{x}'A_2$. By definition of two other matrices $E'_1 := A'_1$ and $E'_2 := -A'_2$, respectively, which are put together again $E'_p := E'_1 + E'_2$ the fulfillment of $\vec{x}'E'_p = \vec{0}$ can be achieved. This shows that the approach which was chosen was appropriate for the derivation of the matrix of constraints we are looking for.

By the application of (6) and (8) to the basic equation (1) via (9) the matrix A' is obtained. From A' the matrix of constraints E'_p is derived as described above. By this procedure, 10 linear independent columns of E'_p are obtained. It should be noticed that E'_p has some additional columns which are linear dependent. This means that 10 constraints are necessary to solve the rank deficiency in this particular model with the unknown parameters of equation (1). This has been confirmed by the authors by an independent numerical method using 'Googe-numbers' (Schwarz, 1978). The final matrix of constraints E' which can be used in the free network adjustment is obtained by selecting 10 columns out of E'_p which have to be linear independent. One possible choice is the following one:

$E' =$

m	a	b	c	d	e	f	u	v	w	
c	0	0	0	0	0	0	0	0	0	c
0	-tanδcosα	-tanδsinα	1	0	0	0	0	0	0	α
0	sinα	-cosα	0	0	0	0	0	0	0	δ
0	-1	0	0	0	0	0	0	0	0	Δε
0	0	1/sinε	0	0	0	0	0	0	0	Δψ
0	0	0	0	0	0	-1/ω	0	0	0	DUT1
0	0	0	0	0	1	0	0	0	0	x_p
0	0	0	0	1	0	0	0	0	0	y_p
x	0	0	-y	0	z	-y	1	0	0	x
y	0	0	x	-z	0	x	0	1	0	y
z	0	0	0	y	-x	0	0	0	1	z

(10)

The scale factor m, six rotations a, ..., f and three translations u, v, and w are necessary as transformation parameters. If fewer parameters are to be solved for a different matrix of constraints is obtained. If, for instance, the nutation parameters shall not be estimated the respective rows - i. e. the fourth and fifth in matrix E' in (10) - and the columns beneath the rotation parameters a and b - i. e. the second and third in the same place - have to be eliminated and the matrix of constraints fits to the problem. Thus, in this case, the matrix of constraints of the new problem is a submatrix of E' in (10).

5. EXAMPLES

A PC-based software package for free network VLBI solutions has been developed at Geodetic Institute,

Bonn and comprehensive tests have been carried out (Plietker, 1990). The software which allows the use of real observing schedules as well as of simulated observing schedules, is based on the geometric VLBI equation (1). It has been shown indeed that by the application of the E' matrix (10) a 'total' free network solution can be performed successfully, i. e. it is not necessary any more to keep some of the parameters fixed as in the 'standard' least squares solution. As already mentioned, this will not generally reduce the rms values of the parameters but it will yield a more equal distribution of the error ellipses of the radio sources and of the error ellipsoids of the VLBI stations. A major application of free network adjustment can be seen in the a priori quality judgement of observation schedules for VLBI. Thus, the following examples show the influence of free network adjustment on DOP factors as criteria for the quality of an VLBI observation schedule. For a more detailed explanation of the schedules which have been used as for the different DOP factors see Plietker and Schuh (1991, this issue).

solution of IRIS-A		1	2	3
free network		no	yes	yes
observations		1022		
unknowns		45	47	47
redundancy		977	976	976
STADOP	WESTFORD	0.04	0.04	0.04
	WETTZELL	1.28	1.34	1.34
	HRAS_085	1.04	1.06	1.06
	RICHMOND	1.09	1.11	1.11
	ONSALA	1.23	1.28	1.28
SSTDOP		2.33	2.41	2.41
QDOP	0106+013	2.28	F 2.30	T 2.34
	0212+735	1.73	F 1.59	T 1.74
	0229+131	1.80	F 1.84	T 1.87
	0420-014	2.21	F 2.26	T 2.29
	0528+134	1.60	F 1.66	T 1.68
	0552+398	-	F 0.80	F 0.76
	OJ287	1.27	F 1.30	T 1.31
	4C39.25	0.88	F 0.91	F 0.85
	1055+018	2.25	F 2.27	T 2.30
	OQ208	1.02	F 1.02	F 0.99
	1633+38	0.97	F 0.95	F 0.90
	1741-038	2.30	F 2.31	T 2.34
	1803+784	2.59	F 2.24	T 2.59
	2121+053	2.36	F 2.35	T 2.40
	VR422201	0.87	F 0.87	F 0.82
QQDOP		6.83	6.78	6.98
GDOP		7.22	7.19	7.39

Table 1: Effects of free network adjustment on the DOP factors of the radio source positions determined in an IRIS-A experiment. In the columns of the free network solution (marked by 'yes') the radio sources which are involved in the matrix of constraints are marked with an 'F'. Those which are totally free are marked with a 'T'.

In the first example an IRIS-A schedule has been analyzed three times with a different choice of the datum to demonstrate the effect of free network adjustment on the determination of the radio source positions. In the least squares fit the radio source positions and the clock and atmosphere parameters have been solved for. The WESTFORD clock has been kept fixed as a reference. All station positions have been kept fixed, too. In the first column of table 1 the results of a conventional solution are given where the position of one radio source (0552+398) has been kept fixed. In the second column the results of a free network solution are shown. All radio sources contribute to the matrix of constraints which means that the average of the corrections to the a priori right ascensions is zero. The sum of the variances of the right ascensions becomes minimal. The last column again shows the results of a free network solution. However, the right ascensions of only five radio sources were considered to contribute to the constraint. As already mentioned in paragraph 1, this procedure corresponds most to the current practice in global VLBI solutions. The radio sources which are supposed to be stable and already well determined are used for the matrix of constraints whereas those which are 'new' or unstable are completely free. This yields an equal distribution of the errors of the source positions and guarantees not to be dependent on only one radio source which might be influenced by systematic effects.

The second example deals with the effects of free network adjustment on the DOP factors of the station coordinates. The DOP factors obtained by two VLBI observation schedules, SWEAT2 and WESK1 which are also described in Plietker and Schuh (1991, this issue), have been analyzed. For each schedule first a conventional solution has been carried out with the station coordinates of WETTZELL kept fixed and than a free network adjustment has been computed. The results of the different solutions can be seen in table 2.

For both schedules the typical effect of free network adjustment can be observed, i. e. a more equal distribution of the errors of the station positions. The DOP factors which are related to the station positions (HDOP - horizontal DOP, VDOP - vertical DOP, PDOP - position DOP) are reduced by the factor 2 to 4 from the conventional to the free network solution. Furthermore, the free network adjustment has also a minimizing effect on the DOP factors of the auxiliary parameters which describe the behaviour of the station clocks (TDOP) and the tropospheric refraction in zenith direction (ATMDOP). Thus, the global DOP (GDOP) is considerably reduced in the free network solutions in both examples as can be seen in the bottom line of table 2.

experiment		SWEAT1		WESK1	
free network		no	yes	no	yes
observations		43	43	223	223
redundancy		30	30	208	208
SHANGHAI	HDOP	7.10	1.51	1.74	0.33
	VDOP	3.27	1.95	1.48	0.28
	PDOP	7.82	2.47	2.29	0.43
	TDOP	11.74	7.49	7.54	7.04
	ATMDOP	0.59	0.57	0.42	0.31
	STADOP	14.12	7.90	7.89	7.06
HARTRAO	HDOP	6.68	1.48	-	-
	VDOP	6.37	1.88	-	-
	PDOP	9.24	2.39	-	-
	TDOP	12.86	6.49	-	-
	ATMDOP	1.85	1.07	-	-
	STADOP	15.94	7.00	-	-
KASHIMA	HDOP	-	-	1.79	0.40
	VDOP	-	-	1.57	0.32
	PDOP	-	-	2.38	0.51
	TDOP	-	-	8.49	7.89
	ATMDOP	-	-	0.47	0.32
	STADOP	-	-	8.83	7.91
WETTZELL	HDOP	-	1.16	-	0.61
	VDOP	-	1.34	-	0.52
	PDOP	-	1.77	-	0.81
	TDOP	-	-	-	-
	ATMDOP	2.15	1.03	0.54	0.34
	STADOP	2.15	2.05	0.54	0.87
	GDOP	21.41	10.75	11.85	10.64

Table 2: Effects of the free network adjustment on the DOP factors of the station positions

6. CONCLUSION

The matrix of constraints E' which is necessary to carry out a free network adjustment of VLBI measurements has been derived analytically and test solutions have been run successfully. This allows for instance a general a priori quality judgement of a VLBI observing schedule.

Based on the free network approach, the concept of the VLBI global soulutions with hundreds to thousands of VLBI sessions and hundred thousands of observables from many stations around the world during several years could be reconsidered. Depending on the goal of the global solution such as plate tectonics, determination of global terrestrial and extragalactic reference systems, the free network adjustment will have several advantages compared to current procedures. For instance the concept of the determination of an optimal datum as used in deformation analysis can be transferred to VLBI.

REFERENCES

Brouwer, F. J. J., [1985]: On the Principles, Assumptions and Methods of Geodetic Very Long Baseline Interferometry; Publications on Geodesy, New Series, vol 7, no 4, Netherlands Geodetic Commission; Delft 1985

Heitz, S., [1986]: Grundlagen kinematischer und dynamischer Modelle der Geodäsie; Mitteilungen aus den Geodätischen Instituten der Rheinischen Friedrich-Wilhelms-Universität Bonn, Nr. 63; 1986

Koch, K. R., [1988]: Parameter Estimation and Hypothesis Testing in Linear Models; Springer Verlag; Berlin, Heidelberg, 1988

Ma, C., D. B. Shaffer, C. de Vegt, K. J. Johnston, and J. L. Russel, [1990]: A Radio Optical Reference Frame. I. Precise Radio Source Positions Determined by MARK III VLBI: Observations from 1979 to 1988 and a Tie to the FK5; Astronomical Journal, vol 99, no 4, American Astronomical Society; 1990

Plietker, B., [1990]: Definition von DOP-Werten und Untersuchung zur freien Netzausgleichung in der VLBI; diploma thesis; Bonn 1990

Plietker, B., and H. Schuh, [1991]: Definitions of DOP Factors for VLBI Solutions; this issue

Schwarz, C. R., [1978]: TRAV10 Horizontal Network Adjustment Program; NOAA Technical Memorandum NOS NGS-12, National Geodetic Survey; Rockville, Md., 1978

DEFINITION OF DOP FACTORS FOR VLBI SOLUTIONS

Berthold Plietker
Institute of Photogrammetry
Stuttgart University, Germany

and

Harald Schuh
DLR (German Aerospace Research Establishment)
Cologne, Germany

ABSTRACT: DOP (Dilution of Precision) factors which already play an important role in GPS scheduling are used for the estimation of the quality of VLBI networks and observing schedules. After an explanation of the objectives and the definition of the DOP factors for VLBI their application is shown by two examples.

1. INTRODUCTION

If a schedule for VLBI observations has to be drawn up it should be known how well the design will correspond to the expectations before starting time consuming and expensive measurement, i. e. criteria are needed on which the quality of the considered network design can be judged. Such criteria should meet various requirements. Besides giving hints about the general quality of the network they also should allow the comparison of individual parameters even if these have got different units. The a priori computability of such quality factors is also presumed.

For navigation and positioning with the Global Positioning System (GPS) DOP factors (Dilution of Precision) have proved to be very efficient for the estimation of the quality of an observing configuration (Wells et. al., 1986). This concept is transferred to VLBI.

2. DEFINITION OF DOP FACTORS

The quality of a network design is tightly connected with the precision of the different parameters solved for. Hence, the factors which determine the quality should be derivated from the variance covariance matrix $D(\vec{\beta}) = \sigma^2 (X'X)^{-}$ which represents the inner precision of the network. However, referring to the requirements given in paragraph 1., i. e. the criteria should be a priori computable and should be comparable for the different parameters, the variances of the parameters have to be normalized by the division by σ^2, i. e. only the inverse of the normal equation matrix is taken into account. The exclusion of the variance of unit weight is justified because it only depends on the quality of the observations. However, relative factors are sufficient if we want to learn about the quality of the network design and its effects on the individual parameters. Thus the a priori computability of the quality factors is given by the normalization. The requirement of the comparability quoted above can be achieved by multiplying the different variances with corresponding multipliers f so that we get all factors with the same unit (in this case dimensionless: [-]). Then combinations and also comparisons of the quality of the different parameters which are solved for in the VLBI least squares solution are possible.

Thus, the following general formula for the DOP factors is obtained:

$$DOP_i = \sqrt{\frac{1}{\sigma^2}\, tr\,(F_i \cdot D(\vec{\beta}))}\ ,$$

where $D(\vec{\beta})$ is the variance covariance matrix and $F_i = diag(f_1, ..., f_j, ..., f_u)$ is the matrix of the corresponding multipliers f which all are equal zero besides those which are needed to determine the respective DOP factor. The corresponding multipliers f of the different parameters are given in the following table:

unit of parameter	multiplier f
time: [s]	1
length: [m]	$(1/c)^2$
angle: [°]	$(2R/c)^2$

Table 1: Corresponding multipliers f of the different parameters

In Table 1 c stands for the velocity of light and R for the mean radius of the Earth, i. e. angles are referred to arcs on the Earth via the basic formula of geodesy.

Below, we introduce some of the DOP factors which can be defined. We distinguish between two groups. The first one contains DOP factors of parameters which are usually estimated in a VLBI solution. That means, the DOP factors can be computed immediately from the inverse normal equation matrix, for instance:

'Position DOP of a station'

$$PDOP = \frac{1}{\sigma_0}\sqrt{\frac{1}{c^2}\cdot(\sigma_x^2 + \sigma_y^2 + \sigma_y^2)}$$

'Clock parameter DOP'

$$TDOP = \frac{1}{\sigma_0}\sqrt{\sigma_{T0}^2 + \sigma_{T1}^2 + \sigma_{T2}^2}$$

'Atmosphere parameter DOP'

$$ATMDOP = \frac{1}{\sigma_0}\sqrt{\sigma_{atm}^2}$$

'Polar motion DOP'

$$POLDOP = \frac{1}{\sigma_0}\sqrt{(\frac{2R}{c})^2\cdot(\sigma_{x_p}^2 + \sigma_{y_p}^2)}$$

The second group contains DOP factors which can be derived by error propagation. E. g., on each VLBI station a horizontal coordinate system (x_H, y_H, y_H) is defined so that we can compute:

'Horizontal component DOP'

$$HDOP = \frac{1}{\sigma_0}\sqrt{\frac{1}{c^2} \cdot (\sigma^2_{x_H} + \sigma^2_{y_H})}$$

'Vertical component DOP'

$$VDOP = \frac{1}{\sigma_0}\sqrt{\sigma^2_{z_H}}$$

Similarly a 'baseline system' or 'arc system' respectively can be defined in which a DOP factor of the baseline length and DOP factors of the components orthogonal to the direction of the length can be computed.

3. EXAMPLES

Two examples will illustrate how DOP factors can be used and how the results can be interpreted. The examples are not to be considered as a thorough investigation of the quality of different VLBI networks but merely as an illustration of the application of DOP factors.

From the first example (tab. 2) follows that factors the results of different experiments are a priori comparable by using DOP. There is not only the possibility of comparing single parameters but also whole parameter groups. In this example all station positions and radio source coordinates and the clock of one reference station are kept fixed in the least squares solutions of different experiments with different duration. The clock parameters of the other stations, the atmosphere parameters and the Earth rotation parameters are to be estimated. The choice of the same set of solve-for parameters allows the comparability of the estimation of the Earth rotation parameters in different experiments. There are two experiments on the SWEAT network as it is called (Wettzell Geodetic Fundamental Station, FRG (WETTZELL) - Hartebeesthoek Radio Astronomy Observatory, RSA (HARTRAO) - Shanghai Astronomical Observatory, PRCh (SHANGHAI)) and one on the IRIS-A network (Westford Observatory, Mass., USA (WESTFORD) - WETTZELL - Fort Davis, Tex., USA (HRAS_085) - Richmond Station, Fla., USA (RICHMOND) - Onsala Space Observatory, Sweden (ONSALA)). For our analysis, the latter schedule has been divided into 3-hour subintervals. At first, each of the new 3-hour-schedules was analyzed separately. Then, the chronologically first and second were merged to form a 6-hour schedule which was analyzed next. Consecutively all the other intervals also were appended chronologically forming each time a 3 hours longer schedule for which the DOP factors of two parameter groups were computed.

exper.	dur.	observables			SSTDOP	ERPDOP			GDOP
		min.	avg.	max.	avg.	min.	avg.	max.	avg.
SWEAT1	4h	-	36	-	367.76	-	2.09	-	367.77
SWEAT2	3h	-	43	-	206.54	-	3.89	-	206.57
IRIS-A	3h	97	109	124	383.04	3.81	4.24	4.70	383.06
"	6h	-	222	-	54.17	-	2.49	-	54.22
"	9h	-	338	-	21.50	-	2.09	-	21.60
"	12h	-	435	-	11.22	-	1.83	-	11.37
"	15h	-	536	-	6.84	-	1.63	-	7.03
"	18h	-	638	-	4.72	-	1.47	-	4.95
"	21h	-	746	-	3.40	-	1.36	-	3.66
"	24h	-	870	-	2.62	-	1.26	-	2.91

SSTDOP	'Combination of station parameter DOPs'
ERPDOP	'Earth rotation parameter DOP'
GDOP	'Global DOP' as a combination of SSTDOP and ERPDOP
min.	minimal value of the eight 3-hour-schedules on IRIS-A network
avg.	average ~
max.	maximal ~

Table 2: Dependency of DOP factors of different experiments on the duration

The high values of SSTDOP - here as a combination of TDOP and ATMDOP - in the short-time experiments are caused by the weak determination of the drift rate of the clocks. The magnitude of ATMDOP is only about 0.1 ... 0.5.

Regarding the determination of the Earth rotation parameters it can be seen that the SWEAT experiments which are especially designed for Earth rotation parameter estimation provide a similar quality of determination as the 24-hour IRIS-A experiment although the SWEAT sessions are carried out within only 3 and 4 hours by fewer observing stations than IRIS-A. Indeed, 9 hours of observations in IRIS-A are needed to get the quality of the 4-hour SWEAT1 schedule (ERPDOP = 2.09). The difference in accuracy between both SWEAT experiments shows that there has to be put much care in selecting the radio sources and choosing the sequence of observations because SWEAT1 determines the Earth rotation parameters with the same ground network with even fewer observations better than SWEAT2. However, the combination of the station parameter DOPs are smaller with the SWEAT2 schedule than with the SWEAT1 schedule because of the higher number of observations within a shorter time.

The second example (tab. 3) deals with the dependency of the DOP factors on the geometry of the network. Here we use again the SWEAT2 schedule lasting 3 hours and the WESK1 schedule as it is called lasting 10 hours. Both of them are triangular networks with one baseline (WETTZELL - SHANGHAI) in common. The third station of SWEAT2 is HARTRAO with a long north-south baseline while the third station of WESK1 is KASHIMA in Japan, giving the network a long west-east but a poor north-south extension. Thus, the WESK1 experiment is expected to be useful for determination of the phase of Earth rotation or rather DUT1 while SWEAT2 should additionally be usable for a good estimation of polar motion.

Again the station and radio source coordinates and the clock of one reference station (WETTZELL) are kept fixed. In the SWEAT2 solution also the drift rates of the other clocks are kept fixed. By this the magnitude of TDOP (clock parameter DOP) is kept on the same level as in the WESK1 solution where the

higher number of observations keeps TDOP low.

experiment		SWEAT2	WESK1
observations		43	223
redundancy		33	211
SHANGHAI	TDOP	7.00	7.16
	ATMDOP	0.22	0.17
	STADOP	7.00	7.16
HARTRAO	TDOP	6.45	-
	ATMDOP	0.45	-
	STADOP	6.48	-
KASHIMA	TDOP	-	7.91
	ATMDOP	-	0.18
	STADOP	-	7.91
WETTZELL	ATMDOP	0.44	0.21
	SSTDOP	9.55	10.67
	POLDOP	2.86	2.99
	UTDOP	2.63	0.86
	ERPDOP	3.88	3.11
	GDOP	10.31	11.12

Table 3: Effects of the network geometry on the Earth rotation parameters

Concerning network geometry the results (table 3) confirm the expectations expressed above. By the WESK1 configuration the polar motion is three times weaker determined than the changes of Earth rotation (2.99 to 0.86). Against that SWEAT2 yields merely very small differences between POLDOP and UTDOP (2.86 to 2.63). Comparing both experiments the precision of the polar motion parameters approximately will be the same (2.99 to 2.86) though SWEAT2 just needs a third of the observing time and a fifth of the observations which WESK1 needs. On the other hand, the phase of Earth rotation (UT1) can be determined better by WESK1 (0.86 to 2.63) firstly having a lot more of observations and secondly possessing a longer east-west component of the baselines.

Both examples show that by DOP factors the quality of a VLBI configuration (station network and schedule) for the determination of different parameters can directly be compared. It is obvious, however, that inaccuracies of the models which have to be applied to the observables, i. e. the model for tropospheric refraction or the model for tidal variations of UT1, are not covered by the DOP factors which purely depend on the geometry.

4. CONCLUSION

DOP factors are introduced as well suited values to determine a priori the quality of a schedule of VLBI measurements. The advantage of DOP factors against the usually used factors of the normal equation matrix is given by the fact that DOP factors allow the direct comparison of parameters with different units, as Earth rotation parameters, station coordinates and clock parameters, and also the combination of

different parameters.

5. REFERENCES

Brouwer, F. J. J. [1985]: On the principles, assumptions and methods of geodetic Very Long Baseline Interferometry; Publications on Geodesy, New Series, vol 7, no 4, Netherlands Geodetic Commission; Delft 1985

Koch, K. R. [1988]: Parameter Estimation and Hypothesis Testing in Linear Models; Springer Verlag; Berlin, Heidelberg 1988

Müller, A. F. [1987]: Einfluß der Satellitenkonfiguration auf die Genauigkeit absoluter und relativer Koordinatenbestimmung; diploma thesis; Bonn 1987

Plietker, B. [1990]: Definition von DOP-Werten und Untersuchung zur freien Netzausgleichung in der VLBI; diploma thesis; Bonn 1990

Wells, D. E., N. Beck, D. Delikaraoglou, A. Kleusberg, E. J. Krakiwsky, G. Lachapelle, R. B. Langley, M. Nakiboglou, K. P. Schwarz, J. M. Tranquilla, and P. Vanicek [1986]: Guide to GPS Positioning; Canadian GPS Associates; Fredericton, N. B., Canada 1986

Design of an Expert System for VLBI Data Analysis

Harald Schuh
German Aerospace Research Establishment (DLR)
Linder Höhe
D-5000 Köln 90, Germany

ABSTRACT. Due to the increasing number of VLBI experiments and due to the necessity of a shorter turn around time from the VLBI session until the availability of the final results, the procedure of data analysis has to be accelerated considerably. Faster and more powerful computers can only marginally improve the duration of data processing because the flow of data analysis and the tasks of the analyst are very complex. The concept of an expert system for the MarkIII Data Analysis System is presented which will support and guide the analysts to make the data analysis faster even by less experienced analysts. The name of the expert system to be developed is VLBIXPS.

1. INTRODUCTION

In the past two decades the field of artificial intelligence has shown to be one of the most fascinating subjects of computer sciences. In particular the applications of expert systems (XPS) have proved to be useful for various fields such as medical diagnosis or production process planning. It will be shown in this paper that an expert system for scientific data analysis such as VLBI data processing will also bring many benefits.

2. GENERAL REMARKS ABOUT EXPERT SYSTEMS (XPS)

This paragraph contains a definition and typical applications of expert systems (XPS) and a short description of the usual structure of an XPS.

A definition similar to the following one was found in Schnupp et al. (1989): An expert system (XPS) is a computer system which can administer specific expert knowledge, store and evaluate it in such a manner that it can provide targeted information to users, or can be used to dispatch certain tasks. It is an intelligent and active system, which contains logic and knowledge representation by rules, facts etc.. Usually it can also be called knowledge-based software.

Typical applications of expert systems are:
- medical diagnosis,
- planning and control of industrial enterprises (production process planning, information management),
- configuration of computer systems,
- maintenance and repair of technical devices (cars, machines, ...),
- control (air traffic control, control of power plants, ...),
- computer-aided instructions,
- data analysis, image processing.

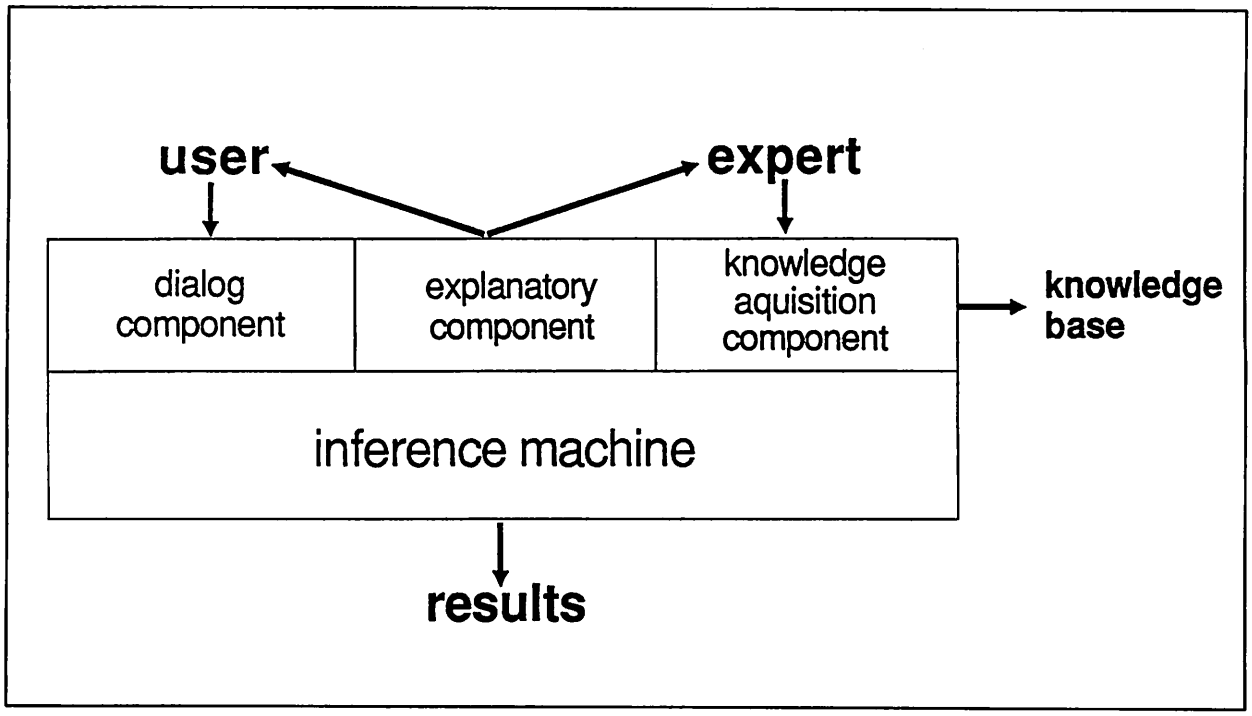

Fig. 1.: Typical structure of an expert system

A usual structure of an XPS is shown on fig. 1. Programming can be done by:
- 'classical' procedural languages (Fortran, Pascal, C, ...),
- AI-languages with facts, rules, objects, symbols, etc. (Prolog, Lisp, ...),
- knowledge-based tools (KEE, OPS5, ...),
- XPS-shells (Emycin, Xi plus, Nexpert Object, ...).

3. EXPERT SYSTEM FOR VLBI DATA ANALYSIS

3.1 REASONS

In the past years a steady increase of the number of radio telescopes around the world and of the number of sessions ('experiments') which take place by using these radio telescopes could be observed. Already now this large amount of observing sessions leads to the necessity of a faster and even semiautomated data flow during the data analysis in particular with respect to the wish to a shorter turn-around time between the date of the observing session and the delivery of final results. However, this can only marginally be achieved by faster computers, because it is well known that the data analysis is very complex and the analyst's (expert's) decisions are often needed which is indeed the time-limiting factor. Already today there is a shortage of qualified experts and the analysts' training takes a long time. Moreover, even by an experienced analyst errors can be made, which then are at least time consuming. Wrong results could even lead to a misinterpretation and to incorrect conclusions. Thus, the goal should be to make the VLBI data analysis faster and safer because of less failures and less errors even by less experienced analysts.

3.2 AN XPS FOR THE MKIII DATA ANALYSIS SYSTEM ('CALC/SOLVE')

3.2.1 GOALS OF THE PROJECT

In the research project described in this article an XPS for the Mark III Data Analysis System (Ryan et al., 1980) will be developed as a knowledge-based assistant for support

and guidance of an analyst who has already a good basic knowledge. The XPS will guide and control the operations done by the analyst and will do all necessary checks if possible automatically. It will give detailed explanations to the analyst (decision support system) in particular when he/her has to chose between different options or has to select specific models or parameters. When failures or problems in the process of data analysis have occured it should advise the analyst how to overcome the problem (diagnostic system). The system will contain a flexible and extensible knowledge-base. In the future an extended version of the expert system shall be developed as instruction system for newcomers and the system can also be extended to cover other aspects of the VLBI process, like scheduling of observing sessions and the correlation of the raw data. The expert system shall be implemented either parallel on a separate computer (PC or workstation) or as a kind of shell with all other (existing) programmes integrated. In the first case the XPS is independent but its use is more elaborate because there is no direct data flow between the existing programmes and the knowledge-based software. In the latter case the direct data flow exists, but the additional software parts are not completely independent of the individual programmes which could cause problems in particular in the case of failures and interrupts. From the very beginning the new knowledge-based software should be designed to be transferable to other VLBI software packages like OCCAM (developed at the Universities of Bonn and Madrid) or MASTERFIT/MODEST (developed at Jet Propulsion Laboratory, Pasadena,CA) because the procedure of data analysis is very similar in all VLBI analysis programmes.

3.2.2 TASKS OF THE XPS FOR VLBI

By looking at the work which is usually done by the analyst during the course of data analysis by the MkIII Data Analysis System, we found that almost all tasks of the analyst can be supported by an XPS. This is shown by the additional blocks in the flow chart of the standard MkIII Data Analysis System in fig. 2. Below, some of the steps will be explained in more detail. It is obvious that not all of those tasks really need an expert system like software. Some of them can be achieved by a comfortable user interface as well or by additional algorithms or crosschecks programmed within the existing software. Some other tasks could be achieved by using 'classical' programming methods but the use of AI languages will accelerate and fascilitate the realization.

Additional knowledge-based software ammendments are proposed for the following steps:

*** Check of completeness**
- Are all data and all information available (type 50 and type 52 files on B-tapes, log-files of stations, ...)?

*** Start DBFT**
- explanations of data entry
- fault diagnosis from error messages (diagnostic system), by giving not only general computer-relevant explanations but VLBI-specific reasons (will be treated in more detail below).

*** Check of #BLOKQ, UT1PM and EPHEM**
- all data in #BLOKQ? (if not — enter data and start SKULL/SKELETON),
- all data in UT1PM? (if not — enter UT1-, polar motion data and/or leap seconds),
- EPHEM files available? (if not — add files).

*** Start KBMSG**
- explanations of data entry,
- fault diagnosis (diagnostic system).

*** Start CALC (SETUP) (X- and S-band databases)**
- explanations of data entry,
- selection of flags (selection system),
  i.e. - ocean loading corrections on/off (cross check with #BLOKQ)?
  - which relativity model to be used?
  - ...

*** START SOLVE (A) (S,-X-band)**
- explanations of data entry, guidance through the menues (connection to CALC!),
- parameter selection system using rule-based knowledge representation,
- ambiguity elimination by a planning system with algorithms (computation of ambiguity spacing) and constraints (the sum of the ambiguity levels within each triangle should be zero); if fully automatic — decision system,
- fault diagnosis (diagnostic system) by giving not only computer-relevant explanations but VLBI-specific reasons as shown by the example in 3.2.3.

*** Start DELOG and DBCAL**
- system for data analysis of MET-, CAB-, and WVR-files (outliers, breaks; ...),
- enter meteorological data and cable calibration data into the database.

*** Start SOLVE (P)**
parameter estimation (station coordinates, Earth rotation parameters, source positions, ...) supported by:
- system for parameter selection,
- system for data analysis,
  * searching for outliers
  * analyzing the residuals:
    - station-dependent variation of residuals,
    - variation of residuals with respect to variation of meteorological data,
    - source-dependent variation of residuals,
- system for choosing a priori sigmas (planning system).

*** Analysis of results**
- check of plausibility: are solved-for parameters reasonable, too big, ...? (consultation system),
- hints, what to check,
- in case of problems, reference where to enter again into the programme flow.

*** Comparison and interpretation of results**
- comparison of the baseline evolutions with existing plate-tectonic models,
- comparison of ERP series with results of other observing techniques,
- use of the baseline results to derive regional deformations and global plate motions,
- investigation of the interactions between the ERPs and other geophysical and atmospheric phenomena.

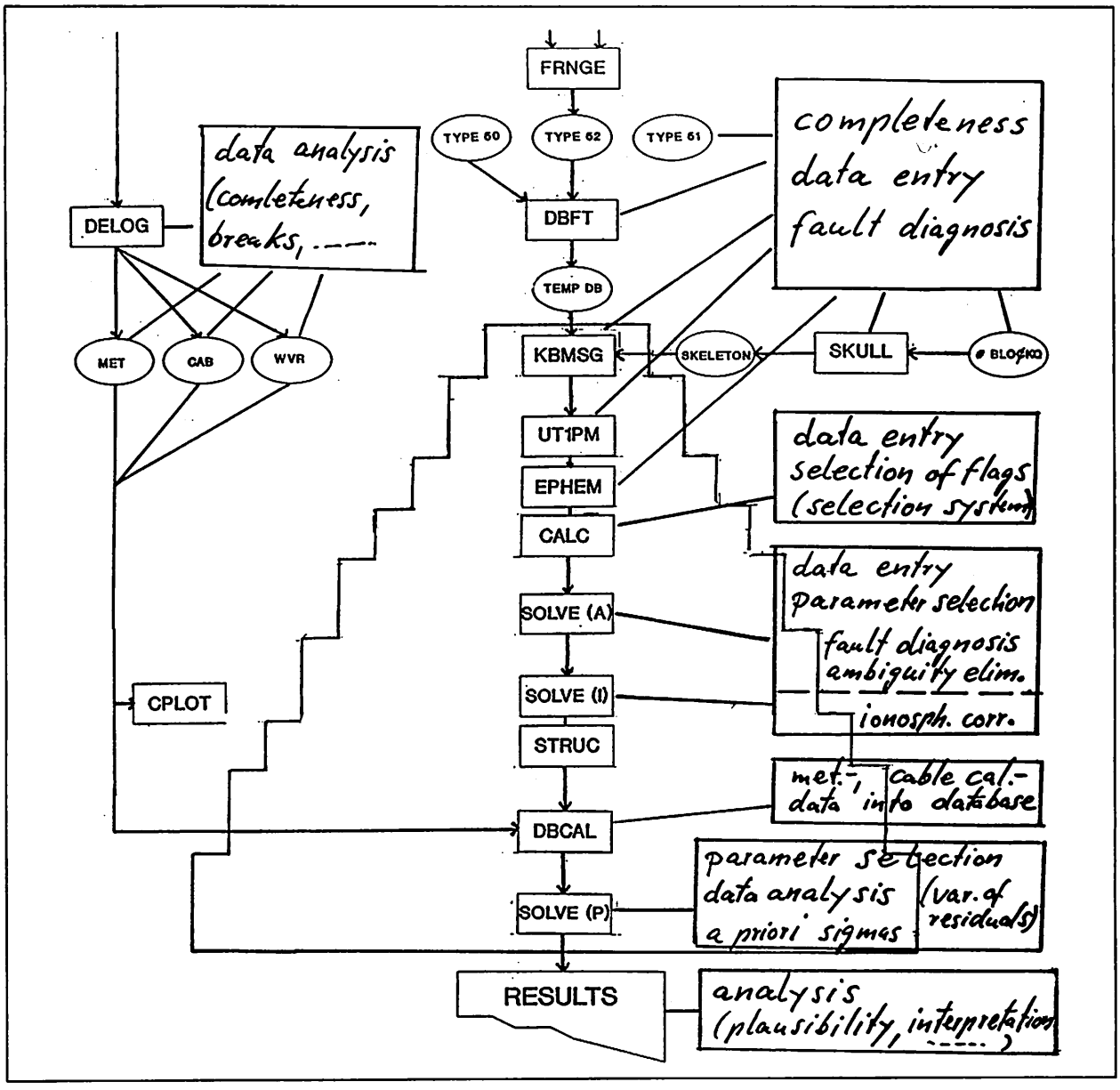

Fig. 2: Flow chart of the standard MarkIII Data Analysis System and all tasks which could be supported by expert system type software amendments.

3.2.3 EXPERT SYSTEM FOR FAULT DIAGNOSIS IN SOLVE

This system must have an explanatory component to tell the user why the problem/ failure/ error message has occured and how it can be solved.

For each error message (i.e. goal) several layers of reasons can be defined by rules. Usually layer 1 is a computer-specific layer whereas the layers 2,3,4, ... are 'VLBI-specific' layers. If those are programmed as rules in Prolog the interpreter finds the goal by backward chaining.

As shown on the fictitious example in fig. 3 the computer gives only a computer-specific error message (error #33). The explanation by the manual would be 'CPU overflow' or 'disk is full'. But the real reason for the CPU overflow must be tracked downwards since it is due to a rank deficiency (layer 2) which could be caused because the number of observations n is less than the number of parameters u or because of the specific selection of the parameters to be solved for (layer 3). For instance there is a rank deficiency if the analyst has solved for all station parameters or for all source parameters or for all clock parameters (layer 4).

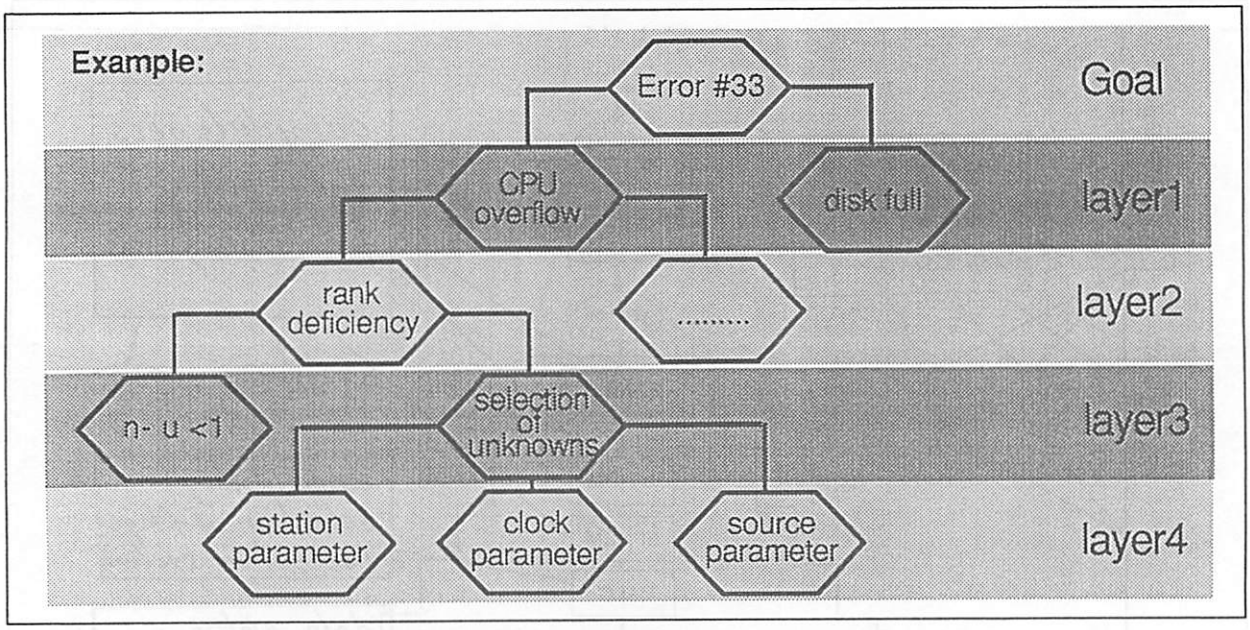

Fig. 3: Example for the structure of rules in an XPS for fault diagnosis in SOLVE

3.2.4 STATUS AND GOAL OF THE PROJECT

In the past months first steps for the development of an XPS for the MarkIII Data Analysis System ('CALC/SOLVE') have been made.
In the first phase, the concept and design for such a knowledge-based assistant shall be completed by the knowledge acquisition, the formalization of knowledge and the knowledge representation by rules, facts, etc.. In the next phase exemplary PC-based prototypes of specific parts shall be realized using Prolog (and/or Lisp) to represent rule-based knowledge. The use of Fortran 77/88 is also possible in particular if connection to existing software is desired. The first version of the system will be designed to support the current version of the MarkIII Data Analysis System as presently implemented at the Geodetic Institute of the University of Bonn (GIUB). If the concept and a prototype of the XPS have been designed once, the flexible knowledge-base will allow an easy transition to any new version of the MkIII Data Analysis System. The implementation of such new version of the VLBI-software on a new HP workstation at GIUB is planned for 1992/93.

The name of the expert system (knowledge-based assistant) to be developed is **VLBIXPS**. In the future the full integration into the HP environment is planned. The development and implementation of the complete expert system will take several person years. The transfer to other VLBI software packages shall be supported as well as the extension of the system to other tasks within the VLBI process. There are several other programmes which also need the expertise of high-qualified researchers and engineers. These are for instance scheduling of observing sessions and the correlation process of the raw data. The processing of GPS-observations in the stationary mode, i.e. for geodetic application, has considerable similarities with geodetic VLBI. Thus, many of the ideas which are behind VLBIXPS will be tranferable to GPS data processing, too.

4. REFERENCES

Schnupp, P. Nguyen Huu, C.T. and Bernhard, L.W.: Expert Systems Lab Course. Springer-Verlag Berlin Heidelberg, 1989.

Ryan, J.W., Ma, C. and Vandenberg, N.R.: The Mark III VLBI Data Analysis System, NASA Goddard Space Flight Center, publication X-945-80-25, August, 1980.

INTRODUCTION TO THE OCCAM V2.0 MODELS

N. Zarraoa, A. Rius, E. Sardón
Instituto de Astronomía y Geodesia, CSIC-UCM
MADRID, SPAIN

H. Schuh
Geodetic Institute of Bonn University
BONN, GERMANY

ABSTRACT

In this paper we will summarize the models that are presently available in the software package OCCAM (release version 2.0) for the geodetic analysis of VLBI experiments. The models will be briefly explained and we will include the references in which they can be found in detail.
The availability of the program for interested users will be presented, as well as the plans for future improvements.

1. INTRODUCTION

OCCAM V2.0 is a research and development package for the analysis of geodetic VLBI experiments. Some references describing the Bonn VLBI Software System (BVSS), antecedent of OCCAM, and previous implementations of the program, can be found in Schuh (1987) **[31]** and Zarraoa et al. (1990) **[39]**.

Recent comparisons with CALC V7.0 (Rius et al. 1991 **[28]**), have shown discrepancies below three picoseconds in the models, in baselines up to 3000 Km.

Some characteristics of this package are:

- It is written in FORTRAN 77
- The package runs on IBM AT compatible computers under MS-DOS
- End to end process
- Up to date IERS standard models for the computation of VLBI theoretical delays are implemented and checked (see IERS Technical Note 3 **[17]**). Other models are also available.
- Single or multibaseline processing methods
- Interactive menu system to operate the program

The software is provided freely to any group interested in data processing and/or software upgrading. Contributions to improve and upgrade the program by every member of the informal "user group" are welcome. From the valuable modifications a next standard version of OCCAM will be released and will be distributed by the OCCAM coordinator.

For more information on the availability of the software, contact the OCCAM coordinator:

Néstor Zarraoa
Instituto de Astronomía y Geodesia
Facultad de Ciencias Matemáticas
28040 MADRID
Spain

Phone 34 - 1 - 394 45 78 Fax 34 - 1 - 543 94 89
Telex 41802 UCMAT E E-mail W057@EMDUCM11.BITNET

2. OCCAM STRUCTURE

The OCCAM software contains several FORTRAN programs and a set of MS-DOS batch files that allow the use of interactive menus to operate the system.

The user must provide input data files containing:

- A VLBI data file with delays, delay rates and their formal errors, surface meteorological data, ionospheric or cable calibration corrections (if available), etc.
- Catalogues with coordinates of stations and sources
- A file with tables of the EOP and of the ephemeris for Sun, Earth and Moon for several dates around the experiment.
- Ocean loading amplitudes and phases for the stations.
- An "options file" for the data process.

This information is stored by the package in the "OCCAM Standard Data Files" that are used by all the programs to read or add information from or to those files.

The program is divided in two main parts. The first computes all the models and the partial derivatives. The seconds performs the least squares adjustment of the parameters. Several utilities have been added to the software for printing, backing up or adding external information.

The partial derivatives are computed based on a simplified model of the geometric delay, which is expected to be good up to one part in 10^4. If the a-priori values of the parameters are very unaccurate, an iterative estimation process might be needed.

In table 1 there is a list of all the effects that are currently modeled and those that should be added in the near future, along with the reference describing the models available or suggested for each effect.

Effect	Implemented	Default model	Alternative / Suggested Model
Ionospheric Correction	No		[30]
Sun-Earth-Moon Ephemeris	Yes	[2]	[35]
Precession	Yes	[21]	
Nutation	Yes	[32] [37]	
Earth Tides	Yes	[23]	[5]
Ocean Loading	Yes	[13] [25] [17]	
Atmospheric Loading	Partially	[26]	
Antenna Deformation	No		[27]
Pole Tide	Yes	[33]	
Short Period UT1 Variations	Yes	[38]	
Oceanic Tide UT1 Variations	Yes	[3]	
Antenna axis offset	Yes	[33]	
Tropospheric Zenith Delay	Yes	[22]	
Tropospheric Mapping Func.	Yes	[19]	[8] [9] [22]
Plate Motions	No		[10] [24]
Geometric Model	Yes	[40]	[11]
Clock Breaks	Yes	[29]	

Table 1

3. MODEL COMPUTATION

This part of the program performs the computation of all the geometrical, geophysical and relativistic models of the VLBI observables. The IERS standard models **[17]** are available as well as other alternative models for several items.

The task is done in four steps. First, the input data provided by the user is reallocated and indexed in the OCCAM Standard Data Files in order to be easily handled by the rest of the programs. Second, the models that depend only on the observation time and/or the observed radiosource are computed. They cover items like precession and nutation, EOP and ephemeris interpolation, etc. Third, all the models depending on time and station are computed. These include several geophysical models (Earth tides, ocean loading, etc.), the computation of partial derivatives with respect to station and source coordinates, etc. Finally, the relativistic geometrical models are computed to get the theoretical delays and delay rates.

The a-priori positions of the VLBI stations and the radio sources observed should be good enough if we want to get an accurate modeling of the VLBI observables. There are several catalogs of sites and sources that are frequently used in geodetic VLBI experiments. The most standard are those compiled by the Goddard Space Flight Center (GSFC), or those included in the IERS Celestial and Terrestrial Reference Network (ICRF and ITRF). See Caprette et al. (1990) **[6]** and IERS Annual Report (1991) **[18]**.

A. Models depending on radiosource and time

This option performs the transformation between the J2000.0 Celestial Reference Frame for the quasars to their apparent positions in the observation time.

The ephemeris of Earth, Sun and Moon can be obtained from the Massachussets Institute of Technology (MIT) PEP ephemeris or the Jet Propulsion Laboratory DE200/LE200 ephemeris. The latter are published in the Astronomical Almanac (or equivalent) **[2]** every year, with a format compatible with that expected by OCCAM. EOP information can be obtained from the Bulletin B of the International Earth Rotation Service (IERS) **[16]**, that is released monthly.

EOP and Ephemeris data for Sun, Earth and Moon are interpolated to each observation time. The Aitken-Lagrange interpolation method is presently used in the program. For reference see Hildebrand (1956) pp 49-50 **[15]**.

If there is no ephemeris information available, the program includes an analytical method to obtain the heliocentric and barycentric earth positions that is described in Stumpff (1980) **[35]**.

The relation between the Greenwich Mean Sidereal Time and the Universal Time is given by Aoki et al. (1982) **[1]**.

The precession and nutation theory implemented in OCCAM is described in the IERS Technical Note 3 (1989) **[17]**. The rotation angles for the precession matrix are obtained from Lieske et al. (1977) **[21]** and the nutation theory is the IAU 1980 standard, Wahr

(1981) [37] and Seidelmann (1982) [32].

Corrections to the IAU nutation model derived from VLBI experiments, have been published by Carter and Herring (1987) [7] but they have not been implemented in the software yet.

To get the apparent position of the sources in order to compute their local azimuth-elevation coordinates, a correction term for the annual aberration is included based on Stumpff (1979) [34].

B. Models depending on station and time

Several geophysical effects on the station positions are modeled, like Earth tides, ocean loading, pole tide, atmospheric loading, short UT1 variation or the effect of ocean tides on Earth's rotation.

The effect of Earth tides in the station coordinates is computed using two alternative models. The standard model uses the ephemeris positions of Sun and Moon to compute the tidal potential. This is transformed into station displacements by using the Love numbers. This approach can be found in Melchior (1978) [23]. The nominal Love numbers used by the program are described in the IERS Standards [17] p. 27.

The alternative model is based on the harmonic development of the tidal potential ETMB 85. Its application to the program is described in Büllesfeld & Schuh, 1986 [5], and includes the 95 major constituents from the complete model.

The model used to compute the radial and horizontal displacements of the station positions due to ocean loading has been described by different authors (Goad, 1980 [13] or Pagiatakis, 1984 [25]). The amplitude and phase coefficients for each station have been obtained from the IERS Technical Note 3 [17] and from Scherneck (1989, private communication). The computation of the angular arguments for the tide components is done using a FORTRAN routine that can be found in the IERS Technical Note 3 [17].

The atmospheric loading model derived by Rabbel and Schuh (1987) [26] is implemented in the software. However, the correction is not presently applied to the position of the stations.

The antenna deformation due to the gravitational force and other mechanical and thermal influences could be modeled using a method described in Rius et al. (1987) [27]. However, the practical application of this model is not presently implemented in the software.

The model for the displacement induced by the pole tide is from Yoder and it is described in Sovers & Fanselow (1987) p. 15 [33].

The UT1 is affected by high frequency tidal effects that must be accounted for. Yoder et al (1981) **[38]**, describe a model for the short period fluctuations on UT1. In addition, the ocean tides may induce periodic fluctuations of the UT1. The model implemented in OCCAM for this effect can be found in Baader et al. (1983) **[3]**. The implementation of a new model given by Brosche and co-workers is planned for the near future. This model has allowed to detect the very small influence of the ocean tides in the UT1 results of dedicated VLBI experiments (See Brosche et al. (1991) **[4]**)

The antenna mounting geometry can induce several systematic effects on the observables. Some of them are indistinguishable from clock offsets, but other effects must be corrected because their effect is variable as the Earth and the antenna move. In particular, the effect of non-crossing axes of the antenna has to be accurately modeled. A detailed explanation of the problem and how to model it can be found in Sovers and Fanselow (1987) **[33]**.

The observed VLBI delays are strongly affected by the delay induced on the signal as it passes through the Earth's atmosphere. In this effect, the contributions of the ionosphere and of the troposphere are of different nature and they are calibrated with completely diffe-rent models.

The ionospheric contribution to the delays is dispersive, e.g. depends on the frequency observed. Therefore, the use of dual frequency observations permits the calibration of this contribution. See Scheid (1985) **[30]**.

The calibration of the ionospheric effect in the VLBI data is not performed by OCCAM. Hence, the input data should have been already calibrated or the correction terms should be present in the input data file. One of the future extensions of the program will be the implementation of the dual frequency (S and X band) calibration of the ionospheric effect. We are studying the application of ionospheric information derived from dual frequency GPS measurements to model its contribution when only single frequency VLBI data is available.

The tropospheric contribution is (basically) independent of the observed frequency. The models for this contribution are based on the estimation of an a-priori value of the tropospheric delay in the zenith direction and the use of a mapping function to relate this value to the delay induced at different elevations. In addition, a correction term for the zenith contribution ca be determined as a parameter in the OCCAM estimation process.

There are several models for the mapping function. The available models in OCCAM can be found in Chao (1974) **[8]**, Marini (1972) **[22]**, Davis et al. (1985) **[9]** and Lanyi (1984) **[19]**. The model used to estimate the zenith delay induced by the troposphere as a function of surface meteorological data can be found in Marini (1972) **[22]**.

Presently there is no model of global plate motions implemented in the program. Since the current models like RM2 (Minster & Jordan, 1978 **[24]**) or NUVEL-1 (De Mets et al. 1990 **[10]**) predict velocities of up to several centimeters per year between different plates, this effect should be modeled in future versions of the program.

C. Models depending on baseline and time

This part of the package computes the theoretical delays and delay rates for each observable, according to several relativistic models implemented in OCCAM.

The available models are those from Finkelstein et al. (1985) **[11]**, Zhu & Groten (1988) **[40]** and a modified version of the latter.

The default model is from Zhu and Groten **[40]**, which is included in the 1989 IERS Standards **[17]**. The modified version is equivalent to the original at the picosecond level and incorporates some modifications that assimilates the model to that of Shapiro & Herring, 1989 as described in the IERS Standards **[17]**. The reference system in which the theoretical delay is computed is the Terrestrial Reference Frame.

The model from Finkelstein et al. **[11]** differs from that of Zhu & Groten in the lack of an additional term comprising the potential at the Earth's geocenter, which appears as a relativistic effect on the spatial coordinate transformation. Hence, this model should be less accurate than the Zhu & Groten model.

4. PARAMETER ESTIMATION

The program can estimate in the single baseline mode up to 31 parameters using a least squares approach. The parameters include baseline cylindrical coordinates, source coordinates (up to all sources but one right ascension fixed), clock model (second order polynomial for each station except one reference), atmospheric zenith correction term (one offset for each station), and polar motion (wobble and UT1-UTC).

In addition there is an automatic system to detect clock breaks and adjust additional clock parameters if necessary. The algorithm is described in Sardón et al. (1990) **[29]**.

In the multiexperiment mode the station coordinates, clock offsets and atmospheric correction term can be solved for each station except one reference station for coordinates and clocks. In addition the Earth Orientation Parameters and a deformation matrix can be adjusted. This step uses the single baseline results as input for the least squares estimation.

The least squares method description can be found in many books. In Lawson & Hanson (1974) **[20]** there is a complete treatment of the method, with examples and FORTRAN programs to solve least squares problems. Our least squares application makes use of a pseudo-inverse routine for the inversion of matrices (it is equivalent to a standard inversion for regular matrices) and it can include a non-diagonal weighting matrix and linear equality constraints. See also Golub & Reinsch (1970) **[14]**.

A global multistation-multiexperiment processing algorithm is now implemented in an experimental version, which is not ready for release yet. The inversion is based on sequential Kalman Filtering of the observables. This technique is described in Genin (1980) **[12]** or Tarantola (1989) **[36]**. Our application of the filter can be found in Sardón et al. (this volume) or in Rius et al. (1991) **[28]**.

Before the experimental version described above can be implemented into the standard OCCAM, some work on the user-friendliness of the program must be done. In addition some new capabilities must be added to deal with the estimation of other parameters than those included now.

5. REFERENCES

[1] Aoki, S., B. Guinot, G.K. Kaplan, H. Kinoshita, D.D. McCarthy, P.K. Seidelmann, (1982). "The new definition of Universal Time". Astron. & Astrophys, 105 (359-361).

[2] Astronomical Almanac, (yearly) U.S. Government Printing Office.

[3] Baader, H.R., P. Brosche, W. Hövel, (1983) "Ocean Tides and Periodic Variations of the Earth's Rotation". J. Geophysics, 52 (140-142).

[4] Brosche, P., J. Wunsch, J. Campbell, H. Schuh, (1991). Ocean Tide Effects in Universal Time Detected by VLBI. Astronomy and Astrophysics,245,2,(676-682)

[5] Büllesfeld, F.J., H. Schuh, (1986). "New Harmonic Development of the Tide-Generating Potential ETMB 85 with Application on VLBI Data Analysis". Proc. X Int. Symp. on Earth Tides (933-942), Ed. R. Vieira, Madrid.

[6] Caprette D.S., J.W. Ryan, C. Ma, (1990). "VLBI Geodetic Results 1979-1989 / CDP Data Analysis 1990", NASA Technical Memorandum 100765.

[7] Carter, W.E., T. Herring, (1988). Annual Report of the BIH for 1987. p. D-105.

[8] Chao, C.C. (1974). "The Troposphere Calibration Model for Mariner Mars 1971". Tech. Report 32-1587 (61-76), JPL.

[9] Davis, J.L., T.A. Herring, I.I. Shapiro, A.E.E. Rogers, G. Elgered, (1985). "Geodesy by Radio Interferometry: Effects of Atmospheric Modeling Errors on Estimated Baseline Length". Radio Science 20, (1593-1607).

[10] De Mets, C., R.G. Gordon, D.F. Argus, S. Stein, (1990). "Current Plate Motions". Geophys. J. Int. 101 (425-478).

[11] Finkelstein, A.M., V.J. Kreinovitch, N.S. Pandey, (1983). "Relativistic Reductions for Radiointerferometric Observables". Astrophys. Space Sci., 94 (233-247).

[12] Genin, Y., (1970). "Further Comments on the Derivation of Kalman Filters, Section II: Gaussian Estimates and Kalman Filtering". Theory and Applications of Kalman Filtering (55-63), AGARDOgraph 139, C.T. Leondes, ed.

[13] Goad, C.C. (1980). "Gravimetric Tidal Loading Computed from Integrated Green's Functions". J. Geophys. Res. 85, (2679-2683).

[14] Golub, G.H., C. Reinsch, (1970). "Singular Value Decomposition and Least Squares Solutions". Numerische Mathematik, 14 (403-420).

[15] Hildebrand, F.B. (1956). "Introduction to Numerical Analysis". Ed. McGraw-Hill.

[16] IERS Bulletin B. (monthly). Observatoire de Paris.

[17] IERS Technical Note 3. (1989). Ed. D.D. McCarthy. Observatoire de Paris.

[18] IERS Annual Report for 1990, (1991). Observatoire de Paris.

[19] Lanyi, G.E. (1984). "Tropospheric Delay Effects in Radio Interferometry". TDA Progress Report 42-78 (152-159). JPL.

[20] Lawson, C.L., R.J. Hanson, (1974). "Solving Least Squares Problems". Ed. Prentice-Hall.

[21] Lieske, J.H., T. Lederle, W. Fricke, B. Morando, (1977). "Expression for the Precession Quantities Based upon the IAU (1976) System of Astronomical Constants". Astron. & Astrophys., 58 (1-16).

[22] Marini, J.W. (1972). "Correction of Satellite Tracking Data for an Arbitrary Tropospheric Profile". Radio Science 7, (223-231)

[23] Melchior, P. (1978). "The Tides of the Planet Earth". Ed. Pergamon Press, Oxford.

[24] Minster, J.B., T.H. Jordan, (1978). "Present-Day Plate Motions". J. Geophys. Res. 83 (5331-5354).

[25] Pagiatakis, S.D., R.B. Langley, P. Vanicek, (1984). "Ocean Tide Loading: A Global Model for the Analysis of VLBI Observa-

tions". Proceedings of the 3rd International Symposium on the Use of Artificial Satellites for Geodesy & Geodynamics (328-340). Ed. G. Veis, Athens.

[26] Rabbel, W., H. Schuh, (1986). "The Influence of Atmospheric Loading on VLBI Experiments". J. Geophysics, 59 (164-170)

[27] Rius, A., J. Rodríguez, J. Campbell, (1987). "Geodetic VLBI with Large Antennas". VLBI & Doppler Papers pres. by the Geod. Ins. of the Univ. of Bonn 1983-1987 (59-67). Ed. J. Campbell & H. Schuh.

[28] Rius, A., N. Zarraoa, E. Sardón, (1991). "Repeatability of VLBI baseline estimates". Presented at the XVI Gen. Assembly of the EGS, Wiesbaden, Germany.

[29] Sardón, E., N. Zarraoa, A. Rius, (1990). "Automatic Modeling of Clock Breaks in Geodetic VLBI Analysis". Proc. VII European VLBI Meeting, (103-109). Ed. A. Rius.

[30] Scheid, J.A. (1985). "Comparison of the Calibration of Ionospheric Delay in VLBI Data by the Methods of Dual Frequency and Faraday Rotation". TDA Progress Report 42-82 (11-23). NASA-JPL.

[31] Schuh, H. (1987). "Die Radiointerferometrie auf langen Basen zur Bestimmung von Punktverschiebungen und Erdrotationsparametern". Ph. D. Thesis. Deutsche Geodätische Kommission Nr. 328.

[32] Seidelmann, P.K. (1982). "1980 IAU Nutation: The Final Report of the IAU Working Group on Nutation". Celestial Mechanics, 27 (79-106).

[33] Sovers, O.J., J.L. Fanselow, (1987). "Observation Model and Parameter Partials for the JPL VLBI Parameter Estimation Software MASTERFIT-1987". JPL Publication 83-39 Rev. 3.

[34] Stumpff, P. (1979). "The rigorous treatment of stellar aberration and Doppler shift, and the barycentric motion of the Earth". Astron. & Astrophys. 78 (229-238).

[35] Stumpff, P. (1980). "Two self-consistent FORTRAN-Subroutines for the computation of the Earth's motion". Astron. & Astrophys. Supplement, 41 (1-8).

[36] Tarantola, A. (1987). "Inverse Problem Theory. Methods for Data Fitting and Model parameter Estimation". Ed. Elsevier.

[37] Wahr, J.M. (1981). "The Forced Nutations of an Elliptical, Rotating, Elastic, and Oceanless Earth". Geophys. J. Roy. Astron. Soc., 64 (705-727).

[38] Yoder, C.F., J.G. Williams, M.E. Parke, (1981). "Tidal Variations of Earth Rotation". J. Geophys. Res. 86, (881-891).

[39] Zarraoa, N., A. Rius, E. Sardón, H. Schuh, J. Vierbuchen, (1989). "OCCAM: A Compact and Transportable Tool for the Analysis of VLBI Experiments". Proceed. VII European VLBI Meeting (92-102). Ed. A. Rius.

[40] Zhu, S.Y., E. Groten, (1988). "Relativistic Effects in the VLBI Time Delay Measurements". Manuscripta Geodaetica, 13, (33-39).